

# A Homogeneous Second-Order Descent Method for Nonconvex Optimization

Chuwen Zhang<sup>\*1</sup>, Dongdong Ge<sup>2</sup>, Chang He<sup>1</sup>, Bo Jiang<sup>1</sup>, Yuntian Jiang<sup>1</sup>, Chenyu Xue<sup>1</sup>, and Yinyu Ye<sup>3</sup>

<sup>1</sup>School of Information Management and Engineering, Shanghai University of Finance and Economics

<sup>2</sup>Antai College of Economics and Management, Shanghai Jiao Tong University

<sup>3</sup>Department of Management Science and Engineering, Stanford University

May 8, 2024

## Abstract

In this paper, we introduce a *Homogeneous Second-Order Descent Method* (HSODM) using the homogenized quadratic approximation to the original function. The merit of homogenization is that only the leftmost eigenvector of a gradient-Hessian integrated matrix is computed at each iteration. Therefore, the algorithm is a single-loop method that does not need to switch to other sophisticated algorithms and is easy to implement. We show that HSODM has a global convergence rate of  $O(\epsilon^{-3/2})$  to find an  $\epsilon$ -approximate second-order stationary point, and has a local quadratic convergence rate under the standard assumptions. The numerical results demonstrate the advantage of the proposed method over other second-order methods.

## 1 Introduction

In this paper, we consider the following unconstrained optimization problem:

$$\min_{x \in \mathbb{R}^n} f(x), \quad (1.1)$$

where  $f : \mathbb{R}^n \mapsto \mathbb{R}$  is a twice continuously differentiable function and  $f_{\inf} := \inf f(x) > -\infty$ . Given a tolerance level  $\epsilon > 0$ , we aim to find an  $\epsilon$ -approximate second-order stationary point (SOSP)  $x$  satisfying

$$\|\nabla f(x)\| \leq O(\epsilon), \quad (1.2a)$$

$$\lambda_{\min}(\nabla^2 f(x)) \geq \Omega(-\sqrt{\epsilon}), \quad (1.2b)$$

---

<sup>\*</sup>This research is partially supported by the National Natural Science Foundation of China (NSFC) [Grant NSFC-72150001, 72225009, 11831002]

where  $\lambda_{\min}(A)$  denotes the smallest eigenvalue of matrix  $A$ . When  $f$  is nonconvex, it has been shown that the gradient descent (GD) method finds an  $\epsilon$ -approximate first-order stationary point satisfying (1.2a) in  $O(\epsilon^{-2})$  iterations under the standard  $L$ -Lipschitz continuous gradient condition. If the second-order condition (1.2b) is further required, first-order methods may fail, and a common practice is to consider second-order methods such as some variants of Newton’s method [9].

In each iteration, second-order methods usually construct a simple model function by leveraging the second-order information to approximate the original function at the current iterate  $x_k$ , and then compute the next update direction  $d_k$ . For example, the Newton’s method utilizes the following quadratic approximation to compute  $d_k$ :

$$d_k = \arg \min_d m_k(d) := g_k^T d + \frac{1}{2} d^T H_k d, \quad (1.3)$$

where  $g_k = \nabla f(x_k)$  and  $H_k = \nabla^2 f(x_k)$ . In the nonconvex case, despite the excellent performance in practice, Cartis et al. [5] show that Newton’s method, perhaps surprisingly, has a worst-case complexity of  $O(\epsilon^{-2})$  similar to that of GD method. Therefore, some advanced techniques are needed to improve the convergence performance of Newton’s method. Nesterov and Polyak [37] introduces the cubic regularization (CR) and consider the following subproblem:

$$d_k^{\text{CR}} = \arg \min_d m_k^{\text{CR}}(d) := g_k^T d + \frac{1}{2} d^T H_k d + \frac{\sigma_k}{3} \|d\|^3, \quad (1.4)$$

where  $\sigma_k > 0$ . They show that the cubic regularized Newton’s method has an improved iteration complexity of  $O(\epsilon^{-3/2})$ . Later, Cartis et al. [6, 7] propose an adaptive and inexact version of cubic regularization (ARC) with the same complexity. Another widely-used technique is the trust-region (TR) method. It computes the update direction based on the same model function as Newton’s method, but restrains it within the pre-specified trust-region radius  $\Delta_k$ , and accepts it if the corresponding acceptance ratio  $\rho_k$  exceeds some threshold [9]:

$$d_k^{\text{TR}} = \arg \min_{\|d\| \leq \Delta_k} m_k(d), \quad (1.5a)$$

$$\rho_k := \frac{f(x_k + d_k) - f(x_k)}{m_k(d_k) - m_k(0)}. \quad (1.5b)$$

However, it is more challenging to establish the improved  $O(\epsilon^{-3/2})$  iteration complexity for TR method. To our best knowledge, Ye [46] is the only early work proving that TR with a fixed radius strategy enjoys the  $O(\epsilon^{-3/2})$  complexity. Recently, Curtis et al. [12] point out that traditional TR method fails in satisfying the sufficient decrease property required to obtain the  $O(\epsilon^{-3/2})$  complexity by classical  $\rho_k$ -based acceptance rule and linearly updated radius. To overcome this issue, they develop an algorithm named TRACE [12, 16], which attains the desired complexity result but has a sophisticated rule of expanding and contracting  $\Delta_k$  due to the nonlinearity between  $\|d_k^{\text{TR}}\|$  and the dual variable of problem (1.5a). More recently, Jiang et al. [26] propose a gradient regularized TR method, which attains the complexity of  $O(\epsilon^{-3/2})$  with a cleaner analysis. Royer and Wright [42]

uses a line-search Newton framework and obtains a similar complexity. Their algorithm alternates between Newton and regularized Newton steps based on the smallest eigenvalue of the Hessian  $H_k$ , and the stepsize is chosen under a similar acceptance rule used in [6, 12]. Nevertheless, all the above methods solve Newton systems, where the cost of  $O(n^3)$  are typical. It is possible to find inexact solutions with better complexity performance. In that sense, many classical algorithms are open for improvement with techniques such as applying negative curvature oracles, conjugate gradient method [42, 43, 15].

## 1.1 Our contribution

In this paper, we introduce a new second-order method (Algorithm 1) and analyze its convergence rate. Firstly, we “homogenize” the local quadratic approximation  $m_k(d)$ . Our motivation originated in semidefinite relaxations of quadratic programming [44, 47] and find “negative curvature” even when the Hessian matrix is near positive semidefinite. Then, we show the resulting problem is essentially an eigenvalue problem and can be solved by the random starting Lanczos algorithm [30], which allows a dimension-independent complexity of  $\tilde{O}((n+1)^2\epsilon^{-1/4})$  in high probability. We demonstrate that the leftmost eigenvalue of the homogenized matrix is always negative; namely, the “homogenized negative curvature” exists. Similar to the gradient descent method, where a first-order stationary point is reached by moving along the negative gradient direction, we can attain a second-order stationary point by *exclusively* moving along the direction corresponding to the homogenized negative curvature.

Secondly, we propose a new second-order method called the Homogeneous Second-Order Descent Method (HSODM) with the homogenized quadratic model as the subproblems. We offer two stepsize strategies to utilize the homogenized negative curvature, including the fixed-radius strategy and a simple backtracking line search method. Our method achieves a better iteration complexity of  $O(\epsilon^{-3/2})$  to converge to a SOSP than the  $O(\epsilon^{-2})$  complexity of the standard trust-region method [13] and the negative-curvature-based method [10]. Accounting for subproblems it requires  $\tilde{O}((n+1)^2\epsilon^{-7/4})$  arithmetic operations. In sharp comparison to [4, 2, 28, 42], HSODM only relies on the homogenized model and *does not* alternate between different subroutines. The algorithm is elegant in a simple form and believed to be highly favorable for practitioners. To make a clear comparison, we provide the following Table 1.1 that includes the algorithms with the state-of-the-art complexity results.

Finally, the numerical results of the proposed method are also encouraging. In particular, two variants of HSODM outperform the standard second-order methods including the standard trust-region method, the cubic regularized Newton method in the CUTEst dataset.

Table 1.1: A Brief comparison of several second-order algorithms.  $p \in (0, 1)$  represents the failure probability of the randomized Lanczos method.

| Algorithm           | Iteration Complexity | Subproblem Complexity                          |
|---------------------|----------------------|--|
| HSODM               | $O(\epsilon^{-3/2})$ | $O((n+1)^2 \epsilon^{-1/4} \log(n/p\epsilon))$ |
| ARC [7]             | $O(\epsilon^{-3/2})$ | $O(n^3 + n^2 \log(1/\epsilon))$                |
| TRACE [11]          | $O(\epsilon^{-3/2})$ | $O(n^3 + n^2 \log(1/\epsilon))$                |
| [15, Algorithm 4.1] | $O(\epsilon^{-3/2})$ | $O(n^2 \epsilon^{-1/4} \log(n/p\epsilon))$     |
| Newton-CG [42, 43]  | $O(\epsilon^{-3/2})$ | $O(n^2 \epsilon^{-1/4} \log(n/p\epsilon))$     |

## 1.2 Related works

There is a recent trend on the study of the improved first-order algorithms [4, 2, 28] that can find  $\epsilon$ -approximate second-order stationary point. Thus, this type of algorithms can serve as a scalable alternative to the second-order ones. Notably, some of these algorithms also enable faster first-order convergence to (1.2a) in  $\tilde{O}(\epsilon^{-7/4})$  function and gradient evaluations. The basic idea is to extend Nesterov’s accelerated gradient descent method (AGD) [36] to the nonconvex case. This is achieved by properly embedding second-order information to make the AGD maintain its theoretical property in convex and semiconvex cases. For example, Carmon et al. [4] apply the Hessian-vector products and randomized Lanczos methods to explore the negative curvature (NC), which then is used as a descent direction if (2.1) is satisfied; otherwise,  $f$  becomes locally semiconvex and AGD is invoked to solve the subproblem. The later work in [28, 45] also require NC but avoid Hessian-vector products and the complexities remain the same. Beyond using NC, Agarwal et al. [2] achieve the same complexity bound by applying fast matrix inversion to cubic regularized steps. Recently, Li and Lin [32] introduced a restarted AGD that drops the logarithmic term  $O(\log(\epsilon^{-1}))$  in the complexity bound if the solution is required to only satisfy the first-order condition, but it also losses second-order guarantees. To make AGD work in a comfort zone, these algorithms create sophisticated nested loops that may be hard to implement and tune. Nevertheless, they are designed to be less “dimension-dependent” than pure second-order methods such as [37, 6] and are suitable for large-scale problems in theory.

Coming back to the second-order methods, Royer and Wright [42] separate their method into two cases if (2.1) is absent. In one case the smallest eigenvalue  $\lambda_{\min}(H_k) > -\sqrt{\epsilon}$ , regularized Newton step is used to provide the descent step. In the other case when  $\lambda_{\min}(H_k) > \sqrt{\epsilon}$  is certified, it turns to the ordinary Newton step. Therefore, in the worst case, this method must solve an eigenvalue problem and a Newton step in one iteration. It is unclear if one can unify these procedures as a whole. Recently, Doikov and Nesterov [17] and Mishchenko [35] propose the Gradient Regularized Newton method for convex minimization problems. The subproblem at each iteration is simpler than that of the Cubic Regularized Newton method. Later, Gratton et al. [22] generalizes the

Gradient Regularized Newton method to exploit negative curvature for nonconvex optimization problems. However, their method alternates between regularized Newton and negative curvature steps.

For trust-region methods (1.5),  $\lambda_{\min}(H_k) \leq -\sqrt{\epsilon}$  implies that the Lagrangian dual variable is at least in order of  $\sqrt{\epsilon}$ . When the curvature is properly utilized, it also implies an  $O(\epsilon^{3/2})$  progress as long as the stepsize is carefully selected. This fact can be easily recognized by using the optimality conditions (for example, see [46, 13]). Moreover, it remains true even when the subproblems are solved inexactly or only optimal in the subspace [7, 11, 48]. Curtis et al. [15] further propose a variant of trust-region method that does not alternate between steps, but rather solves a slightly perturbed trust-region subproblem. Later, Jiang et al. [26] show that the parameter of the regularization can be chosen in proportion to the square root of the gradient norm. For fixed-radius strategies [46, 48], if (2.1) does not hold, then the algorithm safely terminates. The case is different for adaptive radius ones. Since the trust-region method uses an acceptance ratio  $\rho_k$  in (1.5) and adjusts the radius linearly, a step may become too small with respect to the dual variable. A workaround can be found in [12, 11] with a delicate control over function progress and the gradient norm:

$$f_k - f_{k+1} \geq \Omega(\|d_k\|^3) \text{ and } \|d_k\| \geq \Omega(\|g_{k+1}\|^{1/2}).$$

Similar conditions are also needed in the analysis of cubic regularization methods [7]. However, these adaptations can be less straightforward to be understood, implemented, and tuned.

In addition, our work is also related to solving trust-region subproblems by eigenvalue procedures [41], which use the same  $(n+1)$ -dimensional symmetric matrix. The idea is later extended to solve cubic regularized subproblems or generalized trust-region subproblems; see, for example, [1, 33]. Both papers introduce the matrix pencils that raise the dimension to  $2(n+1)$  without providing the convergence analysis. While the aforementioned works mainly focus on solving subproblems, we use the homogenized matrix in a generic method that finds stationary points of the main problem. We also provide a complexity analysis of its global and local convergence. Besides, the matrices they construct have larger dimensions than ours, which brings more computational cost when solving the corresponding eigenvalue problem.

### 1.3 Notations, assumptions and organization of the paper

In this subsection, we introduce the notations and assumptions used throughout the paper.

Denote the standard Euclidean norm in space  $\mathbb{R}^n$  by  $\|\cdot\|$ . Let  $B(x_c, r)$  denote the ball whose center is  $x_c$  and radius is  $r$ , i.e.,  $B(x_c, r) = \{x \in \mathbb{R}^n \mid \|x - x_c\| \leq r\}$ . For a matrix  $A \in \mathbb{R}^{n \times n}$ ,  $\|A\|$  represents the induced  $\mathcal{L}_2$  norm, and  $\lambda_{\min}(A)$  denotes its smallest eigenvalue. We also denote  $g_k = \nabla f(x_k)$  and  $H_k = \nabla^2 f(x_k)$ . We use order notations  $O, \Omega$  in the usual sense, whereas  $\tilde{O}$  hides the logarithmic terms.

The rest of the paper is organized as follows. In [Section 2](#), we briefly describe our approach based on the homogenized quadratic model. By solving the homogenized model as an eigenvalue problem, the corresponding HSODM is introduced in [Algorithm 1](#). In [Section 3](#) and [Section 4](#), we give analyses of global and local convergence of HSODM. Our results indicate that HSODM has a global complexity of  $O(\epsilon^{-3/2})$  for an  $\epsilon$ -approximate second-order stationary point. If one does not early terminate the algorithm, it bears a local quadratic converge speed. We address the inexactness in HSODM in [Section 5](#). A Lanczos method with skewed initialization is introduced to utilize the Ritz approximation to homogeneous curvature. In [Section 6](#), we demonstrate the effectiveness of our method by providing fruitful computational results in the CUTEst benchmark compared to other standard second-order methods.

## 2 The Homogenized Quadratic Model and A Second-Order Descent Method

### 2.1 Motivation of Homogenization

The negative curvature of the Hessian matrix empowers many optimization methods in nonconvex optimization. By the term, we say the existence of  $\xi_k \in \mathbb{R}^n$  such that the Rayleigh quotient  $\mathcal{R}_k(\xi_k)$  of  $H_k$  is sufficiently negative, i.e.,

$$\mathcal{R}_k(\xi_k) := \frac{\xi_k^T H_k \xi_k}{\|\xi_k\|^2} \leq -\sqrt{\epsilon}, \quad (2.1)$$

if and only if the Hessian  $H_k \prec -\sqrt{\epsilon} \cdot I$  at some iterate  $x_k$ . Computationally, it is known that such a direction  $\xi_k$  can be found at the cost of  $\tilde{O}(n^2 \cdot \epsilon^{-1/4})$  arithmetic operations, using a randomized Lanczos method [\[30\]](#). When facilitating this direction with a proper stepsize  $\eta$ , the function value must decrease by  $\Omega(\epsilon^{3/2})$  under second-order Lipschitz continuity. This property is widely used in the negative-curvature-based first-order methods [\[4, 28\]](#). However, if [\(2.1\)](#) is invalid, one must switch to other subroutines [\[4, 2, 28, 42\]](#), which complicates the iteration procedure and thus is hard for efficient implementation and parameter tuning.

Unfortunately, a negative curvature never exists if the problem is near convex. To alleviate this issue, we apply the homogenization trick (e.g., see [\[47, 44\]](#)) to the second-order Taylor expansion [\(1.3\)](#) at  $x_k$ :

$$\begin{aligned} t^2 \left( m_k(d) - \frac{1}{2} \delta \right) &= t^2 \left( g_k^T(v/t) + \frac{1}{2} (v/t)^T H_k (v/t) - \frac{1}{2} \delta \right) && (d := v/t) \\ &= t \cdot g_k^T v + \frac{1}{2} v^T H_k v - \frac{1}{2} \delta t^2 = \frac{1}{2} \begin{bmatrix} v \\ t \end{bmatrix}^T \begin{bmatrix} H_k & g_k \\ g_k^T & -\delta \end{bmatrix} \begin{bmatrix} v \\ t \end{bmatrix}, \quad F_k := \begin{bmatrix} H_k & g_k \\ g_k^T & -\delta \end{bmatrix} \end{aligned} \quad (2.2)$$

namely, the second equation is the homogenized quadratic model. The nice property of the “homogenized” matrix  $F_k$  is that it can be indefinite even if  $H_k$  is positive definite, and thus, the “homogenized negative curvature” can be computed from the  $(n+1)$ -dimensional lifted matrix. To make connection to the Rayleigh quotient given in (2.1), we impose a ball constraint  $\|[v; t]\| \leq 1$  on model (2.2) and obtain the subproblem that is solved in our method.

## 2.2 Overview of the method

We present the HSODM in Algorithm 1. The rest of this paper discusses the method that uses the “homogenized” matrix in the iterates. We formally define the homogenized quadratic model as follows. Given an iterate  $x_k \in \mathbb{R}^n$ , let  $\psi_k(v, t; \delta)$  be the homogenized quadratic model,

$$\psi_k(v, t; \delta) := \begin{bmatrix} v \\ t \end{bmatrix}^T \begin{bmatrix} H_k & g_k \\ g_k^T & -\delta \end{bmatrix} \begin{bmatrix} v \\ t \end{bmatrix}, \quad v \in \mathbb{R}^n, t \in \mathbb{R}, \quad (2.3)$$

where  $\delta \geq 0$  is a predefined constant. For each iteration, the HSODM minimizes the model at the current iterate  $x_k$ , i.e.,

$$\min_{\|[v; t]\| \leq 1} \psi_k(v, t; \delta). \quad (2.4)$$

Denote the optimal solution of problem (2.4) as  $[v_k; t_k]$ . As the subproblem (2.4) is essentially an eigenvalue problem, and  $[v_k; t_k]$  is the eigenvector corresponding to the smallest eigenvalue of  $F_k$ . Therefore, we can solve this subproblem using an eigenvector-finding procedure, see [4, 30, 42].

After solving (2.4), we construct a descent direction  $d_k$  based on this optimal solution  $[v_k; t_k]$  and carefully select the stepsize  $\eta_k$  to ensure sufficient decrease. Intuitively, if  $|t_k|$  is relatively small, it means that the Hessian matrix  $H_k$  dominates the homogenized model, and thus we choose the truncated direction  $v_k$  directly (Line 8). Otherwise, the predefined parameter  $-\delta$  becomes significant, and we choose  $v_k/t_k$  as the descent direction instead (Line 10). For the stepsize rule, we provide two strategies for selecting the stepsize: the first is to use line search to determine  $\eta_k$ , and the second is to adopt the idea of the fixed-radius trust-region method [34, 48] such that  $\|\eta_k d_k\| = \Delta$ , where  $\Delta$  is some pre-determined constant. By iteratively performing this subroutine, our algorithm will converge to an  $\epsilon$ -approximate second-order stationary point.

---

**Algorithm 1:** Homogeneous Second-Order Descent Method (HSODM)

---

**Data:** initial point  $x_1$ ,  $\nu \in (0, 1/2)$ ,  $\Delta = \Theta(\sqrt{\epsilon})$

```
1 for  $k = 1, 2, \dots$  do
2   Solve the subproblem (2.4), and obtain the solution  $[v_k; t_k]$ ;
3   if  $|t_k| > \sqrt{1/1 + \Delta^2}$  then                                     // small value case
4      $d_k \leftarrow v_k/t_k$ ;
5     Update  $x_{k+1} \leftarrow x_k + d_k$ ;
6     (Early) Terminate (or set  $\delta = 0$  and proceed);
7   if  $|t_k| \geq \nu$  then                                             // large value case (a)
8      $d_k \leftarrow v_k/t_k$ 
9   else                                                                 // large value case (b)
10     $d_k \leftarrow \text{sign}(-g_k^T v_k) \cdot v_k$ 
11  end
12  Choose a stepsize  $\eta_k$  by the fixed-radius strategy or the line search strategy (see
    Algorithm 2);
13  Update  $x_{k+1} \leftarrow x_k + \eta_k \cdot d_k$ ;
14 end
```

---

### 2.3 Preliminaries of the Homogenized Quadratic Model

In this subsection, we present some preliminary analysis of the homogenized quadratic model. First, we study the relationship between the smallest eigenvalues of the Hessian  $H_k$  and  $F_k$ , and the perturbation parameter  $\delta$ . Then we give the optimality conditions of problem (2.4) and provide some useful results based on those conditions.

**Lemma 2.1** (Relationship between  $\lambda_{\min}(F_k)$ ,  $\lambda_{\min}(H_k)$  and  $\delta$ ). *Let  $\lambda_{\min}(H_k)$  and  $\lambda_{\min}(F_k)$  be the smallest eigenvalue of  $H_k$  and  $F_k$  respectively. Denote by  $\mathcal{S}_{\lambda_{\min}}$  the eigenspace corresponding to  $\lambda_{\min}(H_k)$ . If  $g_k \neq 0$  and  $H_k \neq 0$ , then the following statements hold,*

- (1)  $\lambda_{\min}(F_k) < -\delta$  and  $\lambda_{\min}(F_k) \leq \lambda_{\min}(H_k)$ ;
- (2)  $\lambda_{\min}(F_k) = \lambda_{\min}(H_k)$  only if  $\lambda_{\min}(H_k) < 0$  and  $g_k \perp \mathcal{S}_{\lambda_{\min}}$ .

*Proof.* We first prove the statement (1). By the Cauchy interlace theorem [40], we immediately obtain  $\lambda_{\min}(F_k) \leq \lambda_{\min}(H_k)$ . Now we need to prove that  $\lambda_{\min}(F_k) < -\delta$ . It suffices to show that the matrix  $F_k + \delta I$  has a negative eigenvalue.



Let us consider the direction  $[-\eta g_k; t]$ , where  $\eta, t > 0$ . Define the following function of  $(\eta, t)$ :

$$\begin{aligned} f(\eta, t) &:= \begin{bmatrix} -\eta g_k \\ t \end{bmatrix}^T (F_k + \delta I) \begin{bmatrix} -\eta g_k \\ t \end{bmatrix}, \\ &= \eta^2 g_k^T (H_k + \delta I) g_k - 2\eta t \|g_k\|^2. \end{aligned}$$

For any fixed  $t > 0$ , we have

$$f(0, t) = 0 \quad \text{and} \quad \frac{\partial f(0, t)}{\partial \eta} = -2t \|g_k\|^2 < 0.$$

Therefore, for sufficiently small  $\eta > 0$ , it holds that  $f(\eta, t) < 0$ , which shows that  $[-\eta g_k; t]$  is a negative curvature. Hence,  $\lambda_{\min}(F_k) < -\delta$ .

The proof of the statement (2) is similar to the one of Theorem 3.1 in [41], so we omit it here for succinctness of the paper.

□

**Lemma 2.1** shows that we can control the smallest eigenvalue of the homogenized matrix  $F_k$  by adjusting the perturbation parameter  $\delta$ . It helps us find a better direction to decrease the value of the objective function. We also note that the case  $g_k \perp \mathcal{S}_{\lambda_{\min}}$  is often regarded as a hard case in solving the trust-region subproblem. However, this challenge will not incapacitate HSODM in our convergence analysis. In the following, we will show the function value has a sufficient decrease under this scenario. Thus, the subproblem in HSODM is much easier to solve than the trust-region subproblem due to the non-existence of the hard case.

We remark that **Lemma 2.1** is a simpler version of Lemma 3.3 in [41], where the authors give a more detailed analysis of the relationship between the perturbation parameter  $\delta$  and the eigenpair of the homogenized matrix  $F_k$ . However, the difference is that they try to obtain a solution to the trust-region subproblem via the homogenization trick, while our goal is to seek a good direction to decrease the function value. Furthermore, if the homogenized model is used, then we can show that HSODM has the optimal  $O(\epsilon^{-3/2})$  iteration complexity. If instead, the homogenization trick is put on solving the trust-region subproblem as in [41], one still needs a framework like the one in Curtis et al. [12] to guarantee the same convergence property. Moreover, a sequence of homogenized problems needs to be solved in each iteration of the framework.

In the following lemma, we characterize the optimal solution  $[v_k; t_k]$  of problem (2.4) based on the optimality condition of the standard trust-region subproblem.

**Lemma 2.2** (Optimality condition).  *$[v_k; t_k]$  is the optimal solution of the subproblem (2.4) if and*

only if there exists a dual variable  $\theta_k > \delta \geq 0$  such that

$$\begin{bmatrix} H_k + \theta_k \cdot I & g_k \\ g_k^T & -\delta + \theta_k \end{bmatrix} \succeq 0, \quad (2.5)$$

$$\begin{bmatrix} H_k + \theta_k \cdot I & g_k \\ g_k^T & -\delta + \theta_k \end{bmatrix} \begin{bmatrix} v_k \\ t_k \end{bmatrix} = 0, \quad (2.6)$$

$$\|[v_k; t_k]\| = 1. \quad (2.7)$$

Moreover,  $-\theta_k$  is the smallest eigenvalue of the perturbed homogeneous matrix  $F_k$ , i.e.,  $-\theta_k = \lambda_{\min}(F_k)$ .

*Proof.* By the optimality condition of standard trust-region subproblem,  $[v_k; t_k]$  is the optimal solution if and only if there exists a dual variable  $\theta_k \geq 0$  such that

$$\begin{bmatrix} H_k + \theta_k \cdot I & g_k \\ g_k^T & -\delta + \theta_k \end{bmatrix} \succeq 0, \quad \begin{bmatrix} H_k + \theta_k \cdot I & g_k \\ g_k^T & -\delta + \theta_k \end{bmatrix} \begin{bmatrix} v_k \\ t_k \end{bmatrix} = 0, \quad \text{and } \theta_k \cdot (\|[v_k; t_k]\| - 1) = 0.$$

With [Lemma 2.1](#), we have  $\lambda_{\min}(F_k) < -\delta \leq 0$ . Therefore,  $\theta_k \geq -\lambda_{\min}(F_k) > \delta \geq 0$ , and further  $\|[v_k; t_k]\| = 1$ . Moreover, by [\(2.6\)](#), we obtain

$$\begin{bmatrix} H_k & g_k \\ g_k^T & -\delta \end{bmatrix} \begin{bmatrix} v_k \\ t_k \end{bmatrix} = -\theta_k \begin{bmatrix} v_k \\ t_k \end{bmatrix}.$$

Multiplying the equation above by  $[v_k; t_k]^T$ , we have

$$\min_{\|[v; t]\| \leq 1} \psi_k(v, t; \delta) = -\theta_k$$

Note that with [\(2.7\)](#), the optimal value of problem [\(2.4\)](#) is equivalent to the smallest eigenvalue of  $F_k$ , i.e.,  $\lambda_{\min}(F_k)$ . Thus,  $-\theta_k = \lambda_{\min}(F_k)$ . Then the proof is completed. □

With the above optimality condition, we can derive the following corollaries.

**Corollary 2.1.** *The equation [\(2.6\)](#) in [Lemma 2.2](#) can be rewritten as,*

$$(H_k + \theta_k I)v_k = -t_k g_k \quad \text{and} \quad g_k^T v_k = t_k(\delta - \theta_k). \quad (2.8)$$

Furthermore,

(1) *If  $t_k = 0$ , then we have*

$$(H_k + \theta_k I)v_k = 0 \quad \text{and} \quad g_k^T v_k = 0, \quad (2.9)$$

*implying that  $(-\theta_k, v_k)$  is the eigenpair of the Hessian matrix  $H_k$ .*

(2) If  $t_k \neq 0$ , then we have

$$g_k^T d_k = \delta - \theta_k \quad \text{and} \quad (H_k + \theta_k \cdot I)d_k = -g_k \quad (2.10)$$

where  $d_k = v_k/t_k$ .

The corollary above is a direct application of [Lemma 2.2](#), so we omit its proof in the paper.

**Corollary 2.2** (Nontriviality of direction  $v_k$ ). *If  $g_k \neq 0$ , then  $v_k \neq 0$ .*

*Proof.* We prove by contradiction. Suppose that  $v_k = 0$ . Then, we have  $t_k g_k = 0$  with equation (2.8) in [Corollary 2.1](#). It further implies that  $t_k = 0$  due to  $g_k \neq 0$ . However,  $[v_k; t_k] = 0$  contradicts to the equation  $\|[v_k; t_k]\| = 1$  in the optimality condition. Therefore, we have  $v_k \neq 0$ . □

This corollary shows that a nontrivial direction  $v_k$  always exists, thus [Algorithm 1](#) will not get stuck.

**Corollary 2.3.** *For the sign function value  $\text{sign}(-g_k^T v_k)$ , we always have  $\text{sign}(-g_k^T v_k) \cdot t_k = |t_k|$ .*

*Proof.* By the second equation of optimal condition (2.8), and  $\delta < \theta_k$ , we obtain that

$$\text{sign}(-g_k^T v_k) = \text{sign}(t_k),$$

and it implies

$$\text{sign}(-g_k^T v_k) \cdot t_k = \text{sign}(t_k) \cdot t_k = |t_k|.$$

This completes the proof. □

As a byproduct, we also have the following result.

**Corollary 2.4** (Trivial case,  $g_k = 0$ ). *Suppose that  $g_k = 0$ , then the following statements hold,*

- (1) *If  $\lambda_{\min}(H_k) > -\delta$ , then  $t_k = 1$ .*
- (2) *If  $\lambda_{\min}(H_k) < -\delta$ , then  $t_k = 0$ .*

*Proof.* When  $g_k = 0$ , the homogenized matrix  $F_k = [H_k, 0; 0, -\delta]$ , and the subproblem (2.4) is

$$\min_{\|[v; t]\| \leq 1} \psi_k(v, t; \delta) = v^T H_k v - t^2 \cdot \delta.$$

We first prove the statement (1) by contradiction. Suppose that  $t_k \neq 1$ , then we have  $v_k \neq 0$  by the equation (2.7). Thus,

$$\psi_k(v_k, t_k; \delta) = (v_k)^T H_k v_k - t_k^2 \cdot \delta > -\delta = \psi_k(0, 1; \delta), \quad (2.11)$$

where the inequality holds due to  $(v_k)^T H_k v_k \geq \lambda_{\min}(H_k) \|v_k\|^2 > -\delta \|v_k\|^2$ . The equation (2.11) contradicts to the optimality of  $(v_k, t_k)$ , and thus  $t_k = 1$ . The second statement can be proved by the same argument, and we omit the proof here.

□

### 3 Global Convergence Rate

In this section, we analyze the convergence rate of the proposed HSODM. To facilitate the analysis, we present two building blocks considering the large and small values of  $\|d_k\|$ , respectively. For the large value case of  $\|d_k\|$ , we show that the function value decreases by at least  $\Omega(\epsilon^{3/2})$  at every iteration after carefully selecting the perturbation parameter  $\delta$ . In the latter case, we prove that the next iterate  $x_{k+1}$  is already an  $\epsilon$ -approximate second-order stationary point, and thus the algorithm can terminate. Throughout the paper, we make the following standard assumptions.

**Assumption 3.1.** *Assume that  $f$  has  $M$ -Lipschitz continuous Hessian on an open convex set  $X$  containing all the iterates  $x_k$ , i.e., for some  $M > 0$ , we have*

$$\|\nabla^2 f(x) - \nabla^2 f(y)\| \leq M \|x - y\|, \quad \forall x, y \in X, \quad (3.1)$$

and that the Hessian matrix is bounded,

$$\|\nabla^2 f(x_k)\| \leq U_H, \quad \forall k \geq 0, \quad (3.2)$$

for some  $U_H > 0$ .

We also recall the next lemma for preparation.

**Lemma 3.1** (Nesterov [36]). *If  $f : \mathbb{R}^n \mapsto \mathbb{R}$  satisfies Assumption 3.1, then for all  $x, y \in \mathbb{R}^n$ ,*

$$\|\nabla f(y) - \nabla f(x) - \nabla^2 f(x)(y - x)\| \leq \frac{M}{2} \|y - x\|^2, \quad (3.3a)$$

$$\left| f(y) - f(x) - \nabla f(x)^T (y - x) - \frac{1}{2} (y - x)^T \nabla^2 f(x) (y - x) \right| \leq \frac{M}{6} \|y - x\|^3. \quad (3.3b)$$

#### 3.1 Analysis for the large value of $\|d_k\|$

In HSODM, we define the large-value case of  $\|d_k\|$  as the case that its norm is larger than the trust-region radius  $\Delta$ , i.e.,  $\|d_k\| > \Delta$ , or equivalently  $|t_k| \leq \sqrt{1/1 + \Delta^2}$ . In this situation, the homogenized direction can be either  $d_k = \text{sign}(-g_k^T v_k) \cdot v_k$  or  $d_k = v_k/t_k$ . The following discussion shows that both stepsize selection strategies result in a sufficient decrease. The analysis for the fixed-radius strategy is more concise and clear, but it mainly serves as a theoretical result. On the contrary, the line search stepsize selection strategy is more practical in spite of a slightly more complicated analysis.

### 3.1.1 Fixed-radius strategy

For the fixed-radius strategy, the next iterate  $x_{k+1}$  is constrained to satisfy  $\|x_{k+1} - x_k\| = \Delta$ , and hence the stepsize is selected as  $\Delta/\|d_k\|$ . Firstly, we will consider the scenario in which  $|t_k| < \nu$  and  $d_k = \text{sign}(-g_k^T v_k) \cdot v_k$ . We remark that this particular scenario encompasses the so-called ‘‘hard case’’ ( $t_k = 0$ ) in trust-region methods [41]. When  $t_k = 0$ , [Corollary 2.1](#) shows that  $(-\theta_k, v_k)$  is an eigenpair of the Hessian  $H_k$ , and  $v_k$  is a sufficiently negative curvature direction due to  $-\theta_k < -\delta \leq 0$ . Therefore, moving along the direction of  $v_k$  with an appropriate stepsize will always decrease the function value [4]. We first present a lemma that applies to the case  $|t_k| < \nu$ , and it can be regarded as a generalized descent lemma.

**Lemma 3.2.** *Suppose that [Assumption 3.1](#) holds and set  $\nu \in (0, 1/2)$ . If  $|t_k| < \nu$ , then let  $d_k = \text{sign}(-g_k^T v_k) \cdot v_k$  and  $\eta_k = \Delta/\|d_k\|$ , we have*

$$f(x_{k+1}) - f(x_k) \leq -\frac{\Delta^2}{2}\delta + \frac{M}{6}\Delta^3. \quad (3.4)$$

*Proof.* When  $d_k = \text{sign}(-g_k^T v_k) \cdot v_k$ , with the optimality condition (2.8) in [Corollary 2.1](#) and [Corollary 2.3](#), we obtain

$$d_k^T H_k d_k = -\theta_k \|d_k\|^2 - t_k^2 \cdot (\delta - \theta_k) \quad \text{and} \quad g_k^T d_k = |t_k| \cdot (\delta - \theta_k). \quad (3.5)$$

Since  $\eta_k = \Delta/\|d_k\| \in (0, 1)$ , then  $\eta_k - \eta_k^2/2 \geq 0$ , and further

$$\left(\eta_k - \frac{\eta_k^2}{2}\right) \cdot (\delta - \theta_k) \leq 0. \quad (3.6)$$

By the  $M$ -Lipschitz continuous property of  $\nabla^2 f(x)$ , we have

$$\begin{aligned} f(x_{k+1}) - f(x_k) &= f(x_k + \eta_k d_k) - f(x_k) \\ &\leq \eta_k \cdot g_k^T d_k + \frac{\eta_k^2}{2} \cdot d_k^T H_k d_k + \frac{M}{6} \eta_k^3 \|d_k\|^3 \\ &= \eta_k \cdot |t_k| \cdot (\delta - \theta_k) - \frac{\eta_k^2}{2} \cdot \theta_k \|d_k\|^2 - \frac{\eta_k^2}{2} \cdot t_k^2 \cdot (\delta - \theta_k) + \frac{M}{6} \eta_k^3 \|d_k\|^3 \end{aligned} \quad (3.7a)$$

$$\leq \eta_k \cdot t_k^2 \cdot (\delta - \theta_k) - \frac{\eta_k^2}{2} \cdot \theta_k \|d_k\|^2 - \frac{\eta_k^2}{2} \cdot t_k^2 \cdot (\delta - \theta_k) + \frac{M}{6} \eta_k^3 \|d_k\|^3 \quad (3.7b)$$

$$\begin{aligned} &= \left(\eta_k - \frac{\eta_k^2}{2}\right) \cdot t_k^2 \cdot (\delta - \theta_k) - \frac{\eta_k^2}{2} \cdot \theta_k \|d_k\|^2 + \frac{M}{6} \eta_k^3 \|d_k\|^3 \\ &\leq -\theta_k \cdot \frac{\Delta^2}{2} + \frac{M}{6} \Delta^3 \end{aligned} \quad (3.7c)$$

$$\leq -\frac{\Delta^2}{2}\delta + \frac{M}{6}\Delta^3, \quad (3.7d)$$

where (3.7a) follows from (3.5), and (3.7b) holds due to  $|t_k| < \nu < 1$  and  $\delta - \theta_k < 0$ . The inequality (3.7c) holds by (3.6) and  $\eta_k = \Delta/\|d_k\|$ .  $\square$

Now we turn to the case  $|t_k| \geq \nu$ , and let the update direction  $d_k = v_k/t_k$ . When  $\|d_k\|$  is large enough, i.e.,  $\|d_k\| > \Delta$ , we can obtain the same decrease of function value in the next lemma.

**Lemma 3.3.** *Suppose that [Assumption 3.1](#) holds and set  $\nu \in (0, 1/2)$ . If  $|t_k| \geq \nu$  and  $\|v_k/t_k\| > \Delta$ , then let  $d_k = v_k/t_k$  and  $\eta_k = \Delta/\|d_k\|$ , we have*

$$f(x_{k+1}) - f(x_k) \leq -\frac{\Delta^2}{2}\delta + \frac{M}{6}\Delta^3. \quad (3.8)$$

*Proof.* When  $t_k \neq 0$ , with equation (2.10) in [Corollary 2.1](#), we have

$$d_k^T H_k d_k = -g_k^T d_k - \theta_k \|d_k\|^2 \quad \text{and} \quad g_k^T d_k = \delta - \theta_k \leq 0. \quad (3.9)$$

Since  $\eta_k = \Delta/\|d_k\| \in (0, 1)$ , then  $\eta_k - \eta_k^2/2 \geq 0$ , and further

$$\left(\eta_k - \frac{\eta_k^2}{2}\right) \cdot g_k^T d_k \leq 0. \quad (3.10)$$

By the  $M$ -Lipschitz continuous property of  $\nabla^2 f(x)$ , we have

$$\begin{aligned} f(x_{k+1}) - f(x_k) &= f(x_k + \eta_k d_k) - f(x_k) \\ &\leq \eta_k \cdot g_k^T d_k + \frac{\eta_k^2}{2} \cdot d_k^T H_k d_k + \frac{M}{6} \eta_k^3 \|d_k\|^3 \\ &= \left(\eta_k - \frac{\eta_k^2}{2}\right) \cdot g_k^T d_k - \theta_k \cdot \frac{\eta_k^2}{2} \|d_k\|^2 + \frac{M}{6} \eta_k^3 \|d_k\|^3 \end{aligned} \quad (3.11a)$$

$$\leq -\theta_k \cdot \frac{\eta_k^2}{2} \|d_k\|^2 + \frac{M}{6} \eta_k^3 \|d_k\|^3 \quad (3.11b)$$

$$\leq -\frac{\Delta^2}{2}\delta + \frac{M}{6}\Delta^3, \quad (3.11c)$$

where (3.11a) holds due to equation (3.9), (3.11b) follows from equation (3.10), and in (3.11c) we substitute  $\eta_k$  with  $\Delta/\|d_k\|$  and use  $\theta_k \geq \delta$ .

□

### 3.1.2 Line search strategy

For the line search strategy, we utilize a backtracking subroutine to determine the stepsize  $\eta_k$ , ensuring it produces a sufficient decrease. The details of the subroutine are provided below.

---

**Algorithm 2:** Backtracking Line Search

---

**Data:** Given current iterate  $x_k$ , direction  $d_k$ , initial stepsize  $\eta_k = 1$ ,  $\gamma > 0$ ,  $\beta \in (0, 1)$

- 1 **For**  $j = 0, 1, 2, \dots$  **do:**
  - 2   Compute decrease quantity  $D_k := f(x_k) - f(x_k + \eta_k d_k)$ ;
  - 3   **If**  $D_k \geq \gamma \eta_k^3 \|d_k\|^3 / 6$  **then:**
  - 4     **Break;**
  - 5   **Else:**
  - 6     Update  $\eta_k := \beta \cdot \eta_k$ ;
  - 7 **Output:** stepsize  $\eta_k$ .
- 

Similarly, we derive the descent lemmas with the line search strategy and further upper bound the number of iterations required by the line search procedure. For the cases  $|t_k| < \nu$  and  $|t_k| \geq \nu$ , we obtain the following two lemmas that characterize the sufficient decrease property.

**Lemma 3.4.** *Suppose that [Assumption 3.1](#) holds and set  $\nu \in (0, 1/2)$ . If  $|t_k| < \nu$ , then let  $d_k = \text{sign}(-g_k^T v_k) \cdot v_k$ . The backtracking line search terminates with  $\eta_k = \beta^{j_k}$ , and  $j_k$  is upper bounded by*

$$j_N := \left\lceil \log_{\beta} \left( \frac{3\delta}{M + \gamma} \right) \right\rceil,$$

and the function value associated with the stepsize  $\eta_k$  satisfies,

$$f(x_{k+1}) - f(x_k) \leq - \min \left\{ \frac{\sqrt{3}\gamma}{16}, \frac{9\gamma\beta^3\delta^3}{2(M + \gamma)} \right\}. \quad (3.12)$$

*Proof.* Suppose that the backtracking line search terminate with  $\eta_k = 1$ , then we have

$$\begin{aligned} f(x_k + \eta_k d_k) - f(x_k) &\leq -\frac{\gamma}{6} \eta_k^3 \|d_k\|^3 \\ &= -\frac{\gamma}{6} \|v_k\|^3 \\ &\leq -\frac{\sqrt{3}\gamma}{16}, \end{aligned}$$

where the last inequality is due to  $\|v_k\| = \sqrt{1 - |t_k|^2} \geq \sqrt{1 - \nu^2} \geq \sqrt{3}/2$ . Suppose the algorithm does not stop at the iteration  $j \geq 0$  and the condition in Line 4 is not met, i.e.  $D_k < \frac{\gamma}{6} \beta^{3j} \|d_k\|^3 =$

$\frac{\gamma}{6}\beta^{3j}\|v_k\|^3$ . By using a similar argument in the proof of [Lemma 3.2](#), we have that

$$\begin{aligned}
-\frac{\gamma}{6}\beta^{3j}\|v_k\|^3 &< f(x_k + \beta^j d_k) - f(x_k) \\
&\leq \beta^j \cdot g_k^T d_k + \frac{\beta^{2j}}{2} \cdot d_k^T H_k d_k + \frac{M}{6}\beta^{3j}\|d_k\|^3 \\
&= \beta^j \cdot |t_k| \cdot (\delta - \theta_k) - \frac{\beta^{2j}}{2} \cdot \theta_k \|v_k\|^2 - \frac{\beta^{2j}}{2} \cdot t_k^2 \cdot (\delta - \theta_k) + \frac{M}{6}\beta^{3j}\|v_k\|^3 \\
&\leq \beta^j \cdot t_k^2 \cdot (\delta - \theta_k) - \frac{\beta^{2j}}{2} \cdot \theta_k \|v_k\|^2 - \frac{\beta^{2j}}{2} \cdot t_k^2 \cdot (\delta - \theta_k) + \frac{M}{6}\beta^{3j}\|v_k\|^3 \\
&= \left( \beta^j - \frac{\beta^{2j}}{2} \right) \cdot t_k^2 \cdot (\delta - \theta_k) - \frac{\beta^{2j}}{2} \cdot \theta_k \|v_k\|^2 + \frac{M}{6}\beta^{3j}\|v_k\|^3 \\
&\leq -\frac{\beta^{2j}}{2} \cdot \theta_k \|v_k\|^2 + \frac{M}{6}\beta^{3j}\|v_k\|^3 \\
&\leq -\frac{\beta^{2j}}{2} \cdot \delta \|v_k\|^2 + \frac{M}{6}\beta^{3j}\|v_k\|^3.
\end{aligned} \tag{3.13}$$

Therefore,  $\beta^j > \frac{3\delta}{(M+\gamma)\|v_k\|}$  holds, which further implies that

$$j < \log_\beta \left( \frac{3\delta}{(M+\gamma)\|v_k\|} \right).$$

However,  $j_N := \left\lceil \log_\beta \left( \frac{3\delta}{(M+\gamma)\|v_k\|} \right) \right\rceil \geq \log_\beta \left( \frac{3\delta}{(M+\gamma)\|v_k\|} \right)$  due to  $\|v_k\| \leq 1$ . This means that the inequality (3.13) does not hold when  $j = j_N$ , and thus the condition in Line 4 is satisfied in this case. Therefore, the iteration number of backtracking subroutine  $j_k$  is upper bounded by  $j_N$ , and the function value decreases as

$$\begin{aligned}
f(x_k + \eta_k d_k) - f(x_k) &\leq -\frac{\gamma}{6}\beta^{3j_k}\|v_k\|^3 \\
&= -\frac{\gamma\beta^3}{6}\beta^{3(j_k-1)}\|v_k\|^3 \\
&\leq -\frac{9\gamma\beta^3\delta^3}{2(M+\gamma)^3},
\end{aligned}$$

where the last inequality comes from  $\beta^{j_k-1} \geq \frac{3\delta}{(M+\gamma)\|v_k\|}$ . □

**Lemma 3.5.** *Suppose that [Assumption 3.1](#) holds and set  $\nu \in (0, 1/2)$ . If  $|t_k| \geq \nu$  and  $\|v_k/t_k\| > \Delta$ , then let  $d_k = v_k/t_k$ . The backtracking line search terminates with  $\eta_k = \beta^{j_k}$ , and  $j_k$  is upper bounded by*

$$j_N := \left\lceil \log_\beta \left( \frac{3\delta\nu}{M+\gamma} \right) \right\rceil,$$

and the function value associated with the stepsize  $\eta_k$  satisfies,

$$f(x_{k+1}) - f(x_k) \leq -\min \left\{ \frac{\gamma\Delta^3}{6}, \frac{9\gamma\beta^3\delta^3}{2(M+\gamma)^3} \right\}. \tag{3.14}$$



*Proof.* Similarly, suppose that the backtracking line search terminates with  $\eta_k = 1$ , we have

$$\begin{aligned} f(x_k + \eta_k d_k) - f(x_k) &\leq -\frac{\gamma}{6} \eta_k^3 \|d_k\|^3 \\ &\leq -\frac{\gamma}{6} \Delta^3, \end{aligned}$$

where the last inequality comes from  $\|d_k\| > \Delta$ . If  $\eta_k = 1$  does not lead to sufficient decrease, then for any  $j \geq 0$  where the condition in Line 4 is not met, we have

$$\begin{aligned} -\frac{\gamma}{6} \beta^{3j} \|d_k\|^3 &< f(x_k + \beta^j d_k) - f(x_k) \\ &\leq \beta^j \cdot g_k^T d_k + \frac{\beta^{2j}}{2} \cdot d_k^T H_k d_k + \frac{M}{6} \beta^{3j} \|d_k\|^3 \\ &= (\beta^j - \frac{\beta^{2j}}{2}) \cdot (\delta_k - \theta_k) - \frac{\beta^{2j}}{2} \theta_k \|d_k\|^2 + \frac{M}{6} \beta^{3j} \|d_k\|^3 \\ &\leq -\frac{\beta^{2j}}{2} \delta \|d_k\|^2 + \frac{M}{6} \beta^{3j} \|d_k\|^3. \end{aligned} \tag{3.15}$$

Therefore,  $\beta^j \geq \frac{3\delta}{(M+\gamma)\|d_k\|}$  and it implies that

$$j < \log_{\beta} \left( \frac{3\delta}{(M+\gamma)\|d_k\|} \right).$$

Note that

$$\|d_k\| = \|v_k\|/|t_k| = \frac{\sqrt{1-|t_k|^2}}{|t_k|} \leq \frac{1}{\nu}, \tag{3.16}$$

and  $j_N := \left\lceil \log_{\beta} \left( \frac{3\delta\nu}{M+\gamma} \right) \right\rceil \geq \log_{\beta} \left( \frac{3\delta}{(M+\gamma)\|d_k\|} \right)$ , This means that the inequality (3.15) does not hold when  $j = j_N$ , and thus the condition in Line 4 is satisfied in this case. Therefore, the iteration number of backtracking subroutine  $j_k$  is upper bounded by  $j_N$ , and the function value decreases as

$$\begin{aligned} f(x_k + \eta_k d_k) - f(x_k) &\leq -\frac{\gamma}{6} \beta^{3j_k} \|d_k\|^3 \\ &= -\frac{\gamma\beta^3}{6} \beta^{3(j_k-1)} \|d_k\|^3 \\ &\leq -\frac{9\gamma\beta^3\delta^3}{2(M+\gamma)^3}, \end{aligned}$$

where the last inequality is due to  $\beta^{j_k-1} \geq \frac{3\delta}{(M+\gamma)\|d_k\|}$ .  $\square$

Combining the above two lemmas, we now conclude a unified descent property for homogenized negative curvature equipped with backtracking line search.

**Corollary 3.1.** *Suppose that Assumption 3.1 holds and set  $\nu \in (0, 1/2)$ . Let the backtracking line search parameters  $\beta, \gamma$  satisfy  $\beta \in (0, 1)$  and  $\gamma > 0$ . Then after every outer iterate, the function value decreases as*

$$f(x_{k+1}) - f(x_k) \leq -\min \left\{ \frac{\sqrt{3}\gamma}{16}, \frac{9\gamma\beta^3\delta^3}{2(M+\gamma)}, \frac{\gamma\Delta^3}{6}, \frac{9\gamma\beta^3\delta^3}{2(M+\gamma)^3} \right\}.$$

and the inner iteration for backtracking line search is at most

$$j_N \leq \max \left\{ \left\lceil \log_\beta \left( \frac{3\delta}{M+\gamma} \right) \right\rceil, \left\lceil \log_\beta \left( \frac{3\delta\nu}{M+\gamma} \right) \right\rceil \right\} = \left\lceil \log_\beta \left( \frac{3\delta\nu}{M+\gamma} \right) \right\rceil.$$

**Remark 1.** An interesting implication of [Corollary 3.1](#) is that the amount of value decrease of the objective function is almost unaffected by the choice of  $\nu$ , the truncation parameter. The choice of  $\nu$  only affects the number of iterations for backtracking line search, which is  $O(\log_\beta(\delta\nu))$ . Nevertheless, it is not suggested to choose small  $\nu$ , which will increase the complexity of line search as  $\beta < 1$ .

### 3.2 Analysis for the small value of $\|d_k\|$

In this subsection, we consider the case where  $\|d_k\|$  is small, i.e.,  $\|d_k\| \leq \Delta$ , or equivalently  $|t_k| > \sqrt{1/1 + \Delta^2}$ . We show that if  $\|d_k\| \leq \Delta$ , then the next iterate  $x_{k+1} = x_k + d_k$  is already an  $\epsilon$ -approximate second-order stationary point. Therefore, we can terminate the algorithm after one iteration in the small value case. To prove the result, we provide an upper bound of  $\|g_k\|$  for preparation.

**Lemma 3.6.** Suppose that [Assumption 3.1](#) holds. If  $g_k \neq 0$ , and  $\|d_k\| \leq \Delta \leq \sqrt{2}/2$ , then we have

$$\|g_k\| \leq 2(U_H + \delta)\Delta. \quad (3.17)$$

*Proof.* By [Lemma 2.1](#), we have  $\theta_k - \delta > 0$ . Moreover, with equation (2.10) in [Corollary 2.1](#), we can give an upper bound of  $\theta_k - \delta$ , that is,

$$\theta_k - \delta = -g_k^T d_k \leq \|g_k\| \|d_k\| \leq \Delta \|g_k\|. \quad (3.18)$$

Denote  $h(t) = t^2 + (g_k^T H_k g_k / \|g_k\|^2 + \delta) t - \|g_k\|^2$ . It is easy to see that the equation  $h(t) = 0$  must have two real roots with opposite signs. Let its positive root be  $t_2$ . By  $\theta_k - \delta > 0$ , we have  $\theta_k - \delta \geq t_2$ . Therefore, we must have

$$h(\Delta \|g_k\|) = \Delta^2 \|g_k\|^2 + \left( \frac{g_k^T H_k g_k}{\|g_k\|^2} + \delta \right) \Delta \|g_k\| - \|g_k\|^2 \geq 0.$$

After some algebra, we obtain

$$\begin{aligned} \|g_k\| &\leq \frac{(g_k^T H_k g_k / \|g_k\|^2 + \delta) \Delta}{1 - \Delta^2} \\ &\leq \frac{(U_H + \delta) \Delta}{1 - \Delta^2} \\ &\leq 2(U_H + \delta) \Delta. \end{aligned} \quad (3.19)$$

The second inequality holds due to  $H_k \preceq U_H I$ , which implies  $g_k^T H_k g_k / \|g_k\|^2 \leq U_H$ . The last inequality follows from  $\Delta \leq \sqrt{2}/2$ .

□

When  $\|d_k\| \leq \Delta$ , we let the stepsize  $\eta_k = 1$  and proceed the iteration by  $x_{k+1} = x_k + d_k$ . The following lemma shows that the norm of the gradient at  $x_{k+1}$  can be upper bounded, while the smallest eigenvalue of the Hessian at  $x_{k+1}$  has a lower bound.

**Lemma 3.7.** *Suppose that [Assumption 3.1](#) holds. If  $g_k \neq 0$ , and  $\|d_k\| \leq \Delta$ , then let  $\eta_k = 1$ , we have*

$$\|g_{k+1}\| \leq 2(U_H + \delta)\Delta^3 + \frac{M}{2}\Delta^2 + \delta\Delta, \quad (3.20)$$

$$H_{k+1} \succeq -(2(U_H + \delta)\Delta^2 + M\Delta + \delta)I. \quad (3.21)$$

*Proof.* We first prove (3.20). By the optimality condition (2.10) in [Corollary 2.1](#), we have

$$H_k d_k + g_k = -\theta_k d_k,$$

and with (3.18), we have

$$\theta_k \|d_k\| \leq (\delta + \Delta \|g_k\|) \|d_k\|.$$

Thus, it holds that

$$\|H_k d_k + g_k\| = \theta_k \|d_k\| \leq \delta\Delta + \|g_k\|\Delta^2. \quad (3.22)$$

Now we bound the norm of  $\|g_{k+1}\|$  and obtain,

$$\begin{aligned} \|g_{k+1}\| &\leq \|g_{k+1} - H_k d_k - g_k\| + \|H_k d_k + g_k\| \\ &\leq \frac{M}{2} \|d_k\|^2 + \delta\Delta + \|g_k\|\Delta^2 \end{aligned} \quad (3.23a)$$

$$\leq \frac{M}{2} \Delta^2 + \delta\Delta + 2(U_H + \delta)\Delta \cdot \Delta^2 \quad (3.23b)$$

$$= 2(U_H + \delta)\Delta^3 + \frac{M}{2}\Delta^2 + \delta\Delta,$$

where (3.23a) holds due to the  $M$ -Lipschitz continuity of  $\nabla^2 f(x)$  as well as equation (3.22), and (3.23b) follows from [Lemma 3.6](#).

Second, we prove (3.21). Note that the optimality condition (2.5) in [Lemma 2.2](#) implies that

$$H_k + \theta_k \cdot I \succeq 0.$$

With (3.18) and (3.19), we further obtain

$$\begin{aligned} H_k &\succeq -\theta_k I \succeq -(\Delta \|g_k\| + \delta)I \\ &\succeq -2(U_H + \delta)\Delta^2 I - \delta I. \end{aligned} \quad (3.24)$$

We now turn to bound  $H_{k+1}$  and have that

$$\begin{aligned}
H_{k+1} &\succeq H_k - \|H_{k+1} - H_k\|I \\
&\succeq H_k - M\|d_k\|I \\
&\succeq H_k - M\Delta I,
\end{aligned} \tag{3.25}$$

where the second inequality holds by the  $M$ -Lipschitz continuity of  $\nabla^2 f(x)$ , and the last inequality follows from  $\|d_k\| \leq \Delta$ . Combining with (3.24), we arrive at

$$H_{k+1} \succeq -2(U_H + \delta)\Delta^2 I - \delta I - M\Delta I. \tag{3.26}$$

The proof is then completed. □

### 3.3 The global convergence result

Putting the above pieces together, we present the formal convergence theorems of HSODM in both the fixed-radius and line search strategies in [Theorem 3.1](#) and [Theorem 3.2](#), respectively. It shows that our method achieves  $O(\epsilon^{-3/2})$  iteration complexity to find an  $\epsilon$ -approximate second-order stationary point by properly choosing the perturbation parameter  $\delta$  and the radius  $\Delta$ .

**Theorem 3.1.** *Suppose that [Assumption 3.1](#) holds. Let  $\delta = \sqrt{\epsilon}$ ,  $\Delta = 2\sqrt{\epsilon}/M$  and  $\nu \in (0, 1/2)$ , then the homogeneous second-order descent method (HSODM) with the fixed-radius strategy terminates in at most  $O(\epsilon^{-3/2})$  steps, and the next iterate  $x_{k+1}$  is a second-order stationary point.*

*Proof.* Since we take  $\delta = \sqrt{\epsilon}$  and  $\Delta = 2\sqrt{\epsilon}/M$ , by [Lemma 3.2](#) and [Lemma 3.3](#), we immediately obtain that the function value decreases at least  $\Omega(\epsilon^{3/2})$  for the large step case, i.e.,

$$f(x_{k+1}) - f(x_k) \leq -\frac{2}{3M^2}\epsilon^{3/2}.$$

When the algorithm terminates, by [Lemma 3.7](#), we have

$$\|g_{k+1}\| \leq O(\epsilon) \quad \text{and} \quad \lambda_{\min}(H_{k+1}) \geq \Omega(-\sqrt{\epsilon}). \tag{3.27}$$

Therefore, the next iterate  $x_{k+1}$  is already a second-order stationary point.

Note that the total decreasing amount of the objective function value cannot exceed  $f(x_1) - f_{\inf}$ . Hence, the number of iterations for large step cases is upper bounded by

$$O\left(\frac{3M^2}{2}(f(x_1) - f_{\inf})\epsilon^{-3/2}\right),$$

which is also the iteration complexity of our algorithm. □

**Theorem 3.2.** *Suppose that [Assumption 3.1](#) holds. Let  $\delta = \sqrt{\epsilon}$ ,  $\Delta = 2\sqrt{\epsilon}/M$  and  $\nu \in (0, 1/2)$ , and the backtracking line search parameters  $\beta, \gamma$  satisfy  $\beta \in (0, 1)$  and  $\gamma > 0$ . Then the homogeneous second-order descent method (HSODM) with the backtracking line search terminates in at most  $O(\epsilon^{-3/2} \log_\beta(\epsilon))$  steps, and the next iterate  $x_{k+1}$  is a second-order stationary point. Specifically, the number of iterations is bounded by,*

$$O\left(\max\left\{\frac{2(M+\gamma)}{9\gamma\beta^3}, \frac{3M^3}{4\gamma}, \frac{2(M+\gamma)^3}{9\gamma\beta^3}\right\}\left\lceil\log_\beta\left(\frac{3\sqrt{\epsilon}\nu}{M+\gamma}\right)\right\rceil(f(x_1) - f_{\inf})\epsilon^{-3/2}\right).$$

*Proof.* Since we take  $\delta = \sqrt{\epsilon}$  and  $\Delta = 2\sqrt{\epsilon}/M$ , by [Corollary 3.1](#), we immediately obtain that the function value decreases at least  $\Omega(\epsilon^{3/2})$  for the large step case, i.e.,

$$\begin{aligned} f(x_{k+1}) - f(x_k) &\leq -\min\left\{\frac{\sqrt{3}\gamma}{16}, \frac{9\gamma\beta^3\delta^3}{2(M+\gamma)}, \frac{\gamma\Delta^3}{6}, \frac{9\gamma\beta^3\delta^3}{2(M+\gamma)^3}\right\} \\ &\leq -\min\left\{\frac{9\gamma\beta^3}{2(M+\gamma)}, \frac{4\gamma}{3M^3}, \frac{9\gamma\beta^3}{2(M+\gamma)^3}\right\}\epsilon^{3/2}, \end{aligned}$$

and the inner iteration for backtracking line search is at most

$$j_N \leq \left\lceil\log_\beta\left(\frac{3\delta\nu}{M+\gamma}\right)\right\rceil = \left\lceil\log_\beta\left(\frac{3\sqrt{\epsilon}\nu}{M+\gamma}\right)\right\rceil.$$

When the algorithm terminates, by [Lemma 3.7](#), we have

$$\|g_{k+1}\| \leq O(\epsilon) \quad \text{and} \quad \lambda_{\min}(H_{k+1}) \geq \Omega(-\sqrt{\epsilon}).$$

Therefore, the next iterate  $x_{k+1}$  is already a second-order stationary point.

Note that the total decreasing amount of the objective function value cannot exceed  $f(x_1) - f_{\inf}$ . Hence, the number of iterations for large step case is upper bounded by

$$O\left(\max\left\{\frac{2(M+\gamma)}{9\gamma\beta^3}, \frac{3M^3}{4\gamma}, \frac{2(M+\gamma)^3}{9\gamma\beta^3}\right\}\left\lceil\log_\beta\left(\frac{3\sqrt{\epsilon}\nu}{M+\gamma}\right)\right\rceil(f(x_1) - f_{\inf})\epsilon^{-3/2}\right),$$

which is also the iteration complexity of our algorithm. Since  $\beta < 1$ , this completes the proof.  $\square$

Since  $\delta = \sqrt{\epsilon}$ , we see that the line-search version has an extra overhead of  $O(\log_\beta \epsilon)$  compared to the fixed-radius strategy. In practice, the line-search version can choose steps that are much larger than  $\Delta$  and hence has a fast rate of convergence. This benefit can be observed in the [Section 6](#).

## 4 Local Convergence Rate

In this section, we provide the local convergence analysis of HSODM. In particular, when  $x_k$  is sufficiently close to a second-order stationary point  $x^*$ , we shall show that the stepsize  $\eta_k$  always

equals to 1 and the line search procedure is not required. Consequently, HSODM achieves a local quadratic convergence rate by setting the perturbation parameter  $\delta = 0$  for the subsequent iterations.

We first make the standard assumption [9, 38, 36] to facilitate the local convergence analysis.

**Assumption 4.1.** *Assume that HSODM converges to a strict local optimum  $x^*$  satisfying that  $\nabla f(x^*) = 0$  and  $\nabla^2 f(x^*) \succ 0$ .*

**Remark 2.** *From the above Assumption 4.1, we immediately know that there exists a small neighborhood such that for all  $x \in B(x^*, R)$ ,  $\nabla^2 f(x) \succeq \mu \cdot I$  for some  $\mu > 0$ . In other words,  $x_k$  arrives at the neighborhood of  $x^*$  for sufficiently large  $k$ , hence both  $H_k$  and  $H_k + \theta_k I$  are nonsingular.*

To prove the local convergence rate, we prove the following auxiliary results for preparation.

**Corollary 4.1.** *Suppose that Assumption 4.1 holds, then  $t_k \neq 0$  for sufficiently large  $k$ .*

*Proof.* We prove by contradiction. Suppose that  $t_k = 0$ . Then by Corollary 2.1,  $(-\theta_k, v_k)$  is the eigenpair of  $H_k$ , implying that,

$$\lambda_{\min}(H_k) \leq -\theta_k.$$

Recall that in Lemma 2.2, we have  $\theta_k > 0$ , hence  $\lambda_{\min}(H_k) < 0$ . This makes a contradiction to  $H_k \succ 0$ . Then the proof is completed.  $\square$

The following lemma demonstrates that the step  $d_k$  generated by the HSODM eventually reduces to the small valued case for sufficiently large  $k$ . Consequently, we choose  $\eta_k = 1$  and update the iteration by  $x_{k+1} = x_k + d_k$  as shown in Section 3.2. We remark that it is similar to the case of the classical Newton trust-region method (see [38, Theorem 4.9]), where the updates become asymptotically similar to the pure Newton step.

**Lemma 4.1.** *For sufficiently large  $k$ , we have  $\|d_k\| \leq \Delta$ .*

*Proof.* Due to  $t_k \neq 0$ , by equation (2.10) in Corollary 2.1, we have

$$d_k = -(H_k + \theta_k I)^{-1} g_k,$$

and further

$$\begin{aligned} \|d_k\| &\leq \|(H_k + \theta_k I)^{-1}\| \|g_k\| \\ &\leq \frac{\|g_k\|}{\mu + \theta_k} \leq \frac{\|g_k\|}{\mu}. \end{aligned} \tag{4.1}$$

The above inequalities hold because of  $H_k \geq \mu I$  and  $\theta_k > 0$ . Note that with Assumption 4.1,  $\|g_k\| \rightarrow 0$  as  $k \rightarrow \infty$ , then there exist a sufficiently large  $K \geq 0$ , such that

$$\|g_k\| \leq \Delta \mu, \forall k \geq K. \tag{4.2}$$

Combining (4.1), we conclude that  $\|d_k\| \leq \Delta$  will be satisfied.

□

In the local phase, we set the perturbation parameter  $\delta = 0$ , and solve

$$\min_{\| [v; t] \| \leq 1} \psi_k(v, t; 0) := \begin{bmatrix} v \\ t \end{bmatrix}^T \begin{bmatrix} H_k & g_k \\ g_k^T & 0 \end{bmatrix} \begin{bmatrix} v \\ t \end{bmatrix}. \quad (4.3)$$

We also denote by  $[v_k; t_k]$  the optimal solution to (4.3). Gathering the above results together, we are ready to prove the following theorem.

**Theorem 4.1.** *Suppose that Assumption 3.1 and Assumption 4.1 hold. For sufficiently large  $k$ , the HSODM converges to  $x^*$  quadratically, that is,*

$$\|x_{k+1} - x^*\| \leq O\left(\left(\frac{M}{\mu} + \frac{\Delta M^2}{\mu^2(1-\Delta^2)^2}\right) \|x_k - x^*\|^2\right).$$

*Proof.* By Corollary 4.1, we have  $t_k \neq 0$ . Since we take  $\delta = 0$ , then with equation (2.10) in Corollary 2.1, we have

$$g_k^T d_k = -\theta_k \quad \text{and} \quad (H_k + \theta_k I)d_k = -g_k,$$

implying that

$$\begin{aligned} \|H_k^{-1}g_k + d_k\| &= \|-\theta_k H_k^{-1}d_k\| \\ &\leq \|H_k^{-1}\| \cdot |\theta_k| \|d_k\| \\ &\leq \frac{1}{\mu} \|g_k\| \|d_k\|^2. \end{aligned} \quad (4.4)$$

By Lemma 4.1, we have  $x_{k+1} = x_k + d_k$ . Therefore,

$$\begin{aligned} \|x_{k+1} - x^*\| &= \|x_k + d_k + H_k^{-1}g_k - H_k^{-1}g_k - x^*\| \\ &\leq \|x_k - H_k^{-1}g_k - x^*\| + \|H_k^{-1}g_k + d_k\| \\ &\leq \frac{M}{\mu} \|x_k - x^*\|^2 + \frac{1}{\mu} \|g_k\| \|d_k\|^2 \end{aligned} \quad (4.5a)$$

$$\leq \frac{M}{\mu} \|x_k - x^*\|^2 + \Delta \|d_k\|^2, \quad (4.5b)$$

where (4.5a) holds due to the standard analysis of Newton's method [38] and equation (4.4), and

(4.5b) follows from  $\|g_k\| \leq \Delta\mu$  as stated in [Lemma 4.1](#). Moreover, we have

$$\begin{aligned}
\|d_k\| &= \|x_{k+1} - x^* - (x_k - x^*)\| \\
&\leq \|x_{k+1} - x^*\| + \|x_k - x^*\| \\
&\leq \frac{M}{\mu} \|x_k - x^*\|^2 + \|x_k - x^*\| + \Delta \|d_k\|^2 \\
&\leq \frac{M}{\mu} \|x_k - x^*\|^2 + \|x_k - x^*\| + \Delta^2 \|d_k\|.
\end{aligned} \tag{4.6}$$

Rearranging the terms, we have

$$\|d_k\| \leq O\left(\frac{M}{\mu(1-\Delta^2)} \|x_k - x^*\|\right). \tag{4.7}$$

With (4.5b), we conclude that

$$\|x_{k+1} - x^*\| \leq \frac{M}{\mu} \|x_k - x^*\|^2 + \Delta \|d_k\|^2 = O\left(\left(\frac{M}{\mu} + \frac{\Delta M^2}{\mu^2(1-\Delta^2)^2}\right) \|x_k - x^*\|^2\right). \tag{4.8}$$

□

## 5 An Inexact HSODM

In the above discussion, all the analysis relies on *exact* eigenvalue solution ([Lemma 2.2](#)) of the subproblem (2.4). This provides the performance estimate using matrix factorizations that take  $O((n+1)^3)$  arithmetic operations per iteration. In this section, we propose an inexact HSODM ([Algorithm 3](#)) utilizing a Lanczos method ([Algorithm 4](#)) to solve (2.4). In other words, we construct the iterates from the Ritz pair [20] instead of the exact leftmost eigenpair of  $F_k$ . This results in a probabilistic worst-case complexity of  $\tilde{O}(\epsilon^{-7/4}(n+1)^2)$  arithmetic operations, which has less dependency on  $n$ .

### 5.1 The Lanczos method: a quick review

Since the inexact algorithm uses the Ritz approximation, for the convenience of the readers, we provide a quick review of the Lanczos method and its connection to solving homogeneous subproblems (2.4). Given any symmetric matrix  $A \in \mathbb{R}^{n \times n}$  and an initial unit vector  $q_1$ , recall that the Lanczos method constructs a basis  $\{q_1, \dots, q_j\}$  for the  $j$ -th order Krylov subspace  $\mathcal{K}(j; A, q_1) = \text{span}\{q_1, Aq_1, \dots, A^j q_1\}$  at the  $j$ -th iteration. Denoting  $Q_j = [q_1, \dots, q_j] \in \mathbb{R}^{n \times j}$ , the following result is standard.

**Lemma 5.1** (Basic property of the Lanczos method [20]). *For any symmetric matrix  $A \in \mathbb{R}^{n \times n}$ , suppose the Lanczos method runs until  $J = \text{rank}(\mathcal{K}(n; A, q_1))$ .*



(1) There is an tridiagonal matrix  $T_j$  and an orthonormal basis  $Q_j$ , such that for any  $j = 1, \dots, J$ ,

$$AQ_j = Q_j T_j + \xi_j e_j^T, \quad Q_j^T A Q_j = T_j, \quad Q_j \perp \xi_j,$$

where  $e_j$  represents  $j$ -th unit vector, and  $\xi_j$  is the residual vector.

(2) Suppose  $Y_j = Q_j S_j$  are computed by the  $j$ -th Krylov iteration of the Lanczos method and the real Schur decomposition  $S_j^T T_j S_j = \Gamma_j$ . Let  $\gamma_i$  be the  $i$ -th entry on the diagonal of  $\Gamma_j$ ,  $y_i$  be the  $i$ -th column vector of  $Y_j$ , then we have the following error estimation,

$$Ay_i - \gamma_i y_i = \xi_j (e_j^T S_j e_i) := s_{ji} \xi_j, |s_{ji}| < 1, \forall i \leq j;$$

furthermore,  $y_i \perp \xi_j$ . We call  $(\gamma_i, y_i)$  the  $i$ -th Ritz pair.

When translating the above result into an inexact version of the optimality condition ([Lemma 2.2](#)), we denote the dual variable as  $\gamma_k$  corresponding to the Ritz value. With a slight abuse of notations, at  $k$ -th iterate  $x_k$ , we override  $[v_k; t_k]$  as the approximate solution, while keeping the reference of  $\theta_k = -\lambda_1(F_k)$  to the ‘‘exact’’ eigenvalue, and denoting its eigenvector as  $\chi_k$ . We have the following theorem.

**Theorem 5.1** (Inexact optimality condition by the Lanczos method). *Suppose that the Lanczos method is used to approximately solve (2.4) and returns a Ritz pair  $(-\gamma_k, [v_k; t_k])$ . We have*

$$\begin{aligned} \begin{bmatrix} H_k & g_k \\ g_k^T & -\delta \end{bmatrix} \begin{bmatrix} v_k \\ t_k \end{bmatrix} + \gamma_k \begin{bmatrix} v_k \\ t_k \end{bmatrix} &= \begin{bmatrix} r_k \\ \sigma_k \end{bmatrix} \\ r_k^T v_k + \sigma_k \cdot t_k &= 0 \end{aligned} \quad (5.1)$$

where  $[r_k; \sigma_k] \in \mathbb{R}^n \times \mathbb{R}$  is the Ritz residual.

The second equation follows part (2) of [Lemma 5.1](#). Generally, when adopting the Ritz approximation, we consider some error estimates  $e_k > 0$  such that  $|\theta_k - \gamma_k| \leq e_k$ . In the Lanczos method, the Ritz value is always an underestimate, i.e.,  $\gamma_k \leq \theta_k$  (see, e.g., [\[20\]](#)), so that it is equivalent to state  $\theta_k - e_k \leq \gamma_k \leq \theta_k$ . The following complexity estimates can be provided regarding a prescribed error  $e_k$ .

**Lemma 5.2** (Complexity estimate of Lanczos method). *Suppose that the Lanczos method is used to approximately solve (2.4), and returns a Ritz pair  $(-\gamma_k, [v_k; t_k])$  satisfying  $\theta_k - e_k \leq \gamma_k \leq \theta_k$  for some  $e_k > 0$ . Then, the the number of required iterations can be upper bounded by either of the following quantities.*

(1)

$$1 + \left\lceil 2 \sqrt{\frac{\|F_k\|}{e_k}} \log \left( \frac{16 \|F_k\|}{e_k (q_1^T \chi_k)^2} \right) \right\rceil, \quad (5.2)$$

where  $(\theta_k, \chi_k)$  is the true leftmost eigenvector of  $F_k$  [\[30, 42\]](#);

(2)

$$1 + \left[ \sqrt{\frac{2\|F_k\|}{\lambda_2(F_k) - \lambda_{\min}(F_k)}} \log \left( \frac{8\|F_k\|}{e_k(q_1^T \chi_k)^2} \right) \right], \quad (5.3)$$

where  $\lambda_2(F_k)$  is the second-smallest eigenvalue such that  $\lambda_2(F_k) - \lambda_{\min}(F_k) > 0$  (e.g. [30]).

Finally, we connect the Ritz error to the desired accuracy  $e_k$ . We defer the proofs of [Lemma 5.2](#) and [Lemma 5.3](#) to the Appendix as the results are mostly related to linear algebra.

**Lemma 5.3.** *Suppose that  $F_k$  is constructed as in (2.3), then*

$$\|F_k\| \leq \max\{U_H, \delta\} + \|g_k\|. \quad (5.4)$$

If we let  $\sigma_F := \lambda_2(F_k) - \lambda_{\min}(F_k) > 0$ , then for the  $[r_k; \sigma_k]$  in (5.1), there exists  $\tau \in [0, 1]$  such that

$$\|[r_k; \sigma_k]\| \leq \tau e_k + 2(\max\{U_H, \delta\} + \|g_k\|) \sqrt{\frac{e_k}{\sigma_F}}. \quad (5.5)$$

## 5.2 Overview of the inexact HSODM

We are now ready to introduce the inexact HSODM that utilizes the Krylov iterations to solve the subproblem inexactly. As the following lemma shows ([Lemma 5.5](#) and [Lemma 5.4](#)), the Ritz error  $[r_k; \sigma_k]$  of  $F_k$  (5.1) propagates a few difficulties in convergence analysis. First of all, since  $\gamma_k$  is an inexact dual variable, we cannot guarantee that  $\gamma_k$  exceeds  $\delta$ , which may result in an insufficient “curvature”. Secondly, the existence of Ritz error  $r_k$  prevents the convergence to the first-order stationary point when terminating the algorithm. To address these issues, we first propose a Lanczos method with skewed randomization ([Line 3, Algorithm 4](#)), so that the Ritz value  $\gamma_k$  always achieves a minimal magnitude  $\delta$  with  $\tilde{O}(\epsilon^{-1/4})$  iteration complexity in high probability. For the latter difficulty that appears in the small value case, we adopt a delicate analysis of the spectrum and show that the eigengap is sufficiently large (e.g., in  $\Omega(\sqrt{\epsilon})$ ) therein. This implies that it is possible to pursue a higher precision ([Line 5](#)) indicated by the gap-dependent complexity (5.3).

---

**Algorithm 3:** Inexact Homogeneous Second-Order Descent Method
 

---

**Data:** initial point  $x_1$ ,  $\nu \in (1/4, 1/2)$ ,  $\Delta = \sqrt{\epsilon}/M$ ,  $\epsilon > 0$

```

1 for  $k = 1, 2, \dots$  do
2   Set  $\delta = \sqrt{\epsilon}$ ,  $e_k = \sqrt{\epsilon}$ ,  $J_{\min} = 0$ ;
3   Run Algorithm 4 with  $(e_k, \delta, J_m)$ , and obtain the solution  $[v_k; t_k]$  and error  $[r_k; \sigma_k]$ ;
4   if  $|t_k| > \sqrt{1/1 + \Delta^2}$  then // small value case
5     if  $\|r_k\| > \epsilon$  then
6       Set  $\delta \leftarrow 3\sqrt{\epsilon} + 2\|g_k\|\Delta + (U_H + \gamma_k)\Delta^2$ ,  $e_k = \epsilon^3$ ,  $J_{\min} = n + 1$ ;
7       Go to Line 3
8     else
9       Update  $x_{k+1} = x_k + d_k$ ;
10      (Early) Terminate (or set  $\delta = 0$  and proceed);
11    end
12    if  $|t_k| \geq \nu$  then // large value case (a)
13       $d_k := v_k/t_k$ 
14    else // large value case (b)
15       $d_k := \text{sign}(-g_k^T v_k) \cdot v_k$ 
16    end
17    Choose a stepsize  $\eta_k$  by fixed-radius strategy ;
18 end
  
```

---

As the large value cases (a) and (b) (**Line 12** and **Line 14**) follow a similar manner to the exact HSODM. A preliminary analysis below explicitly shows how the inexactness impacts our algorithm.

**Lemma 5.4.** *Suppose that **Assumption 3.1** holds and set  $\nu \in (1/4, 1/2)$ . If  $|t_k| \geq \nu$  and  $\|v_k/t_k\| \geq \Delta$ , then let  $d_k := v_k/t_k$  and  $\eta_k = \Delta/\|d_k\|$ , we have*

$$f(x_{k+1}) - f(x_k) \leq \left( \eta_k - \frac{1}{2}\eta_k^2 \right) (\delta - \gamma_k) + 4|\sigma_k| - \frac{\gamma_k}{2}\Delta^2 + \frac{M}{6}\Delta^3.$$

*Proof.* Combining the inexact optimal condition (5.1) and  $d_k = v_k/t_k$  gives

$$\begin{aligned} d_k^T H_k d_k + g_k^T d_k &= -\gamma_k \|d_k\|^2 + \frac{r_k^T v_k}{(t_k)^2}, \\ g_k^T d_k &= -\gamma_k + \delta + \frac{\sigma_k}{t_k}. \end{aligned}$$

Therefore, we have

$$\begin{aligned}
f(x_{k+1}) - f(x_k) &= f(x_k + \eta_k \cdot d_k) - f(x_k) \\
&\leq \eta_k \cdot g_k^T d_k + \frac{\eta_k^2}{2} \cdot d_k^T H_k d_k + \frac{M\eta_k^3}{6} \cdot \|d_k\|^3 \\
&= \eta_k \cdot g_k^T d_k + \frac{1}{2}\eta_k^2 \left( \frac{r_k^T v_k}{(t_k)^2} - g_k^T d_k - \gamma_k \|d_k\|^2 \right) + \frac{M\eta_k^3}{6} \cdot \|d_k\|^3 \\
&= \left( \eta_k - \frac{1}{2}\eta_k^2 \right) \left( \frac{\sigma_k}{t_k} + \delta - \gamma_k \right) + \frac{\eta_k^2}{2} \left( \frac{r_k^T v_k}{(t_k)^2} \right) - \frac{1}{2}\gamma_k \|\eta_k d_k\|^2 + \frac{1}{6}M \|\eta_k d_k\|^3 \\
&= \left( \eta_k - \frac{1}{2}\eta_k^2 \right) (\delta - \gamma_k) + (\eta_k^2 - \eta_k) \frac{r_k^T v_k}{(t_k)^2} - \frac{\gamma_k}{2} \Delta^2 + \frac{M}{6} \Delta^3 \\
&= \left( \eta_k - \frac{1}{2}\eta_k^2 \right) (\delta - \gamma_k) - (\eta_k^2 - \eta_k) \frac{\sigma_k}{t_k} - \frac{\gamma_k}{2} \Delta^2 + \frac{M}{6} \Delta^3.
\end{aligned}$$

Note that  $\eta_k \in (0, 1)$ ,  $|t_k| \geq \nu$  and  $\nu \geq 1/4$ , and thus it holds that

$$- (\eta_k^2 - \eta_k) \frac{\sigma_k}{t_k} \leq \left| \frac{\sigma_k}{\nu} \right| \leq 4|\sigma_k|.$$

Finally, we conclude

$$f(x_{k+1}) - f(x_k) \leq \left( \eta_k - \frac{1}{2}\eta_k^2 \right) (\delta - \gamma_k) + 4|\sigma_k| - \frac{\gamma_k}{2} \Delta^2 + \frac{M}{6} \Delta^3.$$

□

**Lemma 5.5.** *Suppose that [Assumption 3.1](#) holds and set  $\nu \in (1/4, 1/2)$ . If  $|t_k| \leq \nu$ , then let  $d_k := \text{sign}(-g_k^T v_k) \cdot v_k$  and  $\eta_k = \Delta/\|d_k\|$ , we have*

$$f(x_{k+1}) - f(x_k) \leq |\sigma_k| - \frac{\gamma_k}{2} \Delta^2 + \frac{M}{6} \Delta^3.$$

*Proof.* From the inexact optimal condition [\(5.1\)](#), we obtain

$$\begin{aligned}
(v_k)^T H_k v_k &= r_k^T v_k - \gamma_k \|v_k\|^2 - t_k g_k^T v_k, \\
g_k^T v_k &= \sigma_k + t_k \cdot (\delta - \gamma_k).
\end{aligned}$$

Consequently, it follows that

$$\begin{aligned}
f(x_{k+1}) - f(x_k) &= f(x_k + \eta_k \cdot d_k) - f(x_k) \\
&\leq \eta_k \cdot g_k^T d_k + \frac{\eta_k^2}{2} \cdot d_k^T H_k d_k + \frac{M\eta_k^3}{6} \cdot \|d_k\|^3 \\
&= \eta_k \cdot \text{sign}(-g_k^T v_k) g_k^T v_k + \frac{1}{2} \eta_k^2 (v_k)^T H_k v_k + \frac{M}{6} \eta_k^3 \|v_k\|^3 \\
&= -\eta_k \cdot |g_k^T v_k| + \frac{1}{2} \eta_k^2 r_k^T v_k - \frac{1}{2} \eta_k^2 t_k g_k^T v_k - \frac{1}{2} \eta_k^2 \gamma_k \|v_k\|^2 + \frac{M}{6} \eta_k^3 \|v_k\|^3 \\
&\leq -\eta_k \cdot |g_k^T v_k| + \frac{1}{2} \eta_k^2 r_k^T v_k + \frac{1}{2} \eta_k^2 |t_k| |g_k^T v_k| - \frac{1}{2} \eta_k^2 \gamma_k \|v_k\|^2 + \frac{M}{6} \eta_k^3 \|v_k\|^3 \\
&= -\frac{1}{2} \eta_k^2 t_k \sigma_k - \left( \eta_k - \frac{1}{2} \eta_k^2 |t_k| \right) |g_k^T v_k| - \frac{\gamma_k}{2} \Delta^2 + \frac{M}{6} \Delta^3,
\end{aligned}$$

where the last equality holds due to  $r_k^T v_k + t_k \sigma_k = 0$  and  $\eta_k = \Delta / \|d_k\| = \Delta / \|v_k\|$ . Note that  $\eta_k < 1$  and  $|t_k| \leq \nu < 1$ , it implies that  $\eta_k^2 |t_k| \leq \eta_k < 1$ . Finally, we conclude

$$f(x_{k+1}) - f(x_k) \leq |\sigma_k| - \frac{\gamma_k}{2} \Delta^2 + \frac{M}{6} \Delta^3.$$

□

The aforementioned two lemmas illustrate how the additional Ritz residual  $[r_k; \sigma_k]$  and the inexact dual variable  $\gamma_k$  obstruct the descent properties. To safeguard convergence, the Lanczos method should provide sufficiently small  $[r_k; \sigma_k]$  and  $\gamma_k \geq \delta$ . However, the classical Lanczos method with random start [30] cannot fulfil the needs. This is the motivation for our adaptation of the algorithm described next.

### 5.3 A Lanczos method with skewed randomization

To bypass these hurdles, we develop a skewed initialization of the Lanczos method (Algorithm 4), allowing us to attain a convergence behavior akin to that of the exact HSODM.

---

**Algorithm 4:** A Lanczos Method with Skewed Randomization
 

---

**Data:** iterate  $x_k, g_k, H_k$ ;  $\delta > 0, p \in (\exp(-n), 1), e_k > 0, \Psi > \Omega\left(\frac{\sqrt{n}}{p^2 \epsilon^4}\right), J_{\min} \geq 0$

1 **Initialization:** take  $b_1, \dots, b_{n+1} \stackrel{i.i.d.}{\sim} \mathcal{N}(0, 1)$  and set  $b := [b_1, \dots, b_n, \Psi \cdot b_{n+1}]^T$ ,  
 $q_1 = b/\|b\|$ ;

2 **Construction:** Let  $F_k = \begin{bmatrix} H_k & g_k \\ g_k^T & -\delta \end{bmatrix}$ ;  $J_m = \max\left\{J_{\min}, 1 + \sqrt{\frac{2\|F_k\|}{e_k}} \log\left(\frac{8}{e_k(q_1^T \chi_k)^2}\right)\right\}$ ;

3 **while**  $j = 1, \dots, J_m$  **do**

4     Compute  $F_k Q_j = Q_j T_j + \xi_j 1_j$ ;

5     **if**  $\|\xi_j\| \leq \epsilon$  **or**  $j \geq n + 2$  **then**

6         | Break;

7      $j \leftarrow j + 1$ ;

8 **end**

9 Compute Schur decomposition  $S_j^T T_j S_j = \Gamma_j$ ;

10 Compute  $Y_j = Q_j S_j$ ;

11 **return**  $(\gamma_k, [v_k, t_k])$  and corresponding error  $[r_k; \sigma_k]$

---

The crux of our method ([Algorithm 4](#)) is the skewed randomization for the starting vector  $q_1$  ([Line 1](#)). The basic idea is to put more weights, say  $\alpha$ , on the last entry of  $q_1$  to obtain a baseline Ritz value  $\gamma_k$ . The following lemma tells that once  $|\alpha|$  is larger than some constant, the inequality  $\gamma_k \geq \delta$  can be guaranteed. Surprisingly, the magnitude of the last entry in the Ritz residual can also be bounded through  $|\alpha|$ .

**Theorem 5.2.** *Given a unit vector  $q_1 = \sqrt{1 - \alpha^2} \cdot [u; 0] + \alpha \cdot [0; 1] \in \mathbb{R}^{n+1}$  with  $u \in \mathbb{R}^n$  and  $\|u\| = 1$ , then we have the following results.*

(1) *For the  $j$ -th Krylov iterations with  $j \geq 2$ , the last entry in each of the later Lanczos vectors  $q_j = [v_j, \beta_j]$  is bounded as:*

$$|\beta_j| = |q_j^T e_{n+1}| \leq 2\sqrt{1 - \alpha^2}.$$

(2) *The last entry of Ritz error  $\sigma_k$  in (5.1) is bounded as:*

$$|\sigma_k| \leq O(\sqrt{1 - \alpha^2})$$

*once the Krylov iteration number  $j$  is larger than 3.*

(3) *If further assume that*

$$\alpha \cdot g_k^T u \leq 0 \quad \text{and} \quad |\alpha| \geq \frac{U_H + \delta}{\sqrt{(U_H + \delta)^2 + 4(g_k^T u)^2}}, \quad (5.8)$$

*then the approximated dual variable  $\gamma_k$  is sufficiently large, i.e.,  $\gamma_k \geq \delta$ .*

Now we show [Algorithm 4](#) fits the purpose.

**Theorem 5.3.** *Consider the skewed initialization ([Line 1](#)) in [Algorithm 4](#), then for any  $p \in (\exp(-n), 1)$  and  $\epsilon > 0$ , with a probability at least  $1 - p$ , it holds that*

$$\alpha^2 \geq \Omega(1 - \epsilon^4), \quad |\sigma_k| \leq O(\epsilon^2) \quad \text{and} \quad q_1^T \chi_k \geq \Omega\left(\frac{p^3 \epsilon^4}{n}\right).$$

We delay the proofs to [Appendix B](#) since the above two theorems are quite technical. Note that [Algorithm 4](#) may rely on a priori  $\|F_k\|$ .

**Remark 3.** *Technically, one can slightly refine [Algorithm 4](#) with the bound estimation [[43](#), [Algorithm 5](#)], in which case  $\|F_k\|$  can be estimated by some  $\hat{F}_k$  such that*

$$\|F_k\| \in [\hat{F}_k/2, \hat{F}_k]. \tag{5.9}$$

*in the first  $O(\log(n))$  iterations in high probability ([[43](#), [Lemma 10](#)]). Then the dependency on a priori  $\|F_k\|$  can be dropped (e.g., at [line 2](#)) at the cost of one trial run.*

## 5.4 Global convergence analysis of the inexact HSODM

In this subsection, we discuss the convergence of [Algorithm 3](#) that inherits the discussion in [Section 3](#). To start with, we show that a sufficient decrease can be achieved thanks to the skewed randomization of the Lanczos method.

**Corollary 5.1.** *Suppose that [Assumption 3.1](#) holds. If we run [Algorithm 4](#) and set the parameters*

$$e_k = \delta = \sqrt{\epsilon}, \quad \Delta = \Theta(\sqrt{\epsilon}).$$

*Then for any  $p \in (\exp(-n), 1)$ , it holds for the large value cases ([Line 12](#), [Line 14](#))*

$$f(x_{k+1}) - f(x_k) \leq -\frac{\delta}{4}\Delta^2 + \frac{M}{6}\Delta^3$$

*with probability at least  $1 - p$ .*

*Proof.* From [Theorem 5.2](#) and [Theorem 5.3](#), with a probability of at least  $1 - p$ , it holds that

$$|\sigma_k| \leq O(\epsilon^2) \quad \text{and} \quad \gamma_k \geq \delta.$$

Therefore, for the case in [Lemma 5.5](#), we have

$$\begin{aligned} f(x_{k+1}) - f(x_k) &\leq |\sigma_k| - \frac{\gamma_k}{2}\Delta^2 + \frac{M}{6}\Delta^3 \\ &\leq O(\epsilon^2) - \frac{\delta}{2}\Delta^2 + \frac{M}{6}\Delta^3 \\ &\leq -\frac{\delta}{4}\Delta^2 + \frac{M}{6}\Delta^3. \end{aligned}$$

The result of the case in [Lemma 5.4](#) can be established similarly. □

For the small value case, as before, it will only happen when  $|t_k| \geq \nu$  and  $d_k = v_k/t_k$ . Under this scenario, we show that the Hessian matrix at iterate  $x_k$  is nearly positive semidefinite. In this view, [Algorithm 3](#) tests whether the Ritz error  $r_k$  is sufficiently small. If not, it increases the perturbation parameter  $\delta$  and recalculates the Ritz pair by [Algorithm 4](#). In this case, we show that the eigengap of the homogeneous matrix now exceeds  $\Omega(\sqrt{\epsilon})$ . Those results are summarized in the following lemma.

**Lemma 5.6.** *Suppose that [Assumption 3.1](#) holds. If we run [Algorithm 4](#) and set the parameters*

$$e_k = \delta = \sqrt{\epsilon}, \quad \Delta = \Theta(\sqrt{\epsilon}),$$

then it holds that

$$\lambda_{\min}(H_k) \geq -2\delta - 2\|g_k\|\Delta - (U_H + \gamma_k)\Delta^2 = \Omega(-\sqrt{\epsilon}).$$

Furthermore, when resetting  $\delta := 3\sqrt{\epsilon} + 2\|g_k\|\Delta + (U_H + \gamma_k)\Delta^2$ , it holds for the resulting homogeneous matrix that

$$\lambda_2(F_k) - \lambda_{\min}(F_k) \geq \sqrt{\epsilon}.$$

*Proof.* From the inexact optimal condition [\(5.1\)](#), it holds that

$$-\gamma_k = -\delta(t_k)^2 + 2t_k g_k^T v_k + (v_k)^T H_k v_k.$$

Rearranging the terms gives

$$\begin{aligned} (\gamma_k - \delta)(t_k)^2 &= -2t_k g_k^T v_k - \left( \gamma_k + \frac{(v_k)^T H_k v_k}{\|v_k\|^2} \right) \|v_k\|^2 \\ &\leq 2t_k \sqrt{1 - (t_k)^2} \|g_k\| - \left( \gamma_k + \frac{(v_k)^T H_k v_k}{\|v_k\|^2} \right) \|v_k\|^2 \\ &\leq 2t_k \sqrt{1 - (t_k)^2} \|g_k\| - (\gamma_k + \lambda_{\min}(H_k)) (1 - (t_k)^2), \end{aligned}$$

and it further implies

$$\gamma_k - \delta \leq 2\Delta\|g_k\| + |\lambda_{\min}(H_k) + \gamma_k|\Delta^2 \leq 2\Delta\|g_k\| + (U_H + \gamma_k)\Delta^2.$$

Recall  $H_k + \theta_k I \succeq 0$  and  $\theta_k \leq \gamma_k + e_k = \gamma_k + \delta$ , we have

$$\lambda_{\min}(H_k) + 2\delta + 2\|g_k\|\Delta + (U_H + \gamma_k)\Delta^2 \geq 0.$$

Due to the choice of parameters  $\delta = \sqrt{\epsilon}$  and  $\Delta = \Theta(\sqrt{\epsilon})$ , it holds that  $\lambda_{\min}(H_k) \geq \Omega(-\sqrt{\epsilon})$ . For the second part, recall the homogeneous matrix has the form

$$F_k = \begin{bmatrix} H_k & g_k \\ g_k^T & -\delta \end{bmatrix}.$$



As we reset  $\delta := 3\sqrt{\epsilon} + 2\|g_k\|\Delta + (U_H + \gamma_k)\Delta^2 \geq \Omega(\sqrt{\epsilon})$ , the Cauchy interlace Theorem gives

$$\lambda_2(F_k) - \lambda_{\min}(F_k) \geq \lambda_{\min}(H_k) + \delta \geq \sqrt{\epsilon}.$$

□

It remains to show that if the increased perturbation is used (Line 5), it either yields a direction with the decrease in function value or achieves  $\epsilon$ -approximate SOSP in the subsequent iteration.

**Lemma 5.7.** *Suppose that Assumption 3.1 holds and we reset*

$$\delta = 3\sqrt{\epsilon} + 2\|g_k\|\Delta + (U_H + \gamma_k)\Delta^2, \quad e_k = \Theta(\epsilon^3), \quad \text{and} \quad \Delta = \Theta(\sqrt{\epsilon})$$

in Algorithm 3. For any  $p \in (\exp(-n), 1)$ , if  $|t_k| > \sqrt{1/1 + \Delta^2}$ , then the next iterate  $x_{k+1} = x_k + d_k$  is already an  $\epsilon$ -approximate SOSP. Otherwise, it holds that

$$f(x_{k+1}) - f(x_k) \leq -\frac{\delta}{4}\Delta^2 + \frac{M}{6}\Delta^3$$

with probability at least  $1 - p$ .

*Proof.* If Algorithm 4 with increased  $\delta$  outputs the  $[v_k, t_k]$  in the small step case, from Lemma 5.6, we know  $\lambda_1(H_k) \geq \Omega(-\sqrt{\epsilon})$ . Since  $\|d_k\| \leq \Delta$ , following the similar argument in Lemma 3.7 gives  $\lambda_1(H_{k+1}) \geq \Omega(-\sqrt{\epsilon})$ . Now we inspect the value of  $\|g_{k+1}\|$ , by second-order Lipschitz continuity, we have

$$\begin{aligned} \|g_{k+1}\| &\leq \|g_{k+1} - g_k - H_k d_k\| + \|g_k + H_k d_k\| \\ &\leq \frac{M}{2}\|d_k\|^2 + \|g_k + H_k d_k\| \\ &= \frac{M}{2}\|d_k\|^2 + \left\| \frac{r_k}{t_k} - \gamma_k d_k \right\| \\ &\leq \frac{M}{2}\Delta^2 + \nu\|r_k\| + |\gamma_k|\Delta. \end{aligned} \tag{5.10}$$

By Lemma 5.3 and  $\lambda_2(F_k) - \lambda_1(F_k) \geq \Omega(\sqrt{\epsilon})$ , We know  $\|r_k\| \leq O(e_k + \sqrt{e_k/\sqrt{\epsilon}}) \leq O(\epsilon^{5/4})$ ; moreover, it holds that

$$|\gamma_k| \leq |g_k^T d_k| + |\delta| + \left| \frac{\sigma_k}{t_k} \right| \leq O(\sqrt{\epsilon}).$$

Therefore, we conclude that  $\|g_{k+1}\| \leq O(\epsilon)$ . □

Finally, we are ready to analyze the complexity of the Lanczos method.

**Corollary 5.2** (Complexity of Algorithm 4). *When Algorithm 4 is invoked in Line 3 in the inexact HSODM, its number of iterations to complete one invoking is upper bounded by*

$$O\left(\sqrt{\|F_k\|}\epsilon^{-1/4}\log(n/(p\epsilon))\right).$$

*Proof.* We first note that only two cases can happen when invoking [Algorithm 4](#) in the inexact HSODM. In the first case, we set  $e_k = \sqrt{\epsilon}$ . By [\(5.2\)](#), the worst-case complexity is thus  $O\left(\sqrt{\|F_k\|}\epsilon^{-1/4}\log(n/(p\epsilon))\right)$ . When setting  $\delta$  to a larger value in [Line 5](#), by [Lemma 5.7](#), we know  $\lambda_2(F_k) - \lambda_{\min}(F_k) \geq \sqrt{\epsilon}$ . Using the gap-dependent estimate [\(5.3\)](#), the same complexity is preserved.  $\square$

In summary, we show that in any case the Lanczos method in [Algorithm 3](#) is guaranteed to terminate in  $\tilde{O}(\epsilon^{-1/4})$  iterations. However, contrasting with the complexity result presented in [\[42, 43\]](#), which depends on  $\|H_k\|$  and can be capped by  $U_H$ , our approach necessitates the magnitude of  $\|F_k\|$ . As per [Lemma 5.3](#),  $\|F_k\| \leq \max\{U_H, \delta\} + \|g_k\| = U_H + \|g_k\|$ , thus a further assumption is required to establish the overall complexity of the inexact HSODM.

**Assumption 5.1.** *Assume that the gradient at each iterate  $x_k$  is upper bounded by some  $U_g > 0$ , that is,*

$$\|\nabla f(x_k)\| \leq U_g, \quad \forall k \geq 1. \quad (5.11)$$

Such an assumption is widely adopted in the analysis of second-order algorithms such as [\[6, 42\]](#). Since the inexact HSODM is monotone, this assumption can be easily satisfied whenever the sublevel set  $\{x : f(x) \leq f(x_1)\}$  is compact. Consequently,  $\|F_k\|$  can be upper bounded by  $U_H + U_g$ , and the total complexity follows below.

**Theorem 5.4** (Complexity of the inexact HSODM). *Suppose that [Assumption 3.1](#) and [Assumption 5.1](#) hold. Then the inexact HSODM ([Algorithm 3](#)) terminates in*

$$K = 12(f(x_1) - f_{\inf})M^2\epsilon^{-3/2}$$

*iterations and returns an iterate  $x_{k+1}$  such that*

$$\|g_{k+1}\| \leq O(\epsilon) \quad \text{and} \quad \lambda_{\min}(H_{k+1}) \geq \Omega(-\sqrt{\epsilon}).$$

*with probability at least  $1 - Kp$ . Furthermore, the arithmetic operations required by [Algorithm 3](#) are bounded from above by*

$$O\left((n+1)^2\epsilon^{-7/4}(f(x_1) - f_{\inf})M^2\sqrt{U_H + U_g}\log(n/(p\epsilon))\right)$$

*Proof.* By selecting  $\delta = \sqrt{\epsilon}$  and  $\Delta = \frac{\sqrt{\epsilon}}{M}$  in [Algorithm 3](#), the function value decreases at least

$$f(x_{k+1}) - f(x_k) \leq -\frac{\delta}{4}\Delta^2 + \frac{M}{6}\Delta^3 = -\frac{\epsilon^{3/2}}{12M^2}.$$

Consequently, we obtain that the number of iterations is bounded above by  $K$  before reaching an  $\epsilon$ -approximate SOSp. For each iteration, since there is a probability  $p$  that the Lanczos method will

fail, we bound the probability of failure during the algorithm by  $Kp$ . Combining with [Corollary 5.2](#), the complexity of the arithmetic operations can be established.

□

Since our algorithm requires arithmetic operations on a “homogenized” matrix of dimension  $(n+1)$ , its dependency on dimension and the complexity associated with eigenvalue procedure ([Corollary 5.2](#)) are slightly worse compared to prior second-order algorithms, such as [\[42, 43, 15, 4, 2\]](#). Regarding the Lipschitz constants, the dependency on Hessian Lipschitz constant  $M$  in our bound is comparatively inferior than those in [\[2, 4\]](#), as our algorithm does not explicitly incorporate this constant; rather, it is only invoked in establishing the overall computational complexity. Nevertheless, our algorithm, HSODM, is characterized by its conciseness and unity, requiring only the eigenvalue procedure at each iteration. Specifically, it achieves computational efficiency superior to Newton-type methods when encountering degeneracy in the Hessian matrix [\[25\]](#). Furthermore, the subsequent section also demonstrates the promising practical performance of HSODM.

## 6 Numerical Results

In this section, we include the CUTEst problems [\[21\]](#) since they serve as a standard dataset to test the performance of algorithms for nonlinear problems. Because the HSODM belongs to the family of second-order methods, we focus on comparisons with Newton trust-region method, and adaptive cubic regularized Newton method [\[6\]](#). Our implementation in Julia programming language [\[3\]](#) is publicly accessible as a part of the package at <https://github.com/bzhangcw/DRSOM.jl>. All experiments are conducted in Julia, and the development is handled by a desktop of Mac OS with a 3.2 GHz 6-Core Intel Core i7 processor.

### 6.1 Implementation details

Apart from the original form of HSODM (see [Algorithm 1](#)), we add a few techniques for practical implementations. We first note that a practical HSODM may not explicitly use the Hessian matrix  $H_k$ . In the computation of  $F_k \cdot [v; t]$  where  $v \in \mathbb{R}^n, t \in \mathbb{R}$ , we have

$$F_k \cdot \begin{bmatrix} v \\ t \end{bmatrix} = \begin{bmatrix} H_k \cdot v + t \cdot g_k \\ g_k^T v - t \cdot \delta \end{bmatrix}.$$

From the above fact, a matrix-free option by utilizing the Hessian-vector product  $H_k v$  is provided as in other inexact Newton-type methods [\[6, 14\]](#).

Not limiting to the backtrack line-search algorithm for theoretical analysis, in practice, the homogeneous direction should work with any well-defined line-search method. In our implementation, we apply the Hager-Zhang line-search method with default parameter settings [\[24\]](#). For eigenvalue

problems, we use the Lanczos method to solve homogenized subproblems with a given tolerance,  $10^{-6}$ . Since these methods are readily provided by a few efficient Julia packages, we directly use the line-search algorithms from `LineSearches.jl` [29], and the Lanczos method from `KrylovKit.jl` [23]. For hyperparameters, we set  $\delta = -\sqrt{\epsilon}$ ,  $\nu = 0.01$ , and  $\Delta = 10^{-4}$ .

**The benchmark algorithms** Orban and Siqueira [39] provided highly efficient Julia packages in the `JuliaSmoothOptimizers` organization that include the Newton trust-region method utilizing the Steihaug-Toint conjugate-gradient method (Newton-TR-STCG) and an adaptive cubic regularization (ARC) with necessary subroutines and techniques including subproblem solutions and Krylov methods. The numerical results are recently reported in [19]. We use the original implementation in [39] and the default settings therein.

## 6.2 Unconstrained problems in CUTEst

We next present the results on a selected subset of the CUTEst dataset. To set a comprehensive comparison, we provide the results of HSODM with readily Hessian matrices, named after HSODM, and a version facilitated by Hessian-vector products (HSODM-HVP). We set an iteration limit of 20,000 and termination criterion as  $\|\nabla f(x_k)\| \leq 10^{-5}$  for all the tested algorithms; we check if this criterion is ensured else marked as failed. We focus on the unconstrained problems with the number of variables  $n \in [4, 5000]$ . For each problem in the CUTEst, if it has different parameters, we select all instances that fit the criterion. Then we have 200 instances in total where a few instances cannot be solved by any method. The complete result can be found in [Table C.2](#) and [Table C.3](#).

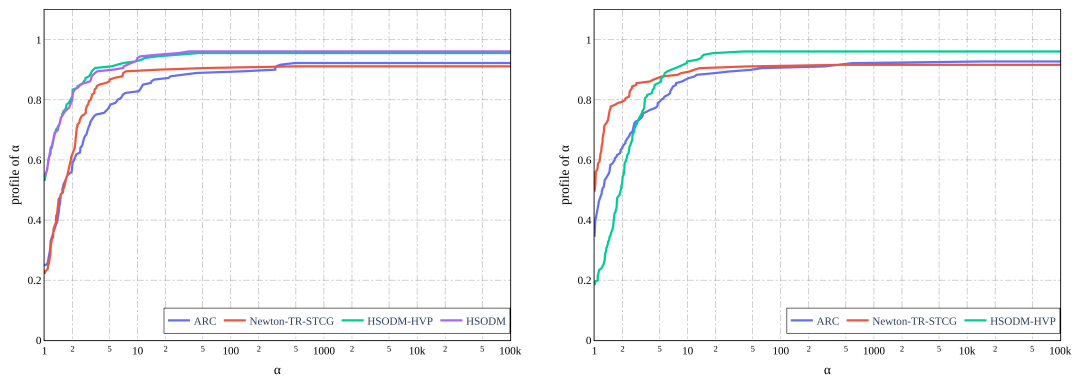
**Overall comparison of the algorithms.** The following [Table 6.1](#) presents a summary of tested algorithms. In this table, we let  $\mathcal{K}$  be the number of successful instances. Besides, we compute performance statistics based on scaled geometric means (SGM), including  $\bar{t}_G, \bar{k}_G, \bar{k}_G^f, \bar{k}_G^g, \bar{k}_G^H$  as (geometric) mean running time, mean iteration number, mean function evaluations, mean gradient evaluations, and mean Hessian evaluations, respectively. The running time is scaled by 1 second, and other metrics are scaled by 50 evaluations or iterations accordingly. Note that the cubic regularization ARC, Newton-TR-STCG, and HSODM-HVP use Hessian-vector products, so that  $\bar{k}_G^H = 0$  and the gradient evaluations in  $\bar{k}_G^g$  actually include the number of Hessian-vector products.

Apart from metrics measured by SGM, we use the performance profile on iteration number as defined in [18]. In essence, the performance profile at point  $\alpha$  in [Figure 6.1](#) of an algorithm indicates the probability of successfully solved instances within  $2^\alpha$  times the best iteration number amongst competitors.

The results from these preliminary implementations show that HSODM and HSODM-HVP outperformed the standard second-order methods, including Newton-TR-STCG and ARC on average. HSODM-HVP and HSODM had better iteration complexity and running time in terms of  $\bar{k}_G, \bar{t}_G$

Table 6.1: Performance in SGM of different algorithms on the CUTEst dataset. Note  $\bar{t}_G, \bar{k}_G$  are scaled geometric means (scaled by 1 second and 50 iterations, respectively). If an instance is failed, its iteration number and solving time are set to 20,000.

| Method         | $\mathcal{K}$ | $\bar{t}_G$ | $\bar{k}_G$ | $\bar{k}_G^f$ | $\bar{k}_G^g$ | $\bar{k}_G^H$ |
|----------------|---------------|-------------|-------------|---------------|---------------|---------------|
| Newton-TR-STCG | 165.00        | 6.14        | 170.44      | 170.44        | 639.64        | 0.00          |
| ARC            | 167.00        | 5.32        | 185.03      | 185.03        | 888.35        | 0.00          |
| HSODM-HVP      | 173.00        | 4.79        | 111.24      | 200.60        | 787.32        | 0.00          |
| HSODM          | 174.00        | 4.86        | 113.30      | 197.46        | 256.20        | 111.28        |



(a) Performance of iteration number

(b) Performance of gradient evaluations

Figure 6.1: Performance profiles of the second-order methods for CUTEst problems. In (a) we report the iteration number. Figure (b) includes the results of gradient evaluations; we only include methods using Krylov subspaces.

among competing algorithms. The HVP variant HSODM-HVP used comparable gradient evaluations with ARC. Since HSODM needs less iterations, more gradient evaluations seem necessary. More function evaluations are needed by extra overhead from the line searches. It is also interesting to see HSODM and also HSODM-HVP (see [EXTROSNB](#)), Newton-TR-STCG (see [ARGLINC](#)) and ARC (see [OSCIGRAD](#)) all had instances on which they performed best.

In terms of performance profile, we see both HSODM and HSODM-HVP had an advantage in iteration numbers. Newton-TR-STCG has the best performance on gradient evaluations in its succeeded instances. HSODM-HVP needs more gradient evaluations since it uses a slightly larger  $n + 1$  dimensional systems. Nevertheless, this disadvantage seems to be mild in practice.

## 7 Conclusion

In this paper, we introduce a homogenized second-order descent method (HSODM) whose global rate of complexity is optimal among a certain broad class of second-order methods (see [8]). The HSODM utilizes the homogenization trick to the quadratic model, which comes from the standard second-order Taylor expansion, such that the resulting homogenized quadratic form can be solved as an eigenvalue problem. We have shown that the homogenized idea is well-defined in both convex and nonconvex cases, where a negative curvature direction always exists. Using the model all along, one can safely stop at a small step to obtain an  $\epsilon$ -approximate second-order stationary point without switching to other methods.

We provide comprehensive experiments of HSODM on nonlinear optimization problems in the CUTEst benchmark. Two variants of HSODM show promising results in these experiments. One future direction is to utilize the method for constrained optimization problems.

## References

- [1] Satoru Adachi, Satoru Iwata, Yuji Nakatsukasa, and Akiko Takeda. Solving the trust-region subproblem by a generalized eigenvalue problem. *SIAM Journal on Optimization*, 27(1):269–291, 2017.
- [2] Naman Agarwal, Zeyuan Allen-Zhu, Brian Bullins, Elad Hazan, and Tengyu Ma. Finding approximate local minima faster than gradient descent. In *Proceedings of the 49th Annual ACM SIGACT Symposium on Theory of Computing*, pages 1195–1199, 2017.
- [3] Jeff Bezanson, Alan Edelman, Stefan Karpinski, and Viral B Shah. Julia: A fresh approach to numerical computing. *SIAM Review*, 59(1):65–98, 2017. doi: 10.1137/141000671. URL <https://epubs.siam.org/doi/10.1137/141000671>.
- [4] Yair Carmon, John C. Duchi, Oliver Hinder, and Aaron Sidford. Accelerated Methods for NonConvex Optimization. *SIAM Journal on Optimization*, 28(2):1751–1772, January 2018. ISSN 1052-6234, 1095-7189. doi: 10.1137/17M1114296. URL <https://epubs.siam.org/doi/10.1137/17M1114296>.
- [5] Coralia Cartis, Nicholas I. M. Gould, and Philippe L. Toint. On the Complexity of Steepest Descent, Newton’s and Regularized Newton’s Methods for Nonconvex Unconstrained Optimization Problems. *SIAM Journal on Optimization*, 20(6):2833–2852, January 2010. ISSN 1052-6234. doi: 10.1137/090774100. URL <https://epubs.siam.org/doi/abs/10.1137/090774100>. Publisher: Society for Industrial and Applied Mathematics.
- [6] Coralia Cartis, Nicholas I. M. Gould, and Philippe L. Toint. Adaptive cubic regularisation methods for unconstrained optimization. Part I: motivation, convergence and numerical results. *Mathematical Programming*, 127(2):245–295, April 2011. ISSN 0025-5610, 1436-4646. doi: 10.1007/s10107-009-0286-5. URL <http://link.springer.com/10.1007/s10107-009-0286-5>.
- [7] Coralia Cartis, Nicholas I. M. Gould, and Philippe L. Toint. Adaptive cubic regularisation methods for unconstrained optimization. Part II: worst-case function- and derivative-evaluation complexity. *Mathematical Programming*, 130(2):295–319, December 2011. ISSN 0025-5610, 1436-4646. doi: 10.1007/s10107-009-0337-y. URL <http://link.springer.com/10.1007/s10107-009-0337-y>.
- [8] Coralia Cartis, Nicholas I. M. Gould, and Philippe L. Toint. *Evaluation Complexity of Algorithms for Nonconvex Optimization: Theory, Computation and Perspectives*. Society for Industrial and Applied Mathematics, Philadelphia, PA, January 2022. ISBN 978-1-61197-698-4 978-1-61197-699-1. doi: 10.1137/1.9781611976991. URL <https://epubs.siam.org/doi/book/10.1137/1.9781611976991>.
- [9] Andrew R. Conn, Nicholas IM Gould, and Philippe L. Toint. *Trust region methods*. SIAM, 2000.

- [10] Frank E. Curtis and Daniel P. Robinson. Exploiting negative curvature in deterministic and stochastic optimization. *Mathematical Programming*, 176(1):69–94, July 2019. ISSN 1436-4646. doi: 10.1007/s10107-018-1335-8. URL <https://doi.org/10.1007/s10107-018-1335-8>.
- [11] Frank E. Curtis and Qi Wang. Worst-Case Complexity of TRACE with Inexact Subproblem Solutions for Nonconvex Smooth Optimization, April 2022. URL <http://arxiv.org/abs/2204.11322>. arXiv:2204.11322 [math].
- [12] Frank E. Curtis, Daniel P. Robinson, and Mohammadreza Samadi. A trust region algorithm with a worst-case iteration complexity of  $O(\epsilon^{-3/2})$  for nonconvex optimization. *Mathematical Programming*, 162(1):1–32, March 2017. ISSN 1436-4646. doi: 10.1007/s10107-016-1026-2. URL <https://doi.org/10.1007/s10107-016-1026-2>.
- [13] Frank E. Curtis, Zachary Lubberts, and Daniel P. Robinson. Concise complexity analyses for trust region methods. *Optimization Letters*, 12(8):1713–1724, December 2018. ISSN 1862-4480. doi: 10.1007/s11590-018-1286-2. URL <https://doi.org/10.1007/s11590-018-1286-2>.
- [14] Frank E. Curtis, Daniel P. Robinson, and Mohammadreza Samadi. An inexact regularized newton framework with a worst-case iteration complexity of  $\mathcal{O}(\epsilon^{-3/2})$  for nonconvex optimization. *IMA Journal of Numerical Analysis*, 39(3):1296–1327, 05 2018.
- [15] Frank E. Curtis, Daniel P. Robinson, Clément W. Royer, and Stephen J. Wright. Trust-region newton-cg with strong second-order complexity guarantees for nonconvex optimization. *SIAM Journal on Optimization*, 31(1):518–544, 2021.
- [16] Frank E. Curtis, Michael J. O’Neill, and Daniel P. Robinson. Worst-Case Complexity of an SQP Method for Nonlinear Equality Constrained Stochastic Optimization, January 2022. URL <http://arxiv.org/abs/2112.14799>. arXiv:2112.14799 [math].
- [17] Nikita Doikov and Yurii Nesterov. Gradient regularization of newton method with bregman distances. *Mathematical Programming*, pages 1–25, 2023.
- [18] Elizabeth D. Dolan and Jorge J. Moré. Benchmarking optimization software with performance profiles. *Mathematical Programming*, 91(2):201–213, January 2002. ISSN 1436-4646. doi: 10.1007/s101070100263. URL <https://doi.org/10.1007/s101070100263>.
- [19] Jean-Pierre Dussault, Tangi Migot, and Dominique Orban. Scalable adaptive cubic regularization methods. *Mathematical Programming*, October 2023. ISSN 1436-4646. doi: 10.1007/s10107-023-02007-6. URL <https://doi.org/10.1007/s10107-023-02007-6>.
- [20] Gene H Golub and Charles F Van Loan. *Matrix computations*. JHU press, 2013.
- [21] Nicholas I. M. Gould, Dominique Orban, and Philippe L. Toint. CUTEst: a Constrained and Unconstrained Testing Environment with safe threads for mathematical optimization.



- Computational Optimization and Applications*, 60(3):545–557, April 2015. ISSN 1573-2894. doi: 10.1007/s10589-014-9687-3. URL <https://doi.org/10.1007/s10589-014-9687-3>.
- [22] Serge Gratton, Sadok Jerad, and Philippe L Toint. Yet another fast variant of newton’s method for nonconvex optimization. *arXiv preprint arXiv:2302.10065*, 2023.
- [23] Jutho Haegeman. KrylovKit, March 2024. URL <https://zenodo.org/records/10884302>.
- [24] William W. Hager and Hongchao Zhang. Algorithm 851: CG\_descent, a conjugate gradient method with guaranteed descent. *ACM Transactions on Mathematical Software (TOMS)*, 32(1):113–137, 2006. Publisher: ACM New York, NY, USA.
- [25] Chang He, Yuntian Jiang, Chuwen Zhang, Dongdong Ge, Bo Jiang, and Yinyu Ye. Homogeneous Second-Order Descent Framework: A Fast Alternative to Newton-Type Methods, June 2023. URL <http://arxiv.org/abs/2306.17516>. arXiv:2306.17516 [math].
- [26] Yuntian Jiang, Chang He, Chuwen Zhang, Dongdong Ge, Bo Jiang, and Yinyu Ye. A universal trust-region method for convex and nonconvex optimization. *arXiv preprint arXiv:2311.11489*, 2023.
- [27] Chi Jin. Lecture 14: Lanczos Algorithm (March 22, 2021). Technical report, 2021.
- [28] Chi Jin, Rong Ge, Praneeth Netrapalli, Sham M. Kakade, and Michael I. Jordan. How to escape saddle points efficiently. In *International Conference on Machine Learning*, pages 1724–1732. PMLR, 2017.
- [29] Patrick K Mogensen and Asbjørn N Riseth. Optim: A mathematical optimization package for Julia. *Journal of Open Source Software*, 3(24):615, April 2018. ISSN 2475-9066. doi: 10.21105/joss.00615. URL <http://joss.theoj.org/papers/10.21105/joss.00615>.
- [30] J. Kuczyński and H. Woźniakowski. Estimating the Largest Eigenvalue by the Power and Lanczos Algorithms with a Random Start. *SIAM Journal on Matrix Analysis and Applications*, 13(4):1094–1122, October 1992. ISSN 0895-4798, 1095-7162. doi: 10.1137/0613066. URL <http://epubs.siam.org/doi/10.1137/0613066>.
- [31] Beatrice Laurent and Pascal Massart. Adaptive estimation of a quadratic functional by model selection. *Annals of statistics*, pages 1302–1338, 2000.
- [32] Huan Li and Zhouchen Lin. Restarted Nonconvex Accelerated Gradient Descent: No More Polylogarithmic Factor in the  $O(\epsilon^{-7/4})$  Complexity, May 2022. URL <http://arxiv.org/abs/2201.11411>. arXiv:2201.11411 [cs, math].
- [33] Felix Lieder. Solving large-scale cubic regularization by a generalized eigenvalue problem. *SIAM Journal on Optimization*, 30(4):3345–3358, 2020.

- [34] David G. Luenberger and Yinyu Ye. *Linear and Nonlinear Programming*, volume 228 of *International Series in Operations Research & Management Science*. Springer International Publishing, Cham, 2021. ISBN 978-3-030-85449-2 978-3-030-85450-8. doi: 10.1007/978-3-030-85450-8. URL <https://link.springer.com/10.1007/978-3-030-85450-8>.
- [35] Konstantin Mishchenko. Regularized newton method with global  $O(1/k^2)$  convergence. *arXiv preprint arXiv:2112.02089*, 2021.
- [36] Yurii Nesterov. *Lectures on convex optimization*, volume 137. Springer, 2018.
- [37] Yurii Nesterov and B.T. Polyak. Cubic regularization of Newton method and its global performance. *Mathematical Programming*, 108(1):177–205, August 2006. ISSN 1436-4646. doi: 10.1007/s10107-006-0706-8. URL <https://doi.org/10.1007/s10107-006-0706-8>.
- [38] Jorge Nocedal and Stephen Wright. *Numerical optimization*. Springer Science & Business Media, 2006.
- [39] Dominique Orban and Abel Siqueira. JuliaSmoothOptimizers, April 2019. URL <https://zenodo.org/record/2655082>. Language: eng.
- [40] Beresford N. Parlett. *The Symmetric Eigenvalue Problem*. Society for Industrial and Applied Mathematics, January 1998. doi: 10.1137/1.9781611971163. URL <http://epubs.siam.org/doi/book/10.1137/1.9781611971163>.
- [41] Marielba Rojas, Sandra A. Santos, and Danny C. Sorensen. A New Matrix-Free Algorithm for the Large-Scale Trust-Region Subproblem. *SIAM Journal on Optimization*, 11(3):611–646, January 2001. ISSN 1052-6234. doi: 10.1137/S105262349928887X. URL <https://epubs.siam.org/doi/abs/10.1137/S105262349928887X>. Publisher: Society for Industrial and Applied Mathematics.
- [42] Clément W. Royer and Stephen J. Wright. Complexity analysis of second-order line-search algorithms for smooth nonconvex optimization. *SIAM Journal on Optimization*, 28(2):1448–1477, 2018. Publisher: SIAM.
- [43] Clément W. Royer, Michael O’Neill, and Stephen J. Wright. A Newton-CG algorithm with complexity guarantees for smooth unconstrained optimization. *Mathematical Programming*, 180(1):451–488, March 2020. ISSN 1436-4646. doi: 10.1007/s10107-019-01362-7. URL <https://doi.org/10.1007/s10107-019-01362-7>.
- [44] Jos F. Sturm and Shuzhong Zhang. On cones of nonnegative quadratic functions. *Mathematics of Operations research*, 28(2):246–267, 2003. Publisher: INFORMS.
- [45] Yi Xu, Rong Jin, and Tianbao Yang. First-order stochastic algorithms for escaping from saddle points in almost linear time. *Advances in neural information processing systems*, 31, 2018.

- [46] Yinyu Ye. Second Order Optimization Algorithms II: Interior-Point Algorithms, 2005.
- [47] Yinyu Ye and Shuzhong Zhang. New results on quadratic minimization. *SIAM Journal on Optimization*, 14(1):245–267, 2003. Publisher: SIAM.
- [48] Chuwen Zhang, Dongdong Ge, Chang He, Bo Jiang, Yuntian Jiang, and Yinyu Ye. DRSOM: A Dimension Reduced Second-Order Method, January 2023. URL <http://arxiv.org/abs/2208.00208>. arXiv:2208.00208 [cs, math].

## A Appendix

### B Additional Proofs

#### B.1 Proof of Lemma 5.2

We provide a sketch here as the results are the combination of the complexity estimates in [27] and Lemma 9 in [42]. Consider the positive semidefinite matrix  $F'_k := \|F_k\|I - F_k$ , and substituting  $\epsilon := \frac{e_k}{2\|F_k\|}$  into the complexity results in [27], the Lanczos method returns an estimate  $\mu_{\max}(F'_k)$  satisfies

$$\mu_{\max}(F'_k) \geq \left(1 - \frac{e_k}{2\|F_k\|}\right) \lambda_{\max}(F'_k)$$

if it starts with the vector  $q_1$  and runs at most

$$1 + 2\sqrt{\frac{\|F_k\|}{e_k}} \log\left(\frac{16\|F_k\|}{e_k(q_1^T \chi_k)^2}\right)$$

iterations (gap-free version). Since  $\mu_{\max}(F'_k) = \|F_k\| - \gamma_k$  and  $\lambda_{\max}(F'_k) = \|F_k\| - \lambda_{\min}(F_k)$ , following the same argument of Lemma 9 in [42], we obtain

$$\gamma_k \leq \lambda_{\min}(F_k) + e_k.$$

The result of the gap-dependent version can be established similarly, and thus we omit it here.

#### B.2 Proof of Lemma 5.3

We first show (5.4).

$$\begin{aligned} \|F_k\| &= \max_{\|[v;t]\|=1} \begin{bmatrix} v \\ t \end{bmatrix}^T \begin{bmatrix} H_k & g_k \\ g_k^T & -\delta \end{bmatrix} \begin{bmatrix} v \\ t \end{bmatrix} \\ &\leq \max_{\|[v;t]\|=1} \begin{bmatrix} v \\ t \end{bmatrix}^T \begin{bmatrix} H_k & 0 \\ 0 & -\delta \end{bmatrix} \begin{bmatrix} v \\ t \end{bmatrix} + \max_{\|[v;t]\|=1} \begin{bmatrix} v \\ t \end{bmatrix}^T \begin{bmatrix} 0 & g_k \\ g_k^T & 0 \end{bmatrix} \begin{bmatrix} v \\ t \end{bmatrix} \\ &\leq \max\{U_H, \delta\} + \|g_k\|, \end{aligned}$$

the proof is completed. For the second argument, denote  $\omega_k = [r_k; \sigma_k]$ , from (5.1), we have

$$[v_k; t_k]^T F_k [v_k; t_k] + \gamma_k = 0. \tag{B.1}$$

We can write  $[v_k; t_k] = \tau \chi_k + s$ , where  $\tau \in [0, 1]$ ,  $s \perp \chi_k$ . Since  $[v_k; t_k]$  is a unit vector, we have

$$\tau^2 + \|s\|^2 = 1. \tag{B.2}$$

Then from (B.1) we have

$$\begin{aligned} -\theta_k + e_k &\geq -\gamma_k = -\theta_k \tau^2 + s^T F_k s \\ &\geq -\theta_k \tau^2 + (-\theta_k + \sigma_F) \|s\|^2. \end{aligned} \quad (\text{B.3})$$

The second equality is obtained by the fact  $s \perp v_1$ . It implies

$$\|s\|^2 \leq \frac{e_k}{\sigma_F}. \quad (\text{B.4})$$

Thus from (5.1) we have

$$\begin{aligned} \omega_k &= F_k[v_k; t_k] + \gamma_k[v_k; t_k] \\ &= (F_k + \gamma_k I)(\tau \chi_k + s) \\ &= \tau(\gamma_k - \theta_k) \chi_k + (F_k + \gamma_k I)s. \end{aligned} \quad (\text{B.5})$$

Hence, the norm of the residual follows

$$\begin{aligned} \|r_k\| &\leq \|\omega_k\| \leq \tau(\theta_k - \gamma_k) + \|(F_k + \gamma_k I)s\| \\ &\leq \tau e_k + \|(F_k + \gamma_k I)\| \sqrt{\frac{e_k}{\sigma_F}} \\ &\leq \tau e_k + 2(\max\{U_H, \delta\} + \|g_k\|) \sqrt{\frac{e_k}{\sigma_F}}. \end{aligned} \quad (\text{B.6})$$

This completes the proof.

### B.3 Proof of Theorem 5.2

For part (1), due to the mechanism of the Lanczos method, for any orthonormal basis  $q_j = [\nu_j, \beta_j]$  with  $j \geq 2$ , we have  $q_j \perp q_1$ . Therefore, it holds that

$$\beta_j \alpha = -\nu_j^T u \sqrt{1 - \alpha^2},$$

and thus

$$|\beta_j| \leq \frac{\sqrt{1 - \alpha^2} \|v_j\| \|u\|}{|\alpha|} \leq 2\sqrt{1 - \alpha^2}. \quad (\text{B.7})$$

For part (2), denote  $F_{n+1} = F_k e_{n+1}$  and  $y = F_{n+1} - (F_{n+1}^T q_1) \cdot q_1 - (F_{n+1}^T q_2) \cdot q_2$ , then  $q_1, q_2, y$  are mutually orthogonal. Therefore,  $y$  is the residual of  $F_{n+1}$  after projecting on the subspace  $\Pi$  spanned by  $q_1, q_2$ , it follows

$$\|y\| = \|(I - \Pi)F_{n+1}\|.$$

By denoting  $\varphi := F_{n+1} - F_k q_1$ , we conclude,

$$\begin{aligned} \|y\| &= \|(I - \Pi)F_{n+1}\| = \|(I - \Pi)(F_k q_1 + \varphi)\| = \|(I - \Pi)\varphi\| \leq \|\varphi\| \\ &= \left\| \begin{bmatrix} (1 - \alpha) \cdot g_k - \sqrt{1 - \alpha^2} \cdot H_k u \\ (1 - \alpha) \cdot (-\delta) - \sqrt{1 - \alpha^2} \cdot g_k^T u \end{bmatrix} \right\| \end{aligned}$$

since  $F_k q_1 \in \mathcal{K}(2; F_k, q_1)$  and  $(I - \Pi)$  is nonexpansive. In this view, we have,

$$\|y\|^2 \leq [(U_H + U_g)^2 + (\delta + U_g)^2] \cdot (1 - \alpha^2) \quad (\text{B.8})$$

as  $1 - \alpha \leq \sqrt{1 - \alpha^2}$  holds for  $\alpha \in (0, 1)$ . Recall that for the Lanczos method, it holds that

$$F_k Q_j - Q_j T_j = \xi_j e_j^T, \quad Q_j = [q_1, \dots, q_j] \in \mathbb{R}^{(n+1) \times j}, \quad T_j \in \mathbb{R}^{j \times j}.$$

Consider the last term of the residual  $\xi_j$ , by  $\xi_{j,n+1}$ , for  $j \geq 3$ , it follows

$$\begin{aligned} \xi_{j,n+1} &= e_{n+1}^T \xi_j = e_{n+1}^T \xi_j e_j^T e_j \\ &= e_{n+1}^T F_k Q_j e_j - e_{n+1}^T Q_j T_j e_j \\ &= F_{n+1}^T q_j - [\beta_1, \dots, \beta_j][0, \dots, 0, T_{j-1,j}, T_{j,j}]^T \\ &= F_{n+1}^T q_j - \beta_{j-1} T_{j-1,j} - \beta_j T_{j,j} \end{aligned}$$

Since  $q_j$  is perpendicular to  $q_1$  and  $q_2$ , we have  $q_j^T F_{n+1} = q_j^T y$ , and thus

$$\begin{aligned} |\xi_{j,n+1}| &= |F_{n+1}^T y - \beta_{j-1} T_{j-1,j} - \beta_j T_{j,j}| \\ &\leq \|F_{n+1}\| \cdot \|y\| + |T_{j-1,j}| \cdot |\beta_{j-1}| + |T_{j,j}| \cdot |\beta_j| \\ &\leq O(\sqrt{1 - \alpha^2}) \end{aligned}$$

where the last inequality follows from (B.7) and (B.8). By the fact of Ritz approximation (Section 10.1.4 in [20]), we conclude

$$|\sigma_k| \leq |\xi_{j,n+1}| \leq O(\sqrt{1 - \alpha^2}).$$

For part (3), from the shift-invariant property of the Krylov subspace, we have

$$\mathcal{K}(j; U_F I_{n+1} - F_k) = \mathcal{K}(j; F_k) := \left\{ q_1, F_k q_1, \dots, F_k^j q_1 \right\}.$$

Since the Ritz value  $-\gamma_k$  is generated in a larger Krylov subspace,  $-\gamma_k \leq q_1^T F_k q_1$  holds. Therefore, it is sufficient to establish that  $q_1^T F_k q_1 \leq -\delta$ . The selection (5.8) implies

$$(U_H + \delta)^2 \cdot (1 - \alpha^2) \leq 4(g^T u)^2 \cdot \alpha^2,$$

and thus it follows

$$\begin{aligned} \begin{bmatrix} \sqrt{1 - \alpha^2} u \\ \alpha \end{bmatrix}^T \begin{bmatrix} H_k & g_k \\ g_k^T & -\delta \end{bmatrix} \begin{bmatrix} \sqrt{1 - \alpha^2} u \\ \alpha \end{bmatrix} &= -\delta \cdot \alpha^2 + 2\alpha \sqrt{1 - \alpha^2} \cdot g^T u + (1 - \alpha^2) \cdot u^T H u \\ &\leq -\delta \cdot \alpha^2 - (1 - \alpha^2) \cdot (U_H + \delta) + (1 - \alpha^2) \cdot U_H \\ &\leq -\delta. \end{aligned}$$

## B.4 Proof of Theorem 5.3

We first show the first inequality. Note that for the randomized initialization, we have

$$|\alpha|^2 = \frac{\Psi^2 x_{n+1}^2}{\sum_{i=1}^n x_i^2 + \Psi^2 x_{n+1}^2}.$$

To ensure  $\alpha^2 \geq \Omega(1 - \epsilon^4)$ , it suffices to set  $\Psi$  satisfying

$$\frac{\Psi^2 x_{n+1}^2}{\sum_{i=1}^n x_i^2} \geq \Omega(\epsilon^{-4}).$$

Note that with a probability at least of  $1 - p$ , it holds

$$\Psi^2 x_{n+1}^2 \geq \frac{\pi}{2} \Psi^2 p^2 > 0.$$

Similarly,  $\sum_{i=1}^n x_i^2$  follows the chi-square distribution of with  $n$  degrees of freedom, with a probability at least of  $1 - e^{-n}$ , we conclude

$$\sum_{i=1}^n x_i^2 \leq 5n.$$

Therefore, choosing

$$\Psi \geq \Omega\left(\frac{\sqrt{n}}{p\epsilon^2}\right)$$

completes the proof.

We first note that for any given  $x \geq 0$ , it holds that

$$1 - \exp(-4x^2/\pi) \geq \operatorname{erf}(x)^2,$$

where  $\operatorname{erf}(x) = \frac{2}{\sqrt{\pi}} \int_0^x e^{-t^2} dt$ . It implies that for any random variable  $X \sim \mathcal{N}(0, 1)$ , we have

$$\operatorname{Prob}(|X| \leq x) = \operatorname{erf}(x/\sqrt{2}) \leq \sqrt{1 - \exp(-2x^2/\pi)}.$$

Note that

$$(v^T q_1)^2 = \frac{(v^T b)^2}{\|b\|^2} = \frac{(\sum_{i=1}^n v_i x_i + \alpha v_{n+1} x_{n+1})^2}{\sum_{i=1}^n x_i^2 + \alpha^2 x_{n+1}^2},$$

and it is sufficient to analyze the two terms  $(v^T b)^2$  and  $\|b\|^2$ , separately.

**Lower bound of  $(q_1^T v)^2$ .** Since  $v \neq 0$ , w.l.o.g., we assume  $\|v\| = 1$ .

- For the case  $\exists v_i \neq 0$  for some  $i = 1, \dots, n$ , it follows

$$\left(\sum_{i=1}^n v_i x_i + \alpha v_{n+1} x_{n+1}\right)^2 \geq \left(\sum_{i=1}^n v_i x_i\right)^2$$

due to the fact that we can set  $\alpha|v_{n+1}x_{n+1}| \gg |\sum_{i=1}^n v_i x_i|$ . Recall  $x_1, \dots, x_n \stackrel{i.i.d.}{\sim} \mathcal{N}(0, 1)$ , we have

$$\sum_{i=1}^n v_i x_i \sim \mathcal{N}\left(0, \sum_{i=1}^n v_i^2\right),$$

and it further implies

$$\text{Prob}\left(\left|\sum_{i=1}^n v_i x_i\right| \leq p\sqrt{\frac{\pi \sum_{i=1}^n v_i^2}{2}}\right) = \text{Prob}\left(\left|\frac{\sum_{i=1}^n v_i x_i}{\sqrt{\sum_{i=1}^n v_i^2}}\right| \leq p\sqrt{\frac{\pi}{2}}\right) \leq \sqrt{1 - \exp(-p^2)} \leq p.$$

Therefore, with a probability at least of  $1 - p$ , we conclude

$$(v^T b)^2 \geq \sqrt{\frac{\pi \sum_{i=1}^n v_i^2}{2}} p > 0.$$

- For the case  $v_1 = \dots = v_n = 0$ , we have  $(v^T b)^2 = \Psi^2 x_{n+1}^2$ . Recall  $x_{n+1} \sim \mathcal{N}(0, 1)$ , it follows that

$$\text{Prob}\left(x_{n+1}^2 \leq \frac{\pi}{2} p^2\right) = \text{Prob}\left(|x_{n+1}| \leq p\sqrt{\frac{\pi}{2}}\right) \leq p.$$

Similarly, with a probability at least of  $1 - p$ , we conclude  $(v^T b)^2 \geq \frac{\pi}{2} \Psi^2 p^2 > 0$ .

Combining the above two cases, it holds that

$$(v^T b)^2 \geq \min\left\{\sqrt{\frac{\pi \sum_{i=1}^n v_i^2}{2}} p, \frac{\pi}{2} \Psi^2 p^2\right\} > 0$$

with a probability of at least  $1 - p$ .

**Upper bound of  $\|b\|^2$ .** First note that

$$\begin{aligned} \|b\|^2 &= \sum_{i=1}^n x_i^2 + \Psi^2 x_{n+1}^2 \\ &\leq \Psi^2 \cdot \sum_{i=1}^{n+1} x_{n+1}^2. \end{aligned}$$

Since the random variable  $\sum_{i=1}^{n+1} x_{n+1}^2$  follows the chi-square distribution of with  $n + 1$  degrees of freedom, the tail bound in [31] implies that

$$\text{Prob}\left(\sum_{i=1}^{n+1} x_{n+1}^2 \geq 5(n+1)\right) \leq e^{-(n+1)}.$$

Therefore, with a probability at least of  $1 - e^{-(n+1)}$ , it holds that

$$\|b\|^2 \leq 5\Psi^2(n+1).$$



Finally, can guarantee

$$(v^T q_1)^2 = \frac{(v_1^T b)^2}{\|b\|^2} \geq \min \left\{ \Omega \left( \frac{p}{\Psi^2 n} \right), \Omega \left( \frac{p^2}{n} \right) \right\}$$

with a probability at least  $\min \{1 - p, 1 - e^{-(n+1)}\}$ .

## C Detailed Computational Results of CUTEst Dataset

For brevity, we use the abbreviations in [Table C.1](#).

Table C.1: Abbreviations of the Methods

| name           | abbreviation |
|----------------|--------------|
| ARC            | A            |
| HSODM          | H            |
| HSODM-HVP      | Hv           |
| Newton-TR-STCG | N            |

Table C.2: Complete Results on CUTEst Dataset, iteration & time

| name       | $n$  | $k$ |      |     |    | $k^g$  |       |      |     | $t$     |         |         |         |
|------------|------|-----|------|-----|----|--------|-------|------|-----|---------|---------|---------|---------|
|            |      | A   | H    | Hv  | N  | A      | H     | Hv   | N   | A       | H       | Hv      | N       |
| ARGLINA    | 200  | 5   | 3    | 3   | 3  | 14     | 12    | 16   | 8   | 3.5e-03 | 9.4e-01 | 3.5e+00 | 1.8e-03 |
| ARGLINB    | 200  | 3   | 4963 | -   | 3  | 8      | 28756 | -    | 8   | 1.6e-03 | 2.0e+02 | 0.0e+00 | 1.6e-03 |
| ARGLINC    | 200  | 32  | 5049 | 5   | 3  | 897590 | 55465 | 52   | 8   | 2.0e+02 | 2.0e+02 | 1.2e+02 | 1.6e-03 |
| ARGTRIGLS  | 200  | 7   | 13   | 13  | 7  | 964    | 57    | 4006 | 963 | 7.4e-01 | 7.8e-01 | 3.6e+00 | 6.5e-01 |
| ARWHEAD    | 1000 | 7   | 6    | 6   | 7  | 25     | 24    | 41   | 25  | 1.2e-03 | 4.0e-03 | 3.7e-02 | 1.9e-03 |
|            | 100  | 7   | 6    | 6   | 7  | 22     | 24    | 41   | 22  | 3.5e-03 | 6.1e-02 | 3.1e-02 | 4.1e-03 |
| BDQRTIC    | 1000 | 12  | 11   | 11  | 12 | 110    | 50    | 185  | 110 | 1.6e-02 | 1.1e-02 | 1.1e-01 | 5.6e-03 |
|            | 100  | 13  | 14   | 14  | 13 | 114    | 66    | 216  | 116 | 1.9e-02 | 1.5e-01 | 1.0e-01 | 1.9e-02 |
| BOXPOWER   | 1000 | 4   | 5    | 5   | 4  | 14     | 18    | 34   | 14  | 7.0e-04 | 1.0e-03 | 3.4e-02 | 7.5e-04 |
|            | 10   | 5   | 7    | 7   | 7  | 18     | 32    | 52   | 26  | 3.4e-03 | 9.2e-02 | 3.9e-02 | 4.9e-03 |
| BOX        | 1000 | 18  | 9    | 9   | 18 | 86     | 41    | 74   | 86  | 2.3e-03 | 2.0e-03 | 5.1e-02 | 1.2e-03 |
|            | 10   | 16  | 45   | 37  | 14 | 82     | 240   | 355  | 68  | 6.5e-03 | 4.3e-01 | 7.2e-01 | 6.8e-03 |
| BROWNAL    | 1000 | 4   | 6    | 5   | 4  | 13     | 25    | 33   | 14  | 6.8e-03 | 2.8e-01 | 3.0e-02 | 3.3e-03 |
|            | 200  | 4   | 4    | 4   | 5  | 12     | 16    | 24   | 15  | 5.7e-02 | 2.0e+01 | 1.4e-01 | 6.9e-02 |
| BROYDN3DLS | 1000 | 6   | 7    | 7   | 6  | 50     | 27    | 116  | 50  | 2.1e-03 | 3.0e-03 | 4.7e-02 | 1.6e-03 |
|            | 50   | 7   | 10   | 10  | 6  | 55     | 45    | 204  | 46  | 5.6e-03 | 1.1e-01 | 7.5e-02 | 6.5e-03 |
| BROYDN7D   | 500  | 102 | 15   | 15  | 36 | 551    | 77    | 477  | 227 | 2.1e-02 | 1.3e-02 | 1.0e-01 | 9.6e-03 |
|            | 50   | 619 | 155  | 162 | 89 | 2857   | 843   | 8223 | 552 | 2.9e-01 | 7.0e-01 | 1.9e+00 | 1.6e-01 |
| BROYDNBDLS | 1000 | 16  | 10   | 10  | 17 | 196    | 43    | 209  | 193 | 5.9e-03 | 1.1e-02 | 6.3e-02 | 7.3e-03 |
|            | 50   | 12  | 14   | 14  | 26 | 176    | 78    | 285  | 215 | 3.8e-02 | 1.9e-01 | 2.0e-01 | 4.4e-02 |
| BRYBND     | 1000 | 16  | 10   | 10  | 17 | 196    | 43    | 209  | 193 | 1.4e-02 | 1.1e-02 | 6.2e-02 | 6.7e-03 |
|            | 50   | 12  | 14   | 14  | 26 | 176    | 73    | 285  | 215 | 3.8e-02 | 2.0e-01 | 2.0e-01 | 5.5e-02 |
| CHAINWOOD  | 1000 | 97  | 40   | 40  | 85 | 425    | 203   | 432  | 435 | 2.1e-02 | 5.0e-03 | 1.9e-01 | 9.2e-03 |

Continued on next page

Table C.2: Complete Results on CUTEst Dataset, iteration & time

| name     | $n$  | $k$   |     |     |      | $k^g$  |      |       |       | $t$     |         |         |         |
|----------|------|-------|-----|-----|------|--------|------|-------|-------|---------|---------|---------|---------|
|          |      | A     | H   | Hv  | N    | A      | H    | Hv    | N     | A       | H       | Hv      | N       |
|          | 4    | 13192 | 585 | 676 | 2124 | 136952 | 2966 | 72418 | 22262 | 1.8e+01 | 7.0e+00 | 1.9e+01 | 1.8e+02 |
| CHNROSNB | 25   | 208   | 36  | 36  | 72   | 1406   | 182  | 948   | 623   | 4.0e-02 | 1.5e-02 | 2.0e-01 | 1.1e-02 |
| CHNRSNBM | 25   | 232   | 39  | 39  | 88   | 1648   | 183  | 1092  | 801   | 5.3e-02 | 1.8e-02 | 2.2e-01 | 1.4e-02 |
| COSINE   | 1000 | 9     | 9   | 12  | 10   | 38     | 39   | 197   | 43    | 2.5e-03 | 6.0e-03 | 7.1e-02 | 2.5e-03 |
|          | 100  | 9     | 8   | 8   | 26   | 32     | 38   | 88    | 149   | 4.7e-03 | 8.2e-02 | 5.1e-02 | 3.0e-02 |
| CRAGGLVY | 1000 | 14    | 12  | 12  | 14   | 259    | 54   | 328   | 259   | 6.3e-03 | 4.0e-03 | 8.4e-02 | 9.6e-03 |
|          | 50   | 15    | 15  | 15  | 14   | 208    | 73   | 390   | 176   | 4.5e-02 | 1.5e-01 | 1.8e-01 | 4.6e-02 |
| CURLY10  | 1000 | 39    | 19  | 19  | 22   | 829    | 106  | 2660  | 646   | 2.0e-02 | 1.3e-01 | 4.0e-01 | 1.4e-02 |
|          | 100  | 46    | 57  | 58  | 18   | 35411  | 298  | 44392 | 5459  | 2.9e+00 | 4.0e+01 | 9.4e+00 | 4.3e-01 |
| CURLY20  | 1000 | 70    | 16  | 16  | 20   | 958    | 92   | 1445  | 503   | 2.8e-02 | 1.1e-01 | 2.8e-01 | 1.4e-02 |
|          | 100  | 77    | 41  | 42  | 17   | 32093  | 211  | 37633 | 6745  | 4.2e+00 | 1.3e+02 | 1.0e+01 | 7.5e-01 |
| CURLY30  | 1000 | 51    | 42  | 41  | 24   | 25457  | 214  | 38609 | 5737  | 4.5e+00 | 2.2e+02 | 1.3e+01 | 1.0e+00 |
| DIXMAANA | 3000 | 7     | 6   | 6   | 8    | 30     | 28   | 48    | 31    | 1.4e-03 | 5.0e-03 | 3.9e-02 | 2.2e-03 |
|          | 90   | 8     | 7   | 7   | 8    | 33     | 35   | 60    | 31    | 1.5e-02 | 4.7e-01 | 5.2e-02 | 1.3e-02 |
| DIXMAANB | 3000 | 8     | 5   | 5   | 11   | 45     | 22   | 40    | 48    | 3.3e-03 | 4.0e-03 | 3.4e-02 | 3.1e-03 |
|          | 90   | 9     | 6   | 6   | 9    | 32     | 28   | 51    | 33    | 1.5e-02 | 4.2e-01 | 4.5e-02 | 1.5e-02 |
| DIXMAANC | 3000 | 9     | 6   | 6   | 13   | 47     | 26   | 52    | 66    | 1.7e-03 | 5.0e-03 | 3.8e-02 | 4.0e-03 |
|          | 90   | 9     | 6   | 6   | 10   | 35     | 28   | 49    | 38    | 1.6e-02 | 4.2e-01 | 4.5e-02 | 1.8e-02 |
| DIXMAAND | 3000 | 10    | 6   | 6   | 15   | 52     | 26   | 50    | 72    | 2.2e-03 | 6.0e-03 | 3.6e-02 | 4.5e-03 |
|          | 90   | 9     | 6   | 6   | 11   | 36     | 29   | 50    | 41    | 1.7e-02 | 4.3e-01 | 4.8e-02 | 1.8e-02 |
| DIXMAANE | 3000 | 11    | 11  | 11  | 10   | 141    | 52   | 214   | 112   | 5.0e-03 | 1.2e-02 | 7.2e-02 | 2.6e-03 |
|          | 90   | 11    | 34  | 34  | 13   | 402    | 172  | 884   | 413   | 1.7e-01 | 2.7e+00 | 7.3e-01 | 1.5e-01 |
| DIXMAANF | 3000 | 13    | 9   | 9   | 19   | 157    | 41   | 170   | 167   | 4.7e-03 | 7.0e-03 | 6.1e-02 | 8.3e-03 |
|          | 90   | 15    | 19  | 19  | 25   | 529    | 94   | 708   | 646   | 2.3e-01 | 1.7e+00 | 6.0e-01 | 3.1e-01 |
| DIXMAANG | 3000 | 14    | 9   | 9   | 17   | 172    | 41   | 159   | 163   | 1.8e-02 | 1.0e-02 | 5.8e-02 | 7.1e-03 |
|          | 90   | 15    | 17  | 17  | 30   | 505    | 84   | 671   | 597   | 2.2e-01 | 1.5e+00 | 5.7e-01 | 2.5e-01 |
| DIXMAANH | 3000 | 14    | 9   | 9   | 25   | 153    | 41   | 166   | 228   | 5.6e-03 | 1.1e-02 | 5.9e-02 | 1.1e-02 |
|          | 90   | 16    | 16  | 16  | 30   | 458    | 79   | 665   | 613   | 2.0e-01 | 1.4e+00 | 6.1e-01 | 2.3e-01 |
| DIXMAANI | 3000 | 12    | 22  | 23  | 14   | 400    | 108  | 1026  | 365   | 7.2e-03 | 3.8e-02 | 1.9e-01 | 1.2e-02 |
|          | 90   | 12    | 85  | 143 | 13   | 5266   | 445  | 14134 | 5761  | 2.2e+00 | 1.3e+01 | 9.3e+00 | 2.1e+00 |
| DIXMAANJ | 3000 | 28    | 13  | 13  | 28   | 580    | 62   | 639   | 658   | 1.5e-02 | 2.9e-02 | 1.4e-01 | 1.9e-02 |
|          | 90   | 54    | 32  | 62  | 36   | 6582   | 164  | 10653 | 5190  | 2.9e+00 | 1.3e+01 | 9.2e+00 | 2.1e+00 |
| DIXMAANK | 3000 | 25    | 13  | 13  | 25   | 528    | 62   | 687   | 518   | 2.2e-02 | 2.8e-02 | 1.4e-01 | 1.7e-02 |
|          | 90   | 57    | 30  | 29  | 40   | 8987   | 154  | 3848  | 4719  | 3.9e+00 | 1.4e+01 | 9.3e+00 | 1.8e+00 |
| DIXMAANL | 3000 | 27    | 15  | 15  | 27   | 642    | 72   | 860   | 437   | 1.8e-02 | 3.0e-02 | 1.6e-01 | 1.5e-02 |
|          | 90   | 87    | 29  | 40  | 64   | 9784   | 150  | 8847  | 10464 | 4.3e+00 | 1.5e+01 | 4.9e+00 | 4.9e+00 |
| DIXMAANM | 3000 | 9     | 30  | 30  | 12   | 341    | 149  | 1121  | 266   | 1.1e+00 | 4.0e-02 | 2.5e-01 | 6.9e-01 |
|          | 90   | 11    | 108 | 297 | 13   | 12793  | 578  | 20134 | 5836  | 6.3e+00 | 1.3e+01 | 1.1e+01 | 2.8e+00 |
| DIXMAANN | 3000 | 15    | 22  | 22  | 18   | 601    | 108  | 839   | 710   | 1.5e-02 | 2.1e-02 | 1.9e-01 | 2.1e-02 |
|          | 90   | 75    | 64  | 48  | 31   | 18601  | 332  | 2758  | 6956  | 8.1e+00 | 1.8e+01 | 8.5e+00 | 2.6e+00 |
| DIXMAANO | 3000 | 15    | 22  | 22  | 19   | 525    | 108  | 825   | 537   | 1.0e-02 | 3.8e-02 | 1.9e-01 | 1.5e-02 |
|          | 90   | 79    | 59  | 171 | 28   | 18310  | 308  | 13239 | 6838  | 7.9e+00 | 2.0e+01 | 8.5e+00 | 3.1e+00 |
| DIXMAANP | 3000 | 18    | 23  | 23  | 25   | 620    | 113  | 922   | 735   | 1.4e-02 | 3.5e-02 | 2.3e-01 | 2.2e-02 |
|          | 90   | 79    | 65  | 91  | 33   | 18703  | 336  | 11944 | 5748  | 8.1e+00 | 2.8e+01 | 9.2e+00 | 2.6e+00 |
| DIXON3DQ | 1000 | 9     | 32  | 33  | 3    | 653    | 161  | 1479  | 166   | 7.5e-02 | 4.1e-02 | 2.4e-01 | 2.5e-03 |
|          | 100  | 11    | 179 | 226 | 5    | 6407   | 963  | 28291 | 2036  | 2.9e-01 | 5.6e+00 | 4.1e+00 | 8.4e-02 |
| DQDRTIC  | 1000 | 5     | 9   | 9   | 4    | 25     | 41   | 91    | 16    | 6.1e-03 | 4.0e-03 | 5.1e-02 | 9.8e-04 |
|          | 50   | 5     | 8   | 8   | 7    | 23     | 36   | 79    | 29    | 3.1e-03 | 7.6e-02 | 4.3e-02 | 4.4e-03 |
| DQRTIC   | 1000 | 24    | 9   | 9   | 25   | 200    | 51   | 116   | 173   | 4.9e-03 | 4.0e-03 | 5.2e-02 | 4.2e-03 |
|          | 50   | 30    | 15  | 15  | 34   | 252    | 107  | 192   | 252   | 1.6e-02 | 1.3e-01 | 8.1e-02 | 1.8e-02 |
| EDENSCH  | 2000 | 12    | 12  | 12  | 17   | 76     | 59   | 156   | 98    | 2.1e-03 | 5.0e-03 | 6.6e-02 | 3.6e-03 |

Continued on next page

Table C.2: Complete Results on CUTEst Dataset, iteration & time

| name      | n    | k     |       |       |       | k <sup>g</sup> |         |         |        | t       |         |         |         |
|-----------|------|-------|-------|-------|-------|----------------|---------|---------|--------|---------|---------|---------|---------|
|           |      | A     | H     | Hv    | N     | A              | H       | Hv      | N      | A       | H       | Hv      | N       |
| EIGENALS  | 36   | 13    | 11    | 11    | 15    | 71             | 58      | 149     | 82     | 2.1e-02 | 3.5e-01 | 9.4e-02 | 2.4e-02 |
|           | 2550 | 10    | 10    | 7     | 9     | 32             | 77      | 50      | 31     | 1.2e-03 | 2.0e-03 | 5.6e-02 | 1.3e-03 |
|           | 6    | 100   | 58    | 135   | 118   | 3914           | 986     | 12184   | 5545   | 2.5e+01 | 2.1e+02 | 2.0e+02 | 3.5e+01 |
| EIGENBLS  | 2550 | 10    | 10    | 8     | 11    | 43             | 71      | 62      | 44     | 1.4e-03 | 2.0e-03 | 4.7e-02 | 1.6e-03 |
|           | 6    | 2045  | 65    | 126   | 451   | 28271          | 355     | 27093   | 23072  | 2.0e+02 | 2.0e+02 | 2.0e+02 | 2.0e+02 |
| EIGENCLS  | 2652 | 93    | 14    | 14    | 24    | 625            | 66      | 381     | 239    | 2.2e-02 | 1.3e-02 | 8.7e-02 | 9.2e-03 |
|           | 30   | 2107  | 70    | 160   | 646   | 26158          | 701     | 25300   | 21199  | 2.0e+02 | 2.1e+02 | 2.0e+02 | 2.0e+02 |
| ENGVAL1   | 1000 | 9     | 8     | 8     | 9     | 55             | 36      | 96      | 55     | 5.6e-03 | 5.0e-03 | 4.6e-02 | 2.2e-03 |
|           | 50   | -     | 8     | 8     | 10    | -              | 34      | 99      | 53     | -       | 8.4e-02 | 5.2e-02 | 9.0e-03 |
| ERRINROS  | 25   | 117   | 81    | 82    | 82    | 880            | 437     | 1837    | 1081   | 3.8e-02 | 2.6e-02 | 3.9e-01 | 1.4e-02 |
| ERRINRSM  | 25   | 314   | 282   | -     | 202   | 2619           | 1514    | -       | 3302   | 8.4e-02 | 7.4e-02 | -       | 3.1e-02 |
| EXTROSNB  | 1000 | 3901  | 9     | 8     | 4092  | 47796          | 85      | 165     | 72504  | 1.7e+00 | 8.0e-03 | 1.5e-01 | 1.9e+02 |
|           | 100  | 3859  | 2346  | 274   | 790   | 47346          | 10621   | 4966    | 10901  | 3.9e+00 | 2.1e+01 | 1.9e+01 | 9.8e+02 |
| FLETBV3M  | 1000 | 31    | 1     | 1     | 5     | 124            | 0       | 2       | 17     | 4.9e-03 | 0.0e+00 | 0.0e+00 | 9.5e-04 |
|           | 10   | 13    | 5     | 5     | 9     | 38             | 30      | 39      | 26     | 8.4e-03 | 5.3e-02 | 3.0e-02 | 6.7e-03 |
| FLETGBV2  | 1000 | 4     | 4     | 4     | 2     | 23             | 16      | 30      | 9      | 1.1e-03 | 1.0e-03 | 2.9e-02 | 4.8e-04 |
|           | 10   | 10    | 19    | 19    | 2     | 3514           | 96      | 4991    | 505    | 4.5e-01 | 1.7e+00 | 1.5e+00 | 6.4e-02 |
| FLETGBV3  | 1000 | 341   | 1     | 1     | 7     | 1167           | 0       | 2       | 27     | 4.8e-02 | 0.0e+00 | 0.0e+00 | 1.3e-03 |
|           | 10   | 20001 | 16946 | 14431 | 2985  | 60002          | 440053  | 418000  | 11921  | 1.1e+01 | 2.0e+02 | 2.0e+02 | 2.8e+02 |
| FLETCHBV  | 1000 | 10    | 114   | 114   | 7     | 83             | 792     | 1283    | 32     | 1.0e-02 | 1.6e-02 | 5.3e-01 | 1.2e-03 |
|           | 10   | 20001 | 18174 | 16120 | 2581  | 80073          | 363037  | 386434  | 10306  | 2.8e+01 | 2.0e+02 | 2.0e+02 | 2.2e+02 |
| FLETCHCR  | 1000 | 469   | 163   | 164   | 368   | 5366           | 776     | 4972    | 3942   | 4.2e-01 | 7.8e-02 | 9.8e-01 | 6.7e-02 |
|           | 100  | 4669  | 1526  | 1526  | 761   | 54891          | 7349    | 50826   | 8458   | 5.8e+00 | 1.4e+01 | 1.6e+01 | 2.3e+02 |
| FMINSRF2  | 16   | 17    | 17    | 17    | 21    | 156            | 82      | 248     | 111    | 6.0e-03 | 4.0e-03 | 9.3e-02 | 3.5e-03 |
|           | 961  | 65    | 131   | 104   | 211   | 2354           | 666     | 6031    | 1096   | 5.6e-01 | 1.8e+00 | 2.2e+00 | 3.0e-01 |
| FMINSURF  | 16   | 17    | 12    | 12    | 23    | 127            | 56      | 154     | 89     | 3.0e-03 | 3.0e-03 | 6.7e-02 | 3.4e-03 |
|           | 961  | 71    | 71    | 74    | 197   | 1943           | 337     | 2176    | 1038   | 4.8e-01 | 1.2e+01 | 3.0e+00 | 2.4e-01 |
| FREUROTH  | 1000 | 15    | 11    | 11    | 13    | 71             | 52      | 138     | 64     | 3.9e-03 | 6.0e-03 | 6.5e-02 | 3.0e-03 |
|           | 50   | 15    | 15    | 15    | 10    | 73             | 73      | 191     | 55     | 1.2e-02 | 1.4e-01 | 1.1e-01 | 1.1e-02 |
| GENHUMPS  | 1000 | 20001 | 229   | 331   | 3888  | 99259          | 1820    | 6401    | 15052  | 6.3e+00 | 2.2e-02 | 1.6e+00 | 2.5e+01 |
|           | 10   | 20001 | 13759 | 8959  | 1386  | 108421         | 120667  | 557579  | 4838   | 2.8e+01 | 1.6e+02 | 2.0e+02 | 1.2e+03 |
| GENROSE   | 100  | 844   | 76    | 74    | 175   | 6581           | 520     | 3553    | 1399   | 3.3e-01 | 5.9e-02 | 5.7e-01 | 3.4e-02 |
|           | 500  | 3823  | 353   | 359   | 836   | 32215          | 2426    | 17279   | 6761   | 1.8e+00 | 1.2e+00 | 3.5e+00 | 4.2e-01 |
| HILBERTA  | 6    | 6     | 11    | 9     | 3     | 31             | 52      | 89      | 12     | 1.2e-03 | 1.0e-03 | 5.0e-02 | 6.2e-04 |
| HILBERTB  | 5    | 5     | 5     | 5     | 4     | 18             | 20      | 35      | 14     | 7.8e-04 | 1.0e-03 | 3.4e-02 | 7.2e-04 |
| INDEFM    | 1000 | 20001 | 20000 | 20000 | 15925 | 81623          | 1039726 | 1102165 | 47857  | 6.5e+00 | 9.1e+00 | 1.1e+02 | 2.3e+02 |
|           | 50   | 20001 | 14992 | 11385 | 758   | 89617          | 776745  | 632944  | 2521   | 1.0e+01 | 2.0e+02 | 2.0e+02 | 5.3e+02 |
| INDEF     | 1000 | 50    | 53    | 54    | 159   | 212            | 273     | 738     | 595    | 7.5e-03 | 1.6e-02 | 2.6e-01 | 2.0e-02 |
|           | 50   | 39    | 63    | 88    | 194   | 194            | 351     | 935     | 823    | 2.9e-02 | 6.0e-01 | 9.5e-01 | 1.4e-01 |
| INTEQNELS | 102  | 4     | 5     | 5     | 4     | 16             | 19      | 38      | 16     | 2.8e-03 | 3.6e-02 | 2.7e-02 | 3.0e-03 |
|           | 502  | 4     | 5     | 5     | 4     | 16             | 19      | 35      | 15     | 5.2e-02 | 3.0e+00 | 1.4e-01 | 4.8e-02 |
| JIMACK    | 1521 | 6239  | 50    | 46    | 52    | 141701         | 488     | 37171   | 2969   | 2.0e+02 | 8.5e+00 | 4.5e+01 | 2.9e+00 |
|           | 81   | 101   | 45    | 8     | 24    | 6236           | 612     | 7119    | 6784   | 2.0e+02 | 2.3e+02 | 2.3e+02 | 2.3e+02 |
| LIARWHD   | 1000 | 11    | 12    | 12    | 11    | 42             | 58      | 99      | 42     | 1.6e-03 | 5.0e-03 | 6.4e-02 | 2.0e-03 |
|           | 36   | 13    | 20    | 20    | 13    | 50             | 102     | 178     | 49     | 7.1e-03 | 2.0e-01 | 1.1e-01 | 8.6e-03 |
| MANCINO   | 50   | 8     | 6     | 6     | 9     | 36             | 27      | 58      | 37     | 2.4e-02 | 2.5e-02 | 6.1e-02 | 2.4e-02 |
| MODBEALE  | 10   | 11    | 11    | 11    | 12    | 94             | 47      | 149     | 86     | 3.4e-03 | 3.0e-03 | 6.3e-02 | 2.3e-03 |
|           | 2000 | 10    | 20    | 20    | 7754  | 132            | 100     | 390     | 236687 | 6.8e-02 | 6.8e-01 | 3.6e-01 | 3.0e+02 |
| MOREBV    | 1000 | 7     | 11    | 11    | 4     | 466            | 51      | 1125    | 217    | 5.2e-03 | 2.7e-02 | 1.4e-01 | 3.6e-03 |
|           | 50   | 3     | 3     | 3     | 3     | 2379           | 11      | 233     | 2446   | 2.1e-01 | 2.4e+00 | 1.3e+00 | 2.1e-01 |
| MSQRTALS  | 4900 | 37    | 12    | 12    | 23    | 446            | 55      | 442     | 373    | 3.3e-02 | 5.5e-02 | 9.9e-02 | 1.6e-02 |

Continued on next page

Table C.2: Complete Results on CUTEst Dataset, iteration & time

| name     | $n$  | $k$   |       |       |      | $k^g$    |        |         |        | $t$     |         |         |         |
|----------|------|-------|-------|-------|------|----------|--------|---------|--------|---------|---------|---------|---------|
|          |      | A     | H     | Hv    | N    | A        | H      | Hv      | N      | A       | H       | Hv      | N       |
| MSQRTBLS | 49   | 34    | 16    | 30    | 39   | 11619    | 81     | 10003   | 12017  | 2.4e+02 | 2.0e+02 | 2.0e+02 | 2.4e+02 |
|          | 4900 | 26    | 13    | 13    | 27   | 454      | 59     | 576     | 446    | 1.4e-02 | 1.9e-02 | 1.1e-01 | 1.9e-02 |
| NCB20B   | 49   | 32    | 16    | 35    | 40   | 11081    | 81     | 10587   | 10835  | 2.3e+02 | 2.0e+02 | 2.2e+02 | 2.2e+02 |
|          | 1000 | 582   | 42    | 52    | 39   | 4143     | 262    | 2405    | 551    | 7.1e-01 | 1.6e-01 | 6.2e-01 | 5.8e-02 |
| NCB20    | 180  | 1458  | 68    | 70    | 131  | 7965     | 425    | 3924    | 1062   | 7.6e+00 | 1.7e+00 | 5.0e+00 | 1.1e+00 |
|          | 1010 | 4219  | 14    | 14    | 41   | 34429    | 187    | 6090    | 1783   | 1.1e+01 | 2.8e-01 | 1.5e+00 | 3.3e-01 |
| NONCVXU2 | 110  | 4199  | 14    | 15    | 48   | 35664    | 169    | 4117    | 2861   | 3.5e+01 | 1.3e+00 | 6.2e+00 | 2.8e+00 |
|          | 1000 | 106   | 10    | 10    | 22   | 496      | 46     | 128     | 99     | 2.5e-02 | 1.0e-03 | 6.0e-02 | 3.5e-03 |
| NONCVXUN | 10   | 3710  | 691   | 721   | 362  | 19119    | 3871   | 33069   | 3386   | 5.6e+00 | 1.2e+01 | 1.7e+01 | 1.1e+00 |
|          | 1000 | 67    | 9     | 9     | 20   | 293      | 41     | 103     | 80     | 2.8e-02 | 2.0e-03 | 5.8e-02 | 3.1e-03 |
| NONDIA   | 10   | -     | 4852  | 2811  | 283  | -        | 26262  | 282701  | 4668   | -       | 2.0e+02 | 2.0e+02 | 1.4e+00 |
|          | 1000 | 11    | 8     | 8     | 14   | 35       | 33     | 61      | 49     | 2.6e-03 | 5.0e-03 | 5.0e-02 | 2.7e-03 |
| NONDQUAR | 90   | 8     | 7     | 7     | 8    | 26       | 29     | 52      | 26     | 3.6e-03 | 7.5e-02 | 3.7e-02 | 4.2e-03 |
|          | 1000 | 71    | 52    | 57    | 22   | 5572     | 253    | 1508    | 643    | 7.1e-02 | 7.2e-02 | 3.7e-01 | 9.5e-03 |
| NONMSQRT | 100  | 87    | 71    | 62    | 114  | 8516     | 350    | 1543    | 8063   | 4.4e-01 | 8.7e-01 | 4.2e-01 | 3.1e-01 |
|          | 4900 | 860   | 20000 | 5332  | 1141 | 18284    | 108076 | 114356  | 51594  | 8.4e-01 | 5.1e+00 | 9.8e+01 | 4.5e+00 |
| OSCIGRAD | 49   | 158   | 119   | 78    | 89   | 14331    | 653    | 14645   | 14859  | 2.0e+02 | 2.0e+02 | 2.1e+02 | 2.0e+02 |
|          | 1000 | 13    | 332   | 12    | 19   | 133      | 2816   | 220     | 168    | 9.9e-03 | 4.4e-02 | 9.5e+01 | 3.5e-03 |
| OSCIPATH | 15   | 14    | -     | 12    | 19   | 160      | -      | 548     | 183    | 2.4e-02 | -       | 1.8e-01 | 3.2e-02 |
|          | 25   | 4     | 3     | 3     | 4    | 22       | 10     | 22      | 22     | 7.0e-04 | 2.0e-03 | 2.5e-02 | 8.2e-04 |
| PENALTY1 | 500  | 4     | 3     | 3     | 4    | 22       | 10     | 22      | 22     | 2.5e-03 | 1.5e-02 | 2.2e-02 | 2.7e-03 |
|          | 1000 | 65    | 50    | 47    | 58   | 196      | 308    | 479     | 193    | 9.8e-03 | 6.0e-02 | 2.3e-01 | 9.0e-03 |
| PENALTY2 | 50   | 29    | 22    | 22    | 33   | 86       | 186    | 265     | 99     | 8.7e-03 | 3.3e+00 | 1.2e-01 | 1.1e-02 |
|          | 1000 | 37    | 13    | 13    | 39   | 242      | 79     | 301     | 353    | 3.8e-02 | 1.4e-02 | 8.3e-02 | 1.4e-02 |
| PENALTY3 | 50   | 0     | 240   | 20000 | 2529 | 3        | 1510   | 161371  | 7581   | 0.0e+00 | 3.1e+02 | 1.3e+02 | 3.0e+02 |
|          | 1000 | 63    | 25    | 25    | 26   | 286      | 129    | 496     | 144    | 3.5e-01 | 5.6e-02 | 3.3e-01 | 6.6e-02 |
| POWELLSG | 60   | 19    | 13    | 13    | 19   | 110      | 64     | 133     | 110    | 1.2e-02 | 6.0e-03 | 7.3e-02 | 3.3e-03 |
|          | 1000 | 20    | 38    | 34    | 20   | 116      | 190    | 357     | 114    | 8.3e-03 | 3.5e-01 | 2.1e-01 | 1.0e-02 |
| POWER    | 1000 | 24    | 8     | 8     | 24   | 253      | 37     | 153     | 253    | 5.8e-03 | 9.0e-03 | 5.3e-02 | 5.0e-03 |
|          | 50   | 30    | 14    | 14    | 30   | 647      | 71     | 723     | 653    | 3.4e-02 | 2.8e+00 | 1.7e-01 | 3.5e-02 |
| QUARTC   | 1000 | 26    | 10    | 10    | 28   | 225      | 59     | 155     | 219    | 6.3e-03 | 7.0e-03 | 5.9e-02 | 5.7e-03 |
|          | 100  | 30    | 15    | 15    | 34   | 252      | 107    | 192     | 252    | 1.6e-02 | 1.3e-01 | 9.2e-02 | 1.6e-02 |
| SBRYBND  | 1000 | 20001 | 112   | 2005  | 251  | 372440   | 678    | 1139968 | 7075   | 1.4e+01 | 2.0e+02 | 9.5e+01 | 9.3e+01 |
|          | 50   | 504   | 18    | 581   | 7130 | 984414   | 149    | 712211  | 810823 | 2.0e+02 | 2.0e+02 | 2.0e+02 | 2.0e+02 |
| SCHMVETT | 1000 | 4     | 6     | 6     | 5    | 37       | 24     | 83      | 47     | 1.3e-03 | 1.0e-03 | 3.8e-02 | 1.4e-03 |
|          | 10   | 5     | 6     | 6     | 5    | 77       | 25     | 116     | 73     | 3.5e-02 | 7.5e-02 | 1.1e-01 | 3.7e-02 |
| SCOSINE  | 1000 | 42    | -     | -     | 4793 | 19355851 | -      | -       | 41338  | 2.0e+02 | -       | -       | 2.3e+02 |
|          | 10   | 12824 | 249   | 56    | 530  | 2048247  | 3964   | 1662    | 54720  | 2.0e+02 | 2.1e+02 | 1.2e+02 | 4.6e+00 |
| SCURLY10 | 1000 | 30    | 4     | 4     | 30   | 103      | 17     | 42      | 103    | 4.5e-03 | 1.0e-03 | 2.8e-02 | 3.9e-03 |
|          | 10   | 30    | 9     | 9     | 31   | 510      | 53     | 232     | 553    | 5.2e-02 | 1.3e-01 | 7.0e-02 | 4.8e-02 |
| SCURLY20 | 1000 | 30    | 8     | 8     | 31   | 378      | 46     | 180     | 389    | 5.8e-02 | 1.5e-01 | 6.6e-02 | 5.1e-02 |
|          | 1000 | -     | 9     | 9     | 31   | -        | 48     | 199     | 350    | -       | 2.1e-01 | 8.0e-02 | 6.6e-02 |
| SENSORS  | 1000 | 40    | 13    | 13    | 18   | 217      | 60     | 174     | 65     | 9.7e-03 | 5.0e-03 | 7.3e-02 | 5.7e-03 |
|          | 10   | 180   | 13    | 13    | 37   | 887      | 68     | 232     | 134    | 1.8e+02 | 1.0e+01 | 5.4e+01 | 2.7e+01 |
| SINQUAD  | 1000 | 33    | 10    | 10    | 13   | 130      | 47     | 93      | 47     | 1.2e-02 | 3.0e-03 | 5.5e-02 | 3.2e-03 |
|          | 50   | 49    | 20    | 20    | 18   | 195      | 106    | 197     | 65     | 5.2e-02 | 1.8e-01 | 2.6e-01 | 1.8e-02 |
| SPARSINE | 1000 | 7     | 9     | 9     | 32   | 183      | 39     | 488     | 433    | 3.4e-03 | 1.6e-02 | 7.6e-02 | 1.2e-02 |
|          | 50   | 11    | 15    | 19    | 32   | 9666     | 71     | 11762   | 5875   | 1.7e+00 | 1.7e+01 | 3.9e+00 | 1.2e+00 |
| SPARSQR  | 1000 | 18    | 5     | 5     | 18   | 156      | 22     | 78      | 156    | 3.8e-03 | 4.0e-03 | 3.4e-02 | 5.6e-03 |
|          | 50   | 22    | 7     | 7     | 22   | 216      | 34     | 91      | 217    | 3.3e-02 | 1.6e-01 | 5.1e-02 | 3.7e-02 |
| SPMSRTL  | 1000 | 21    | 10    | 10    | 22   | 239      | 46     | 377     | 211    | 8.2e-03 | 1.5e-02 | 7.8e-02 | 1.1e-02 |

Continued on next page

Table C.2: Complete Results on CUTEst Dataset, iteration & time

| name     | $n$  | $k$   |       |       |     | $k^g$   |        |        |       | $t$     |         |         |         |
|----------|------|-------|-------|-------|-----|---------|--------|--------|-------|---------|---------|---------|---------|
|          |      | A     | H     | Hv    | N   | A       | H      | Hv     | N     | A       | H       | Hv      | N       |
| SROSENB  | 100  | 20    | 15    | 15    | 21  | 360     | 74     | 503    | 295   | 6.5e-02 | 2.0e-01 | 2.3e-01 | 6.4e-02 |
|          | 500  | 10    | 8     | 8     | 13  | 33      | 32     | 57     | 45    | 1.5e-03 | 4.0e-03 | 4.7e-02 | 2.1e-03 |
|          | 50   | 10    | 8     | 8     | 11  | 35      | 34     | 61     | 38    | 2.8e-03 | 3.2e-02 | 4.5e-02 | 3.7e-03 |
| SSBRYBND | 1000 | 306   | 120   | 1     | 117 | 29656   | 1005   | 2      | 2814  | 5.8e-01 | 2.0e+02 | 1.0e+02 | 4.5e-02 |
|          | 50   | 153   | 30    | 203   | 79  | 292466  | 356    | 194973 | 746   | 5.8e+01 | 2.1e+02 | 2.0e+02 | 3.9e+02 |
| SSCOSINE | 1000 | 20001 | 20000 | 20000 | 51  | 174630  | 153859 | 246624 | 325   | 5.9e+00 | 9.7e-01 | 8.9e+01 | 6.9e-03 |
|          | 10   | 7524  | 73    | -     | 550 | 2025778 | 1016   | -      | 20787 | 2.0e+02 | 2.0e+02 | -       | 2.3e+00 |
| TESTQUAD | 1000 | 7     | 22    | 22    | 8   | 1053    | 109    | 3377   | 1049  | 5.4e-02 | 3.3e+01 | 8.0e-01 | 5.3e-02 |
| TOINTGSS | 1000 | 30    | 6     | 6     | 10  | 156     | 23     | 76     | 59    | 7.2e-03 | 6.0e-03 | 4.2e-02 | 3.1e-03 |
|          | 50   | 7     | 5     | 5     | 9   | 33      | 22     | 43     | 40    | 8.0e-03 | 5.0e-02 | 3.7e-02 | 1.3e-02 |
| TQUARTIC | 1000 | 22    | 14    | 14    | 2   | 71      | 62     | 113    | 6     | 1.0e-02 | 5.0e-03 | 7.5e-02 | 3.0e-04 |
|          | 50   | 12    | 44    | 42    | 8   | 42      | 219    | 369    | 26    | 5.0e-03 | 4.1e-01 | 2.3e-01 | 4.1e-03 |
| TRIDIA   | 1000 | 5     | 10    | 10    | 5   | 128     | 46     | 303    | 116   | 1.2e-03 | 8.0e-03 | 7.1e-02 | 1.6e-03 |
|          | 50   | 6     | 21    | 21    | 7   | 734     | 100    | 1865   | 738   | 3.5e-02 | 2.7e-01 | 3.5e-01 | 3.1e-02 |
| VARDIM   | 200  | 28    | 5     | 5     | 28  | 83      | 23     | 39     | 83    | 5.8e-03 | 3.1e-02 | 3.1e-02 | 5.6e-03 |
| VAREIGVL | 100  | 13    | 9     | 12    | 24  | 116     | 40     | 508    | 1351  | 3.8e-03 | 1.4e-02 | 1.3e-01 | 3.5e-02 |
|          | 500  | 22    | 11    | 12    | 27  | 2130    | 51     | 646    | 2536  | 1.9e-01 | 1.0e-01 | 2.4e-01 | 2.0e-01 |
| WATSON   | 12   | 13    | 103   | 14    | 13  | 99      | 571    | 206    | 98    | 3.1e-03 | 2.6e-02 | 5.0e-01 | 5.1e-03 |
| WOODS    | 4000 | 97    | 40    | 40    | 85  | 425     | 203    | 432    | 435   | 1.3e-02 | 6.0e-03 | 1.9e-01 | 9.4e-03 |
|          | 4    | 99    | 29    | 29    | 62  | 459     | 154    | 317    | 321   | 1.6e-01 | 3.5e+00 | 2.8e-01 | 9.5e-02 |
| YATP1LS  | 120  | 20001 | 36    | 36    | 247 | 53998   | 188    | 328    | 831   | 1.2e+01 | 4.1e-02 | 1.9e-01 | 7.4e-02 |
|          | 2600 | 88    | 33    | 33    | 52  | 278     | 168    | 292    | 188   | 4.2e-01 | 6.4e+00 | 1.1e+00 | 2.8e-01 |
| YATP2LS  | 8    | 38    | 8     | 8     | 56  | 124     | 40     | 65     | 505   | 1.1e-01 | 2.1e+00 | 1.2e-01 | 4.2e-01 |
|          | 2600 | 301   | 7     | 7     | 386 | 1508    | 33     | 54     | 2259  | 1.3e-01 | 2.0e-03 | 4.4e-02 | 8.8e+01 |

Table C.3: Complete Results on CUTEst Dataset, function value & norm of the gradient

| name       | $n$  | $f$      |          |          |          | $\ g\ $ |         |         |         |
|------------|------|----------|----------|----------|----------|---------|---------|---------|---------|
|            |      | A        | H        | Hv       | N        | A       | H       | Hv      | N       |
| ARGLINA    | 200  | +1.2e-22 | +7.0e-28 | +6.7e-29 | +2.8e-26 | 2.2e-11 | 3.7e-13 | 3.1e-14 | 3.4e-13 |
| ARGLINB    | 200  | +5.0e+01 | +5.0e+01 | +0.0e+00 | +5.0e+01 | 1.7e-03 | 1.4e+01 | 0.0e+00 | 2.0e-03 |
| ARGLINC    | 200  | +5.1e+01 | +5.1e+01 | +5.1e+01 | +5.1e+01 | 1.2e+01 | 5.0e+01 | 1.8e-01 | 5.0e-04 |
| ARGTRIGLS  | 200  | +2.1e-19 | +7.1e-23 | +6.9e-17 | +2.2e-19 | 1.4e-08 | 2.4e-08 | 3.3e-06 | 1.5e-08 |
| ARWHEAD    | 1000 | +0.0e+00 | +0.0e+00 | +0.0e+00 | +0.0e+00 | 1.2e-13 | 5.1e-09 | 5.1e-09 | 1.2e-13 |
|            | 100  | +0.0e+00 | +0.0e+00 | +0.0e+00 | +0.0e+00 | 1.1e-11 | 1.4e-07 | 1.4e-07 | 1.1e-11 |
| BDQRTIC    | 1000 | +3.8e+02 | +3.8e+02 | +3.8e+02 | +3.8e+02 | 1.1e-08 | 1.2e-10 | 4.7e-07 | 1.1e-08 |
|            | 100  | +4.0e+03 | +4.0e+03 | +4.0e+03 | +4.0e+03 | 1.4e-08 | 2.9e-06 | 3.0e-06 | 1.4e-08 |
| BOXPOWER   | 1000 | -1.7e-01 | -1.7e-01 | -1.7e-01 | -1.7e-01 | 6.6e-13 | 4.3e-10 | 4.3e-10 | 1.5e-12 |
|            | 10   | -1.8e+02 | -1.8e+02 | -1.8e+02 | -1.8e+02 | 9.3e-10 | 5.7e-06 | 5.7e-06 | 1.6e-08 |
| BOX        | 1000 | +8.0e-09 | +5.2e-16 | +5.2e-16 | +8.6e-09 | 4.0e-07 | 1.5e-06 | 1.5e-06 | 4.4e-07 |
|            | 10   | +1.4e-08 | +7.2e-10 | +2.8e-09 | +1.6e-08 | 4.8e-07 | 8.1e-07 | 2.9e-06 | 8.0e-07 |
| BROWNAL    | 1000 | +6.4e-13 | +2.0e-22 | +4.2e-23 | +2.2e-19 | 1.4e-07 | 5.0e-07 | 2.8e-06 | 1.5e-09 |
|            | 200  | +2.3e-12 | +3.2e-21 | +2.3e-12 | +2.3e-12 | 6.9e-07 | 2.6e-08 | 6.8e-07 | 5.6e-07 |
| BROYDN3DLS | 1000 | +4.9e-15 | +4.6e-29 | +7.5e-17 | +4.7e-15 | 6.5e-07 | 1.1e-10 | 5.8e-07 | 6.4e-07 |
|            | 50   | +6.3e-19 | +7.1e-01 | +7.1e-01 | +3.9e-15 | 7.9e-09 | 7.0e-07 | 1.1e-06 | 6.1e-07 |
| BROYDN7D   | 500  | +1.7e+01 | +1.7e+01 | +1.7e+01 | +1.7e+01 | 7.2e-08 | 4.2e-06 | 4.3e-06 | 1.4e-08 |
|            | 50   | +1.8e+02 | +2.8e+00 | +2.8e+00 | +1.9e+02 | 8.0e-09 | 3.0e-06 | 1.5e-06 | 2.4e-08 |
| BROYDNBDLS | 1000 | +1.5e-17 | +7.7e-19 | +4.6e-15 | +1.2e-17 | 7.7e-09 | 1.4e-06 | 1.5e-06 | 1.5e-08 |

Continued on next page

Table C.3: Complete Results on CUTEst Dataset, function value & norm of the gradient

| name     | n    | $f$      |          |          |          | $\ g\ $ |         |         |         |
|----------|------|----------|----------|----------|----------|---------|---------|---------|---------|
|          |      | A        | H        | Hv       | N        | A       | H       | Hv      | N       |
|          | 50   | +2.2e-14 | +1.1e-22 | +6.6e-17 | +6.2e-18 | 8.9e-07 | 2.4e-10 | 4.9e-08 | 1.3e-08 |
| BRYBND   | 1000 | +1.5e-17 | +7.7e-19 | +4.6e-15 | +1.2e-17 | 7.7e-09 | 1.4e-06 | 1.5e-06 | 1.5e-08 |
|          | 50   | +2.2e-14 | +8.4e-23 | +6.6e-17 | +6.2e-18 | 8.9e-07 | 2.4e-10 | 4.9e-08 | 1.3e-08 |
| CHAINWO  | 1000 | +1.0e+00 | +1.0e+00 | +1.0e+00 | +1.0e+00 | 1.3e-08 | 9.9e-06 | 9.9e-06 | 5.0e-09 |
|          | 4    | +8.5e+02 | +4.2e+02 | +3.8e+02 | +7.9e+02 | 2.7e-08 | 4.4e-10 | 1.4e-06 | 1.7e-07 |
| CHNROSNB | 25   | +1.0e-18 | +9.1e-29 | +3.2e-16 | +6.5e-19 | 1.8e-08 | 6.4e-08 | 3.9e-07 | 9.5e-09 |
| CHNRSNBM | 25   | +2.5e-19 | +1.3e-27 | +2.8e-15 | +2.7e-17 | 1.0e-08 | 8.2e-07 | 1.1e-06 | 5.7e-08 |
| COSINE   | 1000 | -9.9e+01 | -9.9e+01 | -9.9e+01 | -9.9e+01 | 1.4e-07 | 2.2e-09 | 4.4e-06 | 7.7e-09 |
|          | 100  | -1.0e+03 | -1.0e+03 | -1.0e+03 | -1.0e+03 | 7.8e-07 | 1.9e-10 | 2.5e-07 | 4.0e-09 |
| CRAGGLVY | 1000 | +1.5e+01 | +1.5e+01 | +1.5e+01 | +1.5e+01 | 4.0e-08 | 2.5e-06 | 2.7e-06 | 4.2e-08 |
|          | 50   | +3.4e+02 | +3.4e+02 | +3.4e+02 | +3.4e+02 | 1.4e-08 | 2.4e-09 | 9.2e-07 | 9.0e-07 |
| CURLY10  | 1000 | -1.0e+04 | -1.0e+04 | -1.0e+04 | -1.0e+04 | 3.9e-07 | 1.7e-08 | 9.1e-07 | 1.7e-08 |
|          | 100  | -1.0e+05 | -1.0e+05 | -1.0e+05 | -1.0e+05 | 9.4e-07 | 2.4e-07 | 9.3e-06 | 6.4e-04 |
| CURLY20  | 1000 | -1.0e+04 | -1.0e+04 | -1.0e+04 | -1.0e+04 | 1.5e-08 | 1.6e-08 | 9.5e-07 | 1.3e-08 |
|          | 100  | -1.0e+05 | -1.0e+05 | -1.0e+05 | -1.0e+05 | 1.4e-08 | 2.5e-09 | 4.1e-06 | 1.9e-05 |
| CURLY30  | 1000 | -1.0e+05 | -1.0e+05 | -1.0e+05 | -1.0e+05 | 1.5e-08 | 1.6e-03 | 7.5e-06 | 1.6e-04 |
| DIXMAANA | 3000 | +1.0e+00 | +1.0e+00 | +1.0e+00 | +1.0e+00 | 8.7e-12 | 1.6e-06 | 1.6e-06 | 5.0e-17 |
|          | 90   | +1.0e+00 | +1.0e+00 | +1.0e+00 | +1.0e+00 | 8.2e-17 | 3.6e-08 | 3.6e-08 | 6.3e-09 |
| DIXMAANB | 3000 | +1.0e+00 | +1.0e+00 | +1.0e+00 | +1.0e+00 | 8.5e-08 | 3.4e-06 | 3.4e-06 | 2.7e-09 |
|          | 90   | +1.0e+00 | +1.0e+00 | +1.0e+00 | +1.0e+00 | 2.6e-09 | 6.9e-10 | 6.9e-10 | 6.1e-09 |
| DIXMAANC | 3000 | +1.0e+00 | +1.0e+00 | +1.0e+00 | +1.0e+00 | 7.7e-14 | 6.7e-10 | 6.7e-10 | 4.2e-17 |
|          | 90   | +1.0e+00 | +1.0e+00 | +1.0e+00 | +1.0e+00 | 1.3e-14 | 3.4e-08 | 3.4e-08 | 1.2e-19 |
| DIXMAAND | 3000 | +1.0e+00 | +1.0e+00 | +1.0e+00 | +1.0e+00 | 5.8e-12 | 3.0e-08 | 3.0e-08 | 2.6e-12 |
|          | 90   | +1.0e+00 | +1.0e+00 | +1.0e+00 | +1.0e+00 | 4.7e-08 | 8.3e-06 | 8.3e-06 | 1.4e-09 |
| DIXMAANE | 3000 | +1.0e+00 | +1.0e+00 | +1.0e+00 | +1.0e+00 | 1.3e-08 | 1.3e-08 | 9.8e-07 | 5.3e-07 |
|          | 90   | +1.0e+00 | +1.0e+00 | +1.0e+00 | +1.0e+00 | 2.6e-07 | 3.0e-06 | 2.9e-06 | 3.5e-07 |
| DIXMAANF | 3000 | +1.0e+00 | +1.0e+00 | +1.0e+00 | +1.0e+00 | 1.3e-08 | 4.1e-08 | 8.1e-07 | 9.4e-09 |
|          | 90   | +1.0e+00 | +1.0e+00 | +1.0e+00 | +1.0e+00 | 1.5e-08 | 6.1e-06 | 6.0e-06 | 1.6e-08 |
| DIXMAANG | 3000 | +1.0e+00 | +1.0e+00 | +1.0e+00 | +1.0e+00 | 1.1e-08 | 5.6e-08 | 9.3e-07 | 2.5e-07 |
|          | 90   | +1.0e+00 | +1.0e+00 | +1.0e+00 | +1.0e+00 | 7.4e-08 | 5.5e-06 | 5.4e-06 | 8.0e-08 |
| DIXMAANH | 3000 | +1.0e+00 | +1.0e+00 | +1.0e+00 | +1.0e+00 | 3.5e-08 | 1.2e-07 | 8.7e-07 | 1.9e-08 |
|          | 90   | +1.0e+00 | +1.0e+00 | +1.0e+00 | +1.0e+00 | 1.5e-07 | 1.3e-06 | 1.3e-06 | 2.2e-08 |
| DIXMAANI | 3000 | +1.0e+00 | +1.0e+00 | +1.0e+00 | +1.0e+00 | 3.6e-09 | 4.8e-06 | 4.3e-06 | 1.8e-09 |
|          | 90   | +1.0e+00 | +1.0e+00 | +1.0e+00 | +1.0e+00 | 6.7e-07 | 7.2e-06 | 9.4e-06 | 1.3e-08 |
| DIXMAANJ | 3000 | +1.0e+00 | +1.0e+00 | +1.0e+00 | +1.0e+00 | 5.8e-08 | 1.8e-06 | 1.8e-06 | 1.3e-08 |
|          | 90   | +1.0e+00 | +1.0e+00 | +1.0e+00 | +1.0e+00 | 8.6e-07 | 8.1e-06 | 9.4e-06 | 3.3e-07 |
| DIXMAANK | 3000 | +1.0e+00 | +1.0e+00 | +1.0e+00 | +1.0e+00 | 1.3e-07 | 5.7e-07 | 5.9e-07 | 1.4e-08 |
|          | 90   | +1.0e+00 | +1.0e+00 | +1.0e+00 | +1.0e+00 | 4.2e-07 | 7.9e-06 | 9.9e-06 | 7.9e-08 |
| DIXMAANL | 3000 | +1.0e+00 | +1.0e+00 | +1.0e+00 | +1.0e+00 | 1.5e-08 | 7.0e-06 | 7.3e-06 | 7.8e-08 |
|          | 90   | +1.0e+00 | +1.0e+00 | +1.0e+00 | +1.0e+00 | 5.8e-07 | 9.2e-06 | 7.8e-06 | 6.8e-07 |
| DIXMAANM | 3000 | +1.0e+00 | +1.0e+00 | +1.0e+00 | +1.0e+00 | 1.5e-08 | 7.0e-07 | 7.7e-07 | 1.3e-08 |
|          | 90   | +1.0e+00 | +1.0e+00 | +1.0e+00 | +1.0e+00 | 1.6e-07 | 8.4e-06 | 9.9e-06 | 5.0e-08 |
| DIXMAANN | 3000 | +1.0e+00 | +1.0e+00 | +1.0e+00 | +1.0e+00 | 1.5e-08 | 4.6e-06 | 4.6e-06 | 3.7e-08 |
|          | 90   | +1.0e+00 | +1.0e+00 | +1.0e+00 | +1.0e+00 | 7.7e-07 | 7.9e-06 | 1.0e-05 | 3.9e-07 |
| DIXMAANO | 3000 | +1.0e+00 | +1.0e+00 | +1.0e+00 | +1.0e+00 | 8.9e-08 | 4.4e-06 | 4.4e-06 | 2.2e-08 |
|          | 90   | +1.0e+00 | +1.0e+00 | +1.0e+00 | +1.0e+00 | 8.7e-07 | 6.3e-06 | 8.8e-06 | 1.5e-08 |
| DIXMAANP | 3000 | +1.0e+00 | +1.0e+00 | +1.0e+00 | +1.0e+00 | 1.3e-08 | 1.4e-06 | 2.7e-06 | 1.9e-08 |
|          | 90   | +1.0e+00 | +1.0e+00 | +1.0e+00 | +1.0e+00 | 3.0e-07 | 8.1e-06 | 9.5e-06 | 4.3e-07 |
| DIXON3DQ | 1000 | +1.9e-16 | +3.0e-14 | +7.2e-13 | +2.4e-27 | 1.4e-08 | 3.4e-06 | 4.3e-06 | 1.9e-13 |
|          | 100  | +3.2e-08 | +5.7e-10 | +6.1e-12 | +7.8e-17 | 5.7e-07 | 7.6e-06 | 2.8e-06 | 8.3e-09 |
| DQDR TIC | 1000 | +1.2e-23 | +2.7e-29 | +9.4e-18 | +7.1e-30 | 7.0e-12 | 8.4e-08 | 8.4e-08 | 5.4e-15 |

Continued on next page

Table C.3: Complete Results on CUTEst Dataset, function value & norm of the gradient

| name      | n    | $f$      |          |          |          | $\ g\ $ |         |         |         |
|-----------|------|----------|----------|----------|----------|---------|---------|---------|---------|
|           |      | A        | H        | Hv       | N        | A       | H       | Hv      | N       |
|           | 50   | +5.2e-15 | +1.8e-30 | +2.6e-41 | +1.7e-42 | 1.4e-07 | 3.2e-10 | 3.2e-10 | 6.6e-21 |
| DQRTIC    | 1000 | +3.4e-09 | +1.8e-09 | +1.8e-09 | +3.8e-09 | 8.5e-07 | 3.5e-06 | 3.5e-06 | 8.3e-07 |
|           | 50   | +7.5e-07 | +1.4e-10 | +1.4e-10 | +5.1e-07 | 2.3e-05 | 1.1e-06 | 1.2e-06 | 1.7e-05 |
| EDENSCH   | 2000 | +2.2e+02 | +2.2e+02 | +2.2e+02 | +2.2e+02 | 9.0e-07 | 1.1e-07 | 5.3e-07 | 1.6e-08 |
|           | 36   | +1.2e+04 | +1.2e+04 | +1.2e+04 | +1.2e+04 | 7.8e-09 | 1.9e-06 | 1.9e-06 | 7.8e-09 |
| EIGENALS  | 2550 | +1.1e-16 | +7.5e-22 | +7.5e-22 | +5.2e-22 | 2.4e-08 | 2.4e-06 | 2.4e-06 | 1.2e-10 |
|           | 6    | +3.9e-14 | +7.4e+01 | +7.3e+01 | +8.2e-11 | 5.1e-07 | 1.6e+02 | 9.3e+01 | 8.8e-07 |
| EIGENBLS  | 2550 | +1.8e-01 | +9.6e-24 | +1.8e-01 | +1.8e-01 | 7.2e-08 | 2.2e-06 | 8.2e-07 | 3.3e-07 |
|           | 6    | +1.5e-02 | +1.5e-02 | +4.1e-03 | +5.4e-04 | 1.6e-03 | 1.2e-01 | 4.1e-02 | 4.6e-03 |
| EIGENCLS  | 2652 | +3.8e-17 | +2.7e-23 | +9.7e-14 | +5.0e-17 | 1.1e-08 | 4.6e-06 | 4.8e-06 | 1.4e-08 |
|           | 30   | +1.3e+03 | +2.9e+03 | +8.6e+02 | +4.2e-03 | 1.4e+00 | 1.6e+01 | 8.5e+00 | 1.3e-01 |
| ENGVAl1   | 1000 | +5.4e+01 | +5.4e+01 | +5.4e+01 | +5.4e+01 | 8.9e-09 | 5.7e-06 | 5.7e-06 | 8.7e-09 |
|           | 50   | -        | +1.1e+03 | +1.1e+03 | +1.1e+03 | -       | 1.7e-11 | 3.8e-07 | 1.4e-08 |
| ERRINROS  | 25   | +1.8e+01 | +1.8e+01 | +1.8e+01 | +1.8e+01 | 1.3e-08 | 7.4e-08 | 3.8e-06 | 7.2e-07 |
| ERRINRSM  | 25   | +1.8e+01 | +1.8e+01 | -        | +1.8e+01 | 7.6e-10 | 8.0e-06 | -       | 5.5e-08 |
| EXTROSNB  | 1000 | +3.1e-08 | +7.1e-28 | +1.8e-18 | +3.3e-09 | 8.8e-07 | 3.6e-09 | 7.4e-08 | 1.6e-08 |
|           | 100  | +3.3e-08 | +3.0e-09 | +2.4e-09 | +5.1e-07 | 9.7e-07 | 9.4e-06 | 1.0e-05 | 7.4e-04 |
| FLETBV3M  | 1000 | -2.2e-03 | +1.2e-05 | +1.2e-05 | -2.2e-03 | 8.8e-07 | 7.7e-06 | 7.7e-06 | 4.9e-07 |
|           | 10   | -2.0e+03 | -2.0e+03 | -2.0e+03 | -2.0e+03 | 3.6e-12 | 4.4e-11 | 6.6e-07 | 1.6e-08 |
| FLETcbv2  | 1000 | -5.5e-01 | -5.5e-01 | -5.5e-01 | -5.5e-01 | 1.4e-08 | 5.7e-07 | 5.7e-07 | 1.0e-08 |
|           | 10   | -5.0e-01 | -5.0e-01 | -5.0e-01 | -5.0e-01 | 1.5e-08 | 2.8e-06 | 3.0e-06 | 2.1e-09 |
| FLETcbv3  | 1000 | -3.2e-02 | +1.2e-05 | +1.2e-05 | -3.2e-02 | 9.9e-07 | 7.7e-06 | 7.7e-06 | 5.6e-09 |
|           | 10   | -8.0e+07 | -2.9e+11 | -2.5e+11 | -1.0e+11 | 6.3e-01 | 7.5e-01 | 7.6e-01 | 9.4e-01 |
| FLETCHBV  | 1000 | -2.7e+06 | -2.7e+06 | -2.7e+06 | -2.7e+06 | 2.9e-08 | 1.3e-07 | 1.3e-07 | 0.0e+00 |
|           | 10   | -5.6e+19 | -3.0e+19 | -2.7e+19 | -9.2e+18 | 4.7e+07 | 7.3e+07 | 7.4e+07 | 8.8e+07 |
| FLETCHCR  | 1000 | +4.5e-19 | +3.7e-27 | +7.1e-16 | +1.6e-19 | 2.2e-08 | 1.2e-06 | 3.1e-06 | 1.5e-08 |
|           | 100  | +2.8e-19 | +1.4e-22 | +6.5e-18 | +7.6e+02 | 1.9e-08 | 5.3e-06 | 6.9e-07 | 4.6e+00 |
| FMINSRF2  | 16   | +1.0e+00 | +1.0e+00 | +1.0e+00 | +1.0e+00 | 1.6e-09 | 6.1e-06 | 6.1e-06 | 1.4e-08 |
|           | 961  | +1.0e+00 | +1.0e+00 | +1.0e+00 | +1.0e+00 | 2.0e-08 | 5.5e-06 | 8.3e-06 | 1.6e-08 |
| FMINSURF  | 16   | +1.0e+00 | +1.0e+00 | +1.0e+00 | +1.0e+00 | 8.4e-09 | 2.8e-07 | 2.8e-07 | 2.2e-09 |
|           | 961  | +1.0e+00 | +1.0e+00 | +1.0e+00 | +1.0e+00 | 1.1e-07 | 6.1e-07 | 9.6e-07 | 2.7e-08 |
| FREUROTH  | 1000 | +5.9e+03 | +5.9e+03 | +5.9e+03 | +5.9e+03 | 1.3e-08 | 3.3e-07 | 3.3e-07 | 1.4e-08 |
|           | 50   | +1.2e+05 | +1.2e+05 | +1.2e+05 | +1.2e+05 | 9.3e-07 | 3.2e-10 | 4.8e-07 | 2.8e-08 |
| GENHUMPS  | 1000 | +2.9e+04 | +8.6e-32 | +7.5e-20 | +1.3e-17 | 8.5e+01 | 2.2e-08 | 7.9e-07 | 2.1e-09 |
|           | 10   | +1.0e+07 | +4.2e-17 | +5.7e+02 | +1.2e+05 | 1.9e+03 | 7.2e-06 | 2.9e+01 | 5.0e+02 |
| GENROSE   | 100  | +1.0e+00 | +1.0e+00 | +1.0e+00 | +1.0e+00 | 1.8e-08 | 3.9e-07 | 6.9e-07 | 9.3e-09 |
|           | 500  | +1.0e+00 | +1.0e+00 | +1.0e+00 | +1.0e+00 | 1.7e-08 | 7.8e-06 | 5.5e-07 | 8.9e-09 |
| HILBERTA  | 6    | +2.3e-11 | +3.1e-13 | +4.6e-11 | +5.0e-09 | 2.9e-08 | 2.8e-07 | 9.9e-06 | 3.6e-07 |
| HILBERTB  | 5    | +3.4e-19 | +1.2e-31 | +3.1e-23 | +8.9e-20 | 2.8e-09 | 8.5e-09 | 3.7e-07 | 1.3e-09 |
| INDEFM    | 1000 | -1.0e+09 | -2.9e+05 | -9.2e+14 | -2.2e+05 | 7.1e+00 | 7.1e+00 | 7.3e+00 | 1.4e+01 |
|           | 50   | -2.0e+10 | -5.9e+03 | -4.5e+03 | -1.3e+06 | 3.2e+01 | 3.2e+01 | 3.2e+01 | 6.0e+01 |
| INDEF     | 1000 | -5.0e+03 | -4.7e+03 | -4.7e+03 | -4.9e+03 | 1.3e-11 | 3.0e-06 | 6.9e-07 | 2.2e-08 |
|           | 50   | -1.0e+05 | -1.0e+05 | -1.0e+05 | -9.5e+04 | 3.7e-10 | 1.7e-07 | 2.5e-10 | 3.1e-07 |
| INTEQNELS | 102  | +3.2e-18 | +7.9e-31 | +1.1e-17 | +1.1e-18 | 3.7e-09 | 4.9e-10 | 1.7e-07 | 2.2e-09 |
|           | 502  | +1.6e-17 | +9.2e-30 | +7.1e-14 | +1.0e-14 | 8.3e-09 | 3.2e-09 | 5.4e-07 | 2.1e-07 |
| JIMACK    | 1521 | +8.7e-01 | +8.7e-01 | +8.7e-01 | +9.1e-01 | 3.1e-06 | 8.7e-06 | 8.5e-06 | 3.6e-01 |
|           | 81   | +8.9e-01 | +8.7e-01 | +1.1e+00 | +8.9e-01 | 1.6e-02 | 3.4e-04 | 9.4e-01 | 1.7e-02 |
| LIARWHD   | 1000 | +7.4e-19 | +6.2e-28 | +5.6e-28 | +6.8e-19 | 8.9e-09 | 3.1e-06 | 3.1e-06 | 8.5e-09 |
|           | 36   | +1.0e-25 | +4.9e-29 | +0.0e+00 | +7.2e-22 | 2.3e-11 | 4.7e-09 | 4.7e-09 | 1.9e-09 |
| MANCINO   | 50   | +1.5e-21 | +6.0e-24 | +5.9e-20 | +1.3e-21 | 5.4e-08 | 5.6e-07 | 5.6e-07 | 5.2e-08 |
| MODBEALE  | 10   | +2.3e-21 | +9.9e-26 | +1.5e-25 | +1.7e-14 | 1.6e-10 | 3.3e-06 | 3.3e-06 | 2.5e-07 |

Continued on next page

Table C.3: Complete Results on CUTEst Dataset, function value & norm of the gradient

| name     | n    | $f$      |          |          |          | $\ g\ $ |         |         |         |
|----------|------|----------|----------|----------|----------|---------|---------|---------|---------|
|          |      | A        | H        | Hv       | N        | A       | H       | Hv      | N       |
|          | 2000 | +3.0e-15 | +1.8e-25 | +5.2e-14 | +8.0e+00 | 1.3e-07 | 3.5e-08 | 6.7e-07 | 4.8e-04 |
| MOREBV   | 1000 | +6.7e-12 | +7.8e-13 | +3.1e-12 | +1.8e-14 | 2.9e-08 | 5.3e-06 | 7.6e-06 | 5.7e-09 |
|          | 50   | +1.2e-09 | +1.2e-09 | +1.2e-09 | +1.1e-09 | 1.5e-07 | 1.5e-06 | 8.9e-06 | 3.9e-07 |
| MSQRTALS | 4900 | +1.1e-14 | +9.8e-28 | +7.9e-14 | +2.5e-17 | 1.4e-07 | 9.0e-08 | 1.0e-06 | 7.9e-09 |
|          | 49   | +8.5e-04 | +1.5e-01 | +3.6e-04 | +7.7e-05 | 4.9e-01 | 5.9e+00 | 1.7e-01 | 4.6e-03 |
| MSQRTBLS | 4900 | +4.3e-17 | +6.2e-24 | +6.8e-14 | +1.7e-14 | 1.0e-08 | 8.6e-07 | 1.3e-06 | 2.1e-07 |
|          | 49   | +4.5e-03 | +1.6e-01 | +2.2e-04 | +1.3e-05 | 6.1e-01 | 6.0e+00 | 6.6e-02 | 1.8e-03 |
| NCB20B   | 1000 | +1.9e+02 | +1.9e+02 | +1.9e+02 | +1.9e+02 | 1.3e-08 | 4.8e-07 | 9.8e-07 | 3.0e-08 |
|          | 180  | +9.2e+02 | +9.2e+02 | +9.2e+02 | +9.1e+02 | 1.3e-08 | 2.6e-06 | 9.2e-08 | 2.7e-08 |
| NCB20    | 1010 | +3.5e+02 | +3.5e+02 | +3.5e+02 | +3.5e+02 | 3.3e-08 | 1.7e-07 | 8.9e-07 | 4.1e-08 |
|          | 110  | +1.7e+03 | +1.7e+03 | +1.7e+03 | +1.7e+03 | 3.8e-08 | 2.8e-06 | 2.9e-06 | 2.1e-07 |
| NONCVXU2 | 1000 | +2.3e+01 | +2.3e+01 | +2.3e+01 | +2.3e+01 | 1.4e-11 | 1.3e-06 | 1.3e-06 | 7.1e-12 |
|          | 10   | +2.3e+03 | +2.3e+03 | +2.3e+03 | +2.3e+03 | 1.5e-08 | 7.0e-06 | 1.5e-06 | 6.4e-07 |
| NONCVXUN | 1000 | +2.3e+01 | +2.3e+01 | +2.3e+01 | +2.3e+01 | 3.4e-10 | 5.0e-09 | 4.8e-09 | 4.0e-07 |
|          | 10   | -        | +2.3e+03 | +2.3e+03 | +2.3e+03 | -       | 3.0e-02 | 5.3e-02 | 7.0e-02 |
| NONDIA   | 1000 | +3.3e-23 | +5.0e-28 | +0.0e+00 | +2.6e-26 | 4.1e-10 | 3.4e-10 | 3.3e-10 | 9.1e-12 |
|          | 90   | +2.0e-23 | +6.4e-27 | +2.0e-29 | +2.1e-23 | 2.6e-09 | 1.9e-07 | 1.9e-07 | 2.6e-09 |
| NONDQUAR | 1000 | +9.0e-07 | +3.5e-06 | +3.0e-06 | +5.0e-05 | 9.4e-07 | 7.2e-06 | 7.5e-06 | 3.2e-03 |
|          | 100  | +1.6e-06 | +3.5e-06 | +5.0e-06 | +5.3e-07 | 9.8e-07 | 9.1e-06 | 7.0e-06 | 9.0e-07 |
| NONMSQRT | 4900 | +1.1e+00 | +1.1e+00 | +1.1e+00 | +1.1e+00 | 9.5e-07 | 3.1e-02 | 8.5e-02 | 6.4e-07 |
|          | 49   | +7.2e+02 | +7.5e+02 | +7.9e+02 | +7.3e+02 | 2.5e+00 | 4.8e+01 | 6.8e+01 | 3.7e+02 |
| OSCIGRAD | 1000 | +2.8e-09 | +2.8e-09 | +2.4e-09 | +2.8e-09 | 4.6e-08 | 9.2e-06 | 1.3e-03 | 3.6e-08 |
|          | 15   | +5.6e-24 | -        | +1.7e-21 | +3.2e-23 | 6.1e-08 | -       | 6.8e-07 | 8.9e-08 |
| OSCIPTH  | 25   | +1.0e+00 | +1.0e+00 | +1.0e+00 | +1.0e+00 | 4.6e-09 | 2.6e-06 | 2.6e-06 | 4.6e-09 |
|          | 500  | +1.0e+00 | +1.0e+00 | +1.0e+00 | +1.0e+00 | 4.6e-09 | 2.6e-06 | 2.6e-06 | 4.6e-09 |
| PENALTY1 | 1000 | +4.3e-04 | +4.3e-04 | +4.3e-04 | +4.3e-04 | 2.6e-07 | 8.6e-06 | 1.5e-06 | 1.2e-08 |
|          | 50   | +9.7e-03 | +9.7e-03 | +9.7e-03 | +9.7e-03 | 4.3e-03 | 1.8e-07 | 1.8e-07 | 1.9e-03 |
| PENALTY2 | 1000 | +4.3e+00 | +4.3e+00 | +4.3e+00 | +4.3e+00 | 1.4e-08 | 1.6e-09 | 7.7e-06 | 1.9e-07 |
|          | 50   | +1.4e+83 | +4.9e+82 | +4.1e+82 | +1.1e+83 | 4.9e+38 | 9.1e+69 | 2.5e+67 | 2.4e+67 |
| PENALTY3 | 50   | +1.0e-03 | +1.0e-03 | +1.0e-03 | +1.0e-03 | 8.1e-09 | 2.5e-08 | 8.9e-07 | 1.2e-07 |
| POWELLSG | 1000 | +5.1e-10 | +1.6e-11 | +1.8e-11 | +5.1e-10 | 5.5e-07 | 6.9e-06 | 6.9e-06 | 5.4e-07 |
|          | 60   | +1.7e-09 | +6.4e-13 | +7.4e-12 | +1.6e-09 | 6.6e-07 | 3.5e-06 | 2.3e-08 | 6.4e-07 |
| POWER    | 1000 | +1.1e-10 | +1.2e-18 | +2.4e-12 | +1.1e-10 | 7.6e-07 | 3.1e-08 | 4.1e-08 | 7.6e-07 |
|          | 50   | +1.3e-09 | +2.5e-18 | +7.4e-12 | +1.3e-09 | 1.9e-05 | 5.7e-08 | 6.7e-07 | 1.9e-05 |
| QUARTC   | 1000 | +4.6e-09 | +3.1e-10 | +4.5e-10 | +2.8e-09 | 8.9e-07 | 4.6e-06 | 4.7e-06 | 6.0e-07 |
|          | 100  | +7.5e-07 | +1.4e-10 | +1.4e-10 | +5.1e-07 | 2.3e-05 | 1.1e-06 | 1.2e-06 | 1.7e-05 |
| SBRYBND  | 1000 | +1.3e+02 | +4.5e+02 | +4.7e+05 | +3.5e+02 | 4.2e+02 | 2.1e+07 | 3.4e+03 | 1.2e+05 |
|          | 50   | +2.9e+03 | +2.1e+04 | +5.0e+03 | +3.6e+03 | 2.8e+03 | 1.1e+08 | 5.1e+06 | 1.8e+05 |
| SCHMVETT | 1000 | -2.4e+01 | -2.4e+01 | -2.4e+01 | -2.4e+01 | 3.1e-07 | 1.0e-10 | 1.0e-10 | 1.2e-08 |
|          | 10   | -3.0e+03 | -3.0e+03 | -3.0e+03 | -3.0e+03 | 2.5e-08 | 2.1e-07 | 1.0e-06 | 5.4e-08 |
| SCOSINE  | 1000 | +7.1e+00 | -        | -        | -6.5e+00 | 1.3e+05 | -       | -       | 5.9e+00 |
|          | 10   | -4.7e+02 | -1.2e+02 | +8.3e+02 | -4.4e+02 | 4.5e+02 | 9.1e+16 | 1.3e+15 | 6.8e+04 |
| SCURLY10 | 1000 | +1.7e+06 | +9.7e+10 | +9.7e+10 | +1.7e+06 | 5.4e+10 | 1.1e+20 | 1.1e+20 | 5.4e+10 |
|          | 10   | +1.8e+11 | +3.4e+23 | +3.4e+23 | +1.0e+11 | 1.4e+14 | 6.6e+23 | 6.6e+23 | 9.0e+13 |
| SCURLY20 | 1000 | +2.1e+12 | +8.6e+24 | +8.6e+24 | +1.2e+12 | 1.4e+15 | 1.6e+25 | 1.6e+25 | 9.1e+14 |
| SCURLY30 | 1000 | -        | +1.5e+25 | +1.5e+25 | +4.1e+12 | -       | 3.7e+25 | 3.7e+25 | 3.2e+15 |
| SENSORS  | 1000 | -2.0e+01 | -2.1e+01 | -2.1e+01 | -2.0e+01 | 8.6e-11 | 2.1e-10 | 1.2e-07 | 1.9e-08 |
|          | 10   | -2.0e+05 | -2.0e+05 | -2.0e+05 | -2.0e+05 | 1.6e-08 | 9.6e-06 | 9.6e-06 | 7.1e-08 |
| SINQUAD  | 1000 | -1.1e+03 | -1.1e+03 | -1.1e+03 | -1.1e+03 | 2.5e-11 | 9.1e-06 | 9.1e-06 | 2.7e-08 |
|          | 50   | -2.9e+05 | -2.9e+05 | -2.9e+05 | -2.9e+05 | 1.3e-09 | 2.1e-07 | 2.1e-07 | 1.2e-10 |
| SPARSINE | 1000 | +3.6e-18 | +1.4e-27 | +1.8e-15 | +6.3e-18 | 1.5e-08 | 7.5e-08 | 7.1e-07 | 1.0e-08 |

Continued on next page



Table C.3: Complete Results on CUTEst Dataset, function value & norm of the gradient

| name     | n    | $f$      |          |          |          | $\ g\ $ |         |         |         |
|----------|------|----------|----------|----------|----------|---------|---------|---------|---------|
|          |      | A        | H        | Hv       | N        | A       | H       | Hv      | N       |
|          | 50   | +3.2e-18 | +3.3e-20 | +9.8e-13 | +1.7e-11 | 1.9e-08 | 5.3e-09 | 9.6e-06 | 2.8e-04 |
| SPARSQR  | 1000 | +3.8e-10 | +1.2e-13 | +5.3e-13 | +3.8e-10 | 4.7e-07 | 5.5e-09 | 5.5e-09 | 4.7e-07 |
|          | 50   | +2.3e-10 | +1.2e-14 | +5.6e-10 | +2.3e-10 | 3.2e-07 | 1.6e-08 | 1.8e-06 | 3.2e-07 |
| SPMSRTL  | 1000 | +8.9e-17 | +2.5e-17 | +2.7e-13 | +4.4e-16 | 1.1e-08 | 2.5e-06 | 2.5e-06 | 4.1e-08 |
|          | 100  | +5.4e-16 | +4.3e-16 | +2.1e-15 | +8.5e-15 | 1.5e-08 | 3.5e-08 | 9.5e-07 | 3.6e-07 |
| SROSENBR | 500  | +9.4e-17 | +1.4e-28 | +1.2e-28 | +1.8e-18 | 1.7e-08 | 6.5e-07 | 6.5e-07 | 1.3e-09 |
|          | 50   | +3.4e-28 | +6.5e-28 | +1.3e-27 | +2.8e-29 | 7.9e-13 | 4.7e-08 | 4.7e-08 | 1.1e-14 |
| SSBRYBND | 1000 | +2.1e-17 | +1.0e-10 | +1.9e-16 | +1.7e+00 | 2.2e-08 | 1.7e-01 | 2.3e-04 | 1.5e-08 |
|          | 50   | +1.7e-19 | +1.9e+02 | +1.7e-12 | +1.1e+04 | 1.3e-08 | 1.9e+05 | 2.2e-02 | 9.0e+04 |
| SSCOSINE | 1000 | -8.3e+00 | -9.0e+00 | -8.5e+00 | -9.0e+00 | 9.7e-04 | 2.9e-01 | 6.0e+04 | 3.1e-09 |
|          | 10   | -9.9e+02 | +2.5e+01 | -        | -1.0e+03 | 2.4e-02 | 2.4e+10 | -       | 2.9e-03 |
| TESTQUAD | 1000 | +1.2e-16 | +3.0e-19 | +2.4e-17 | +2.8e-17 | 5.3e-08 | 1.5e-07 | 8.5e-08 | 3.3e-08 |
| TOINTGSS | 1000 | +1.0e+01 | +1.0e+01 | +1.0e+01 | +1.0e+01 | 4.5e-07 | 8.1e-09 | 5.4e-07 | 1.5e-08 |
|          | 50   | +1.0e+01 | +1.0e+01 | +1.0e+01 | +1.0e+01 | 4.1e-07 | 4.8e-08 | 1.2e-07 | 5.0e-09 |
| TQUARTIC | 1000 | +8.2e-22 | +4.0e-30 | +2.1e-30 | +1.6e-28 | 5.5e-10 | 2.1e-08 | 2.1e-08 | 3.5e-13 |
|          | 50   | +1.5e-17 | +6.0e-31 | +2.9e-23 | +1.2e-13 | 2.5e-10 | 6.8e-10 | 6.8e-10 | 2.2e-08 |
| TRIDIA   | 1000 | +1.6e-17 | +4.9e-27 | +1.1e-15 | +6.4e-18 | 5.6e-08 | 5.9e-07 | 9.4e-07 | 4.1e-08 |
|          | 50   | +9.5e-19 | +2.7e-25 | +3.2e-16 | +3.5e-19 | 4.0e-08 | 6.1e-10 | 9.3e-07 | 2.2e-08 |
| VARDIM   | 200  | +1.7e-06 | +3.6e-02 | +3.6e-02 | +1.7e-06 | 4.3e+00 | 2.2e+05 | 2.2e+05 | 4.3e+00 |
| VAREIGVL | 100  | +3.9e-18 | +3.2e-26 | +1.6e-13 | +1.9e-11 | 7.5e-09 | 8.4e-07 | 2.9e-06 | 2.0e-07 |
|          | 500  | +8.2e-12 | +3.5e-26 | +6.1e-13 | +7.4e-11 | 1.9e-07 | 9.4e-07 | 4.5e-06 | 8.9e-07 |
| WATSON   | 12   | +1.2e-07 | +1.1e-08 | +1.4e-08 | +1.2e-07 | 9.3e-07 | 9.9e-06 | 4.5e-06 | 9.3e-07 |
| WOODS    | 4000 | +1.0e-19 | +7.4e-24 | +7.4e-24 | +1.3e-20 | 1.3e-08 | 9.9e-06 | 9.9e-06 | 5.0e-09 |
|          | 4    | +1.8e-23 | +3.0e-27 | +1.4e-27 | +1.6e-23 | 1.5e-10 | 1.1e-06 | 1.1e-06 | 1.1e-10 |
| YATP1LS  | 120  | +1.7e+00 | +5.5e-26 | +8.0e-27 | +2.3e-17 | 1.6e+00 | 4.2e-07 | 4.2e-07 | 4.4e-10 |
|          | 2600 | +1.1e-21 | +3.4e-24 | +6.0e-25 | +5.3e-23 | 3.4e-09 | 3.0e-07 | 3.0e-07 | 6.6e-10 |
| YATP2LS  | 8    | +1.1e+02 | +3.7e-31 | +6.3e-28 | +1.1e+02 | 9.9e-07 | 5.2e-10 | 5.2e-10 | 1.9e-07 |
|          | 2600 | +2.6e-29 | +3.8e-28 | +8.0e-27 | +1.3e+02 | 1.2e-13 | 7.5e-12 | 7.3e-12 | 4.0e-07 |